

One-electron singular spectral features of the 1D Hubbard model at finite magnetic field

J. M. P. Carmelo^{1,2,3,4} and T. Čadež^{3,2}

¹*Department of Physics, University of Minho, Campus Gualtar, P-4710-057 Braga, Portugal*

²*Center of Physics of University of Minho and University of Porto, P-4169-007 Oporto, Portugal*

³*Beijing Computational Science Research Center, Beijing 100193, China*

⁴*University of Gothenburg, Department of Physics, SE-41296 Gothenburg, Sweden*

(Dated: 25 May 2016)

The momentum, electronic density, spin density, and interaction dependences of the exponents that control the (k, ω) -plane singular features of the $\sigma = \uparrow, \downarrow$ one-electron spectral functions of the 1D Hubbard model at finite magnetic field are studied. The usual half-filling concepts of one-electron lower Hubbard band and upper Hubbard band are defined for all electronic density and spin density values and the whole finite repulsion range in terms of the rotated electrons associated with the model Bethe-ansatz solution. Such rotated electrons are the link of the non-perturbative relation between the electrons and the pseudofermions. Our results further clarify the microscopic processes through which the pseudofermion dynamical theory accounts for the σ one-electron matrix elements between the ground state and excited energy eigenstates.

PACS numbers: 73.22.Dj, 03.65.Nk, 75.10.Lp, 71.10.Fd

I. INTRODUCTION

The one-dimensional (1D) Hubbard model with nearest-neighbor hopping integral t and on-site repulsion U is an important correlated electronic system whose Bethe ansatz (BA) solution was first derived by the coordinate BA [1, 2], following a similar solution for a related continuous model with repulsive δ -function interaction [3]. For the 1D Hubbard model such a solution is also reachable by the BA inverse-scattering method [4]. In the thermodynamic limit (TL) the imaginary part of its BA complex rapidities simplifies [5]. The Hubbard model was originally introduced as a toy model to study d-electrons in transition metals [6, 7]. It is possibly the most studied lattice system of correlated electrons. Static properties such as the charge and spin stiffnesses of the 1D Hubbard model under periodic boundary conditions can be determined from the use of the response of the energy eigenvalues to an external flux piercing the ring [8, 9].

On the other hand, one of the main challenges in the study of the 1D Hubbard model properties is the calculation of dynamical correlation functions. Its BA solution provides the exact spectrum of the energy eigenstates, yet it has been difficult to apply to the derivation of high-energy dynamical correlation functions. (In this paper we use the designation *high energy* for all energy scales larger than the model low-energy limit associated with the Tomonaga-Luttinger-liquid regime [10–15].) The high-energy dynamical correlation functions of both some integrable models with spectral gap [16–22] and spin lattice systems [23–28] can be studied by the form-factor approach. However, form factors of the 1D Hubbard model $\sigma = \uparrow, \downarrow$ electron creation and annihilation operators involved in the spectral functions studied in this paper remains an unsolved problem.

The low-energy behavior of the correlation functions of the 1D Hubbard model at finite magnetic field was addressed in Refs. [14, 29–31]. On the other hand, in what high-energy behavior of dynamical correlation functions is concerned the method used in Refs. [32, 33] has been a breakthrough to address it for one-electron removal and addition spectral functions at zero magnetic field in the $u \rightarrow \infty$ limit, which have been derived for the whole (k, ω) plane. That method relies on the spinless-fermion phase shifts imposed by Heisenberg spins 1/2. Such elementary objects naturally arise from the zero spin density and $u \rightarrow \infty$ electron wave-function factorization [34–36].

A related pseudofermion dynamical theory (PDT) relying on a representation of the model BA solution in terms of the pseudofermions generated by a unitary transformation from the corresponding pseudoparticles considered in Ref. [37] was introduced in Refs. [38, 39]. It is an extension of the $u \rightarrow \infty$ method of Refs. [32, 33] to the whole $u \equiv U/4t > 0$ range of the 1D Hubbard model. A key property is that the pseudofermions are inherently constructed to their energy spectrum having no interaction terms. This allows the expression of the one-electron spectral functions in terms of convolutions of pseudofermion spectral functions. The price to pay for the lack of pseudofermion energy spectrum interaction terms is that creation or annihilation of pseudofermions under transitions to excited states imposes phase shifts to the remaining pseudofermions. Within the PDT such phase shifts fully control the one- and two-electron spectral-weight distributions over the (k, ω) plane. That approach has been the first breakthrough for the derivation of analytical expressions of the zero-magnetic-field 1D Hubbard model high-energy dynamical correlation functions for the whole finite $u > 0$ range. Recently a modified form of the PDT was used to study the high-energy

spin dynamical correlation functions of the 1D Hubbard model electronic density $n_e = 1$ Mott-Hubbard insulator phase [40].

After the PDT of the 1D Hubbard model was introduced in Refs. [38, 39], a set of novel methods have been developed to also tackle the high-energy physics of 1D correlated quantum problems, beyond the low-energy Tomonaga-Luttinger-liquid limit [41]. In the case of the 1D Hubbard model at zero magnetic field such methods reach the same results as the PDT. For instance, the momentum, electronic density, and on-site repulsion $u = U/4t > 0$ dependence of the exponents that control the line shape of the one-electron spectral function of the model at zero magnetic field calculated in Refs. [42, 43] in the framework of a mobile impurity model using input from the BA solution is exactly the same as that obtained previously by the use of the PDT.

However, the applications to the study of the repulsive 1D Hubbard model one-electron spectral functions of both such methods [42, 43], those of the PDT [44–47], and the time-dependent density-matrix renormalization group (tDMRG) method [48, 49] have been limited to zero magnetic field. The tDMRG studies of Ref. [50] studied the one-electron spectral-weight distributions of the attractive 1D Hubbard model at finite magnetic field. Under the canonical transformation that maps that model into the repulsive 1D Hubbard model, the one-electron spectral-weight distributions plotted in Figs. 1 (c) and Fig. 2 of that reference correspond to electronic densities $n_e = 1$ and $n_e = 0.9$, respectively, and spin density $m = 1/2$. The results refer to a finite system with 40 electrons. While they provide some information on the one-electron spectral-weight distributions, it is not possible to extract from them the momentum dependence of the exponents that *in the TL* control the line shapes near the σ one-electron spectral functions singularities.

The main goal of this paper is to extend the PDT applications to the study of the σ one-electron spectral functions of the repulsive 1D Hubbard model at finite magnetic field h in the TL near their singularities. In the TL the corresponding line shapes are controlled by exponents whose momentum, on-site repulsion $u = U/4t$, electronic density n , and spin density m dependences we study for $u > 0$, $n \in [0, 1]$, and $m \in [0, n_e]$. In addition, the issue of how the σ one-electron creation and annihilation operators matrix elements between the ground state and excited energy eigenstates are accounted for by the PDT introduced in Refs. [38, 39] is further clarified in this paper. Beyond the preliminary analysis of these references, the corresponding microscopic processes are shown to involve the rotated electrons as a needed link of the non-perturbative relation between the electrons and PDT pseudofermions.

Our studies refer to the TL of the Hubbard model under periodic boundary conditions on a 1D lattice with an even number $L \rightarrow \infty$ of sites and in a chemical potential μ and magnetic field h ,

$$\begin{aligned}\hat{H} &= \hat{H}_u + 2\mu \hat{S}_\eta^z + 2\mu_B h \hat{S}_s^z, \\ \hat{H}_u &= -t \sum_{\sigma=\uparrow,\downarrow} \sum_{j=1}^L \left(c_{j,\sigma}^\dagger c_{j+1,\sigma} + c_{j+1,\sigma}^\dagger c_{j,\sigma} \right) + U \sum_{j=1}^L \left(c_{j,\uparrow}^\dagger c_{j,\sigma} - 1/2 \right) \left(c_{j,\downarrow}^\dagger c_{j,\sigma} - 1/2 \right), \\ \hat{S}_\eta^z &= -\frac{1}{2}(L - \hat{N}); \quad \hat{S}_s^z = -\frac{1}{2}(\hat{N}_\uparrow - \hat{N}_\downarrow).\end{aligned}\tag{1}$$

Here the first and second terms of \hat{H}_u are the kinetic-energy operator and the electron on-site repulsion operator, respectively, the operator $c_{j,\sigma}^\dagger$ (and $c_{j,\sigma}$) creates (and annihilates) one spin-projection σ electron at lattice site $j = 1, \dots, L$, and the electron number operators read $\hat{N} = \sum_{\sigma=\uparrow,\downarrow} \hat{N}_\sigma$ and $\hat{N}_\sigma = \sum_{j=1}^L \hat{n}_{j,\sigma} = \sum_{j=1}^L c_{j,\sigma}^\dagger c_{j,\sigma}$. Moreover, μ_B is the Bohr magneton and \hat{S}_η^z and \hat{S}_s^z are the diagonal generators of the Hamiltonian \hat{H}_u global η -spin and spin $SU(2)$ symmetry algebras, respectively. In this paper we use in general units of lattice constant one, so that the number of lattice sites N_a equals the lattice length L . The model properties depend on the ratio U/t and in this paper the corresponding parameter $u = U/4t$ is often used.

The lowest weight states (LWSs) and highest weight states (HWSs) of the η -spin and spin $SU(2)$ symmetry algebras have numbers $S_\alpha = -S_\alpha^z$ and $S_\alpha = S_\alpha^z$, respectively, for $\alpha = \eta, s$. Here S_η is the states η -spin, S_s their spin, and S_η^z and S_s^z are the corresponding projections, respectively, which are the eigenvalues of the spin operators given in Eq. (1). Let $\{|l_r, l_{\eta s}, u\rangle\}$ be the complete set of 4^L energy eigenstates of the Hamiltonian \hat{H} , Eq. (1), associated with the BA solution for $u > 0$. The LWSs of both $SU(2)$ symmetry algebras are here denoted by $|l_r, l_{\eta s}^0, u\rangle$ where the u -independent label $l_{\eta s}$ is a short notation for the set of quantum numbers,

$$l_{\eta s} = S_\eta, S_s, n_\eta, n_s; \quad n_\alpha = S_\alpha + S_\alpha^z = 0, 1, \dots, 2S_\alpha, \quad \alpha = \eta, s.\tag{2}$$

Furthermore, the label l_r refers to the set of all remaining u -independent quantum numbers needed to uniquely specify an energy eigenstate $|l_r, l_{\eta s}, u\rangle$. The latter u -independent quantum numbers naturally emerge from the BA solution and are given below in Section II B.

We call a *Bethe state* an energy eigenstate that is a LWS of both $SU(2)$ symmetry algebras. For a Bethe state one then has that $n_\eta = n_s = 0$ in Eq. (2), so that $l_{\eta s}^0$ stands for $S_\eta, S_s, 0, 0$. The non-LWSs $|l_r, l_{\eta s}, u\rangle$ can be generated

from the corresponding Bethe states $|l_r, l_{\eta s}^0, u\rangle$ as [51],

$$|l_r, l_{\eta s}, u\rangle = \prod_{\alpha=\eta, s} \left(\frac{1}{\sqrt{\mathcal{C}_\alpha}} (\hat{S}_\alpha^+)^{n_\alpha} \right) |l_r, l_{\eta s}^0, u\rangle; \quad \mathcal{C}_\alpha = (n_\alpha!) \prod_{j=1}^{n_\alpha} (2S_\alpha + 1 - j), \quad n_\alpha = 1, \dots, 2S_\alpha,$$

$$\hat{S}_\eta^+ = \sum_{j=1}^L (-1)^j c_{j,\downarrow}^\dagger c_{j,\uparrow}^\dagger; \quad \hat{S}_s^+ = \sum_{j=1}^L c_{j,\downarrow}^\dagger c_{j,\uparrow}^\dagger. \quad (3)$$

Here \mathcal{C}_α are normalization constants and $\alpha = \eta, s$. The model in its full Hilbert space can be described either directly within the BA solution [35, 52] or by application onto the Bethe states of the η -spin and spin $SU(2)$ symmetry algebras off-diagonal generators, as given in Eq. (3).

Relying on the model symmetries, for simplicity and without loss in generality the studies of this paper refer to electronic densities and spin densities in the ranges $n_e \in [0, 1[$ and $m \in [0, n_e]$, respectively. For such electronic densities and spin densities the model ground states are LWSs of both the η -spin and spin $SU(2)$ symmetry algebras so that in the studies of this paper we use the LWS formulation of 1D Hubbard model BA solution.

The PDT is used in it to clarify one of the unresolved questions concerning the physics of the 1D Hubbard model at finite magnetic field, Eq. (1), by deriving the momentum, repulsive interaction $u = U/4t$, electron-density n_e , and spin-density m dependences of the exponents that control the singularities at the σ one-electron spectral functions. These exponents control the line shape near the singularities of the following σ one-electron spectral function $B_{\sigma,\gamma}(k, \omega)$ such that $\gamma = -1$ (and $\gamma = +1$) for one-electron removal (and addition),

$$B_{\sigma,-1}(k, \omega) = \sum_{\nu^-} |\langle \nu^- | c_{k,\sigma} | GS \rangle|^2 \delta(\omega + (E_{\nu^-}^{N_\sigma-1} - E_{GS}^{N_\sigma})) \quad \omega \leq 0,$$

$$B_{\sigma,+1}(k, \omega) = \sum_{\nu^+} |\langle \nu^+ | c_{k,\sigma}^\dagger | GS \rangle|^2 \delta(\omega - (E_{\nu^+}^{N_\sigma+1} - E_{GS}^{N_\sigma})) \quad \omega \geq 0. \quad (4)$$

Here $c_{k,\sigma}$ and $c_{k,\sigma}^\dagger$ are electron annihilation and creation operators, respectively, of momentum k and $|GS\rangle$ denotes the initial N_σ -electron ground state of energy $E_{GS}^{N_\sigma}$. The ν^- and ν^+ summations run over the $N_\sigma - 1$ and $N_\sigma + 1$ -electron excited energy eigenstates, respectively, and $E_{\nu^-}^{N_\sigma-1}$ and $E_{\nu^+}^{N_\sigma+1}$ are the corresponding energies.

The remainder of the paper is organized as follows. In Section II the σ one-electron lower-Hubbard band (LHB) and upper-Hubbard band (UHB) are defined for $u > 0$ and all densities in terms of quantum numbers associated with the σ rotated-electron energy eigenstates occupancies. Moreover, the relation of the β pseudoparticle representation to such σ rotated electrons, which are uniquely defined in terms of the matrix elements of the electron - rotated-electron unitary operator between all model 4^L energy and momentum eigenstates, is an issue also addressed in that section. The PDT suitable for the study of the σ one-electron spectral weights and further information beyond that provided in Refs. [38, 39] on how that dynamical theory accounts for the matrix elements of the σ electron operators between the ground state and the excited energy eigenstates are the issues revisited and studied in Section III. In Section IV the (k, ω) -plane line shape near the singular spectral features of the σ one-electron spectral functions, Eq. (4), is studied. Finally, the concluding remarks are presented in Section V.

II. LOWER- AND UPPER-HUBBARD BANDS AND THE PSEUDOPARTICLE REPRESENTATION EMERGING FROM THE ROTATED ELECTRONS ASSOCIATED WITH THE BA SOLUTION

Concerning the σ one-electron addition processes that contribute to the $\gamma = 1$ spectral function, Eq. (4), important concepts for our study are those of a LHB and a UHB. Those are defined for $u > 0$ and all densities in Section II A by the rotated-electron quantum numbers that define the σ one-electron addition excited energy eigenstates. The corresponding unique definition of the electron - rotated-electron unitary transformation associated with the BA solution and the separation of the rotated-electron occupancy configurations that generate the exact $u > 0$ energy eigenstates into occupancy configurations of three types of fractionalized particles, specifically the spinless c pseudoparticles, the rotated spins $1/2$, and the rotated η -spins $1/2$, are the issues addressed in Section II B. Such a relation allows the introduction and expression in Section II C of operators for the c pseudoparticles, rotated spins $1/2$, and rotated η -spins $1/2$ in terms of the σ rotated-electron creation and annihilation operators. In Section II D the pseudoparticle energy dispersions and other quantities that emerge from the pseudoparticle quantum liquid and determine and control the (k, ω) -plane line shape near the singular spectral features of the $\sigma = \uparrow, \downarrow$ one-electron spectral functions, Eq. (4), are introduced.

A. Definition of σ one-electron lower- and upper-Hubbard bands

The concept of σ one-electron UHB addition is well established at electronic density $n_e = 1$ for $u > 0$ [1, 2, 53]. Below we define the concepts of a LHB and a UHB for $n_e \neq 1$ and $u > 0$ such that due to a quantum phase transition at $n_e = 1$ there is only σ one-electron UHB addition whereas for $n_e \neq 1$ there is both σ one-electron LHB and UHB addition. The Hamiltonian \hat{H} , Eq. (1), quantum phases are associated with different ranges of electronic density n_e and spin density m and are marked by important energy scales. Those correspond to limiting values of the charge energy scale $2\mu = 2\mu(n_e)$ and magnetic energy scale $2\mu_B h = 2\mu_B h(m)$ involving the chemical potential μ and magnetic field h , respectively.

The energy scales $2\mu = 2\mu(n_e)$ and $2\mu_B h = 2\mu_B h(m)$ are odd functions of the hole concentration $(1 - n_e)$ and spin density m , respectively. One may then consider for instance the ranges $n_e \in [0, 1[$ and $m \in [0, n_e]$. The interval $n_e \in]0, 1[$ refers for $m < n_e$ to a metallic quantum phase for which $2\mu = 2\mu(n_e)$ is a continuous function of n_e . It smoothly decreases from $2\mu = (U + 4t)$ for $n_e \rightarrow 0$ to $2\mu = 2\mu_u$ for $n_e \rightarrow 1$ where $2\mu_u < (U + 4t)$ is the Mott-Hubbard gap. On the other hand, at $n_e = 1$ the chemical potential varies in the range $\mu \in [-\mu_u, \mu_u]$ in spite of the electronic density remaining constant, which is a property of the corresponding $n_e = 1$ and $u > 0$ Mott-Hubbard insulator quantum phase.

The $n_e = 1$ Mott-Hubbard gap $2\mu_u$ is the energy scale associated with the phase transition between the two above mentioned quantum phases. For $u > 0$ it remains finite for all spin densities, $m \in [0, 1[$. For instance, in the limits $m \rightarrow 0$ [1, 2, 54] and $m \rightarrow 1$ it reads,

$$\begin{aligned} 2\mu_u &= U - 4t + 8t \int_0^\infty d\omega \frac{J_1(\omega)}{\omega(1 + e^{2\omega u})} = \frac{16t^2}{U} \int_1^\infty d\omega \frac{\sqrt{\omega^2 - 1}}{\sinh\left(\frac{2\pi t\omega}{U}\right)}, \quad m \rightarrow 0, \\ &= \sqrt{(4t)^2 + U^2} - 4t, \quad m \rightarrow 1, \end{aligned} \quad (5)$$

respectively. Its $u \ll 1$ limiting behaviors are $2\mu_u \approx (8/\pi) \sqrt{tU} e^{-2\pi(\frac{1}{t})}$ for $m \rightarrow 0$ and $2\mu_u \approx U^2/8t$ for $m \rightarrow 1$ and the $u \gg 1$ behavior is $2\mu_u \approx (U - 4t)$ for $m \in [0, 1[$.

On the other hand, for the metallic quantum phase corresponding to the spin density interval $m \in [0, n_e[$ for $n_e \in [0, 1[$ the magnetic energy scale $2\mu_B h$ is a continuous function of m . It smoothly increases from zero at $m = 0$ to $2\mu_B h_c$ for $m \rightarrow n_e$. Here h_c is the critical field for the fully polarized ferromagnetism quantum phase transition. Indeed, for $h > h_c$ there is no electron double occupancy, so that the on-site repulsive interaction term in the Hamiltonian, Eq. (1), has no effects and the system is driven into a non-interactive quantum phase.

The magnetic energy scale $2\mu_B h_c$ associated with such a quantum phase transition is an even function of the hole concentration $(1 - n_e)$. For the ranges $n_e \in [0, 1[$ and $m \in [0, n_e]$ it has the following closed-form expression in terms of $u = U/4t$ and the electronic density n_e [55],

$$\begin{aligned} 2\mu_B h_c &= 2t \left[\sqrt{1 + u^2} \left(1 - \frac{2}{\pi} \operatorname{arccot} \left(\frac{\sqrt{1 + u^2}}{u} \tan(\pi n_e) \right) \right) \right. \\ &\quad \left. - 2u n_e - \frac{2}{\pi} \cos(\pi n_e) \operatorname{arctan} \left(\frac{\sin(\pi n_e)}{u} \right) \right]. \end{aligned} \quad (6)$$

In the $n_e \rightarrow 0$ and $n_e \rightarrow 1$ limits this gives,

$$\begin{aligned} 2\mu_B h_c &= 0, \quad n_e \rightarrow 0, \\ &= \sqrt{(4t)^2 + U^2} - U, \quad n_e \rightarrow 1, \end{aligned} \quad (7)$$

respectively. For the density range $n_e \in [0, 1[$ it behaves as $2\mu_B h_c = 4t \sin^2(\pi n_e/2)$ for $u \rightarrow 0$ and as $2\mu_B h_c = (2t n_e/u)[1 - \sin(2\pi n_e)/(2\pi n_e)]$ for $u \gg 1$.

The definition of the σ one-electron LHB and UHB addition for the whole $u > 0$ range, electronic densities $n_e \in [0, 1[$, and spin densities $m \in [0, n_e]$ relies on the occupancy configurations of uniquely defined *rotated electrons*. This involves selecting out of the many choices of $u \rightarrow \infty$ degenerate 4^L energy eigenstates, those obtained from the $u > 0$ Bethe states and corresponding non-LWSs, Eq. (3), as $|l_r, l_{\eta_s}, \infty\rangle = \lim_{u \rightarrow \infty} |l_r, l_{\eta_s}, u\rangle$.

The important point is that for the $u \rightarrow \infty$ energy eigenstates $|l_r, l_{\eta_s}, \infty\rangle$, σ electron single occupancy, double occupancy, and non-occupancy are good quantum numbers. We call V tower the set of energy eigenstates $|l_r, l_{\eta_s}, u\rangle$ with exactly the same u -independent quantum numbers l_r and l_{η_s} and different u values in the range $u > 0$. σ electron single occupancy, electron double occupancy, and electron non-occupancy are not good quantum numbers for the finite- u energy eigenstates $|l_r, l_{\eta_s}, u\rangle$ belonging to the same V tower. For instance, upon decreasing u there emerges for ground states a finite electron double occupancy expectation value, which vanishes for $u \rightarrow \infty$ [56].

Since for any $u > 0$ value the set of energy eigenstates $|l_r, l_{\eta_s}, u\rangle$ that belong to the same V tower are generated by exactly the same occupancy configurations of the u -independent quantum numbers l_r and l_{η_s} given in Eq. (2) and below in Section IIB, respectively, the Hilbert space is the same for the whole $u > 0$ range. Hence for any $u > 0$ there is a uniquely defined unitary operator $\hat{V} = \hat{V}(u)$ such that $|l_r, l_{\eta_s}, u\rangle = \hat{V}^\dagger |l_r, l_{\eta_s}, \infty\rangle$. This operator \hat{V} is the σ electron - rotated-electron unitary operator such that,

$$\tilde{c}_{j,\sigma}^\dagger = \hat{V}^\dagger c_{j,\sigma}^\dagger \hat{V}; \quad \tilde{c}_{j,\sigma} = \hat{V}^\dagger c_{j,\sigma} \hat{V}; \quad \tilde{n}_{j,\sigma} = \tilde{c}_{j,\sigma}^\dagger \tilde{c}_{j,\sigma}, \quad j = 1, \dots, L, \quad \sigma = \uparrow, \downarrow, \quad (8)$$

are the operators that create and annihilate, respectively, the σ rotated electrons as defined here. Moreover, $|l_r, l_{\eta_s}, \infty\rangle = \hat{G}_{l_r, l_{\eta_s}}^\dagger |0\rangle$ where $|0\rangle$ is the electron and rotated-electron vacuum and $\hat{G}_{l_r, l_{\eta_s}}^\dagger$ a uniquely defined operator. It then follows that $|l_r, l_{\eta_s}, u\rangle = \tilde{G}_{l_r, l_{\eta_s}}^\dagger |0\rangle$ where the generator $\tilde{G}_{l_r, l_{\eta_s}}^\dagger = \hat{V}^\dagger \hat{G}_{l_r, l_{\eta_s}}^\dagger \hat{V}$ has the same expression in terms of the σ rotated-electron creation and annihilation operators as $\hat{G}_{l_r, l_{\eta_s}}^\dagger$ in terms of σ electron creation and annihilation operators, respectively. The σ electron - σ rotated-electron unitary operator \hat{V} in Eq. (8) is uniquely defined in Section IIB for $u > 0$ by its matrix elements between all 4^L energy and momentum eigenstates, Eq. (3).

That σ electron single occupancy, electron double occupancy, and electron non-occupancy are good quantum numbers for a $u \rightarrow \infty$ energy eigenstate $|l_r, l_{\eta_s}, \infty\rangle$ then implies that for all the finite- u energy eigenstates $|l_r, l_{\eta_s}, u\rangle$ belonging to the same V tower σ rotated-electron single occupancy, rotated-electron double occupancy, and rotated-electron non-occupancy are good quantum numbers for $u > 0$. For $u > 0$ this applies to all 4^L energy and momentum eigenstates.

Fortunately and as confirmed in Section IIB, the BA quantum numbers are directly related to the numbers of sites singly occupied, doubly occupied, and unoccupied by σ rotated electrons. From the use of that relation it is found that for electronic densities $n_e \in [0, 1[$ and spin densities $m \in [0, n_e]$ the model ground states have zero rotated-electron double occupancy. The σ one-electron LHB addition spectral function $B_{\sigma,+1}^{\text{LHB}}(k, \omega)$ and UHB addition spectral function $B_{\sigma,+1}^{\text{UHB}}(k, \omega)$ are then uniquely defined for $u > 0$ as follows,

$$\begin{aligned} B_{\sigma,+1}(k, \omega) &= B_{\sigma,+1}^{\text{LHB}}(k, \omega) + B_{\sigma,+1}^{\text{UHB}}(k, \omega), \\ B_{\sigma,+1}^{\text{LHB}}(k, \omega) &= \sum_{\nu_0^+} |\langle \nu_0^+ | c_{k,\sigma}^\dagger | GS \rangle|^2 \delta(\omega - (E_{\nu_0^+}^{N_\sigma+1} - E_{GS}^{N_\sigma})) \quad \omega \geq 0, \\ B_{\sigma,+1}^{\text{UHB}}(k, \omega) &= \sum_{\nu_D^+} |\langle \nu_D^+ | c_{k,\sigma}^\dagger | GS \rangle|^2 \delta(\omega - (E_{\nu_D^+}^{N_\sigma+1} - E_{GS}^{N_\sigma})) \quad \omega \geq 0, \end{aligned} \quad (9)$$

where the ν_0^+ and ν_D^+ summations run over the $N_\sigma + 1$ -electron excited energy eigenstates with zero and $D > 0$, respectively, rotated-electron double occupancy and $E_{\nu_0^+}^{N_\sigma+1}$ and $E_{\nu_D^+}^{N_\sigma+1}$ are the corresponding energies.

The σ one-electron spectral functions obey the following sum rules,

$$\begin{aligned} \sum_k \int_{-\infty}^{\infty} d\omega B_{\sigma,-1}(k, \omega) &= N_\sigma; & \sum_k \int_{-\infty}^{\infty} d\omega B_{\sigma,+1}(k, \omega) &= L - N_\sigma, \\ \sum_k \int_{-\infty}^{\infty} d\omega B_{\sigma,+1}^{\text{LHB}}(k, \omega) &= L - N; & \sum_k \int_{-\infty}^{\infty} d\omega B_{\sigma,+1}^{\text{UHB}}(k, \omega) &= N - N_\sigma. \end{aligned} \quad (10)$$

The first two sum rules are well known and exact for all u values. The $B_{\sigma,+1}^{\text{LHB}}(k, \omega)$ and $B_{\sigma,+1}^{\text{UHB}}(k, \omega)$ sum rules are found to be exact both in the limits $n_e \rightarrow 0$ and $n_e \rightarrow 1$ for $u > 0$. Both in the $u \ll 1$ and $u \gg 1$ limits they are exact as well for electronic densities $n_e \in [0, 1[$ and spin densities $m \in [0, n_e]$. They are likely exact also for intermediate u values yet we could not prove it. If otherwise, they are a very good approximation. Fortunately, clarification of this issue is not needed for our studies, as it focuses only on the line shapes in the vicinity of the singularities of the σ one-electron spectral functions and not on the detailed weight distribution over the whole (k, ω) plane. The line shape near the singularities is that observed in experiments on actual condensed matter systems and spin 1/2 ultra-cold atom systems. The important point for the present study is rather the definition of σ one-electron LHB and UHB for $u > 0$, $n_e \in [0, 1]$, and $m \in [0, n_e]$, Eq. (9), which follows from the corresponding unique definition of rotated electrons in Sec. IIB in terms of quantities of the exact BA solution.

The present definition for $u > 0$ and all densities of the concepts of a LHB and a UHB is directly associated with a global lattice $U(1)$ symmetry of the Hamiltonian \hat{H}_u , Eq. (1), beyond its well-known $SO(4) = [SU(2) \otimes SU(2)]/Z_2$ symmetry, which contains the η -spin and spin $SU(2)$ symmetries [57–59]. Such a global lattice $U(1)$ symmetry exists for the model on the 1D and any other bipartite lattice [60] and is behind its global symmetry being actually larger than $SO(4)$ and given by $[SO(4) \otimes U(1)]/Z_2 = [SU(2) \otimes SU(2) \otimes U(1)]/Z_2^2$, which is equivalent to $SO(3) \otimes SO(3) \otimes U(1)$. (The

factor $1/Z_2^2$ follows from the total number 4^L of independent representations of the group $[SU(2) \otimes SU(2) \otimes U(1)]/Z_2^2$ being four times smaller than the dimension 4^{L+1} of the group $SU(2) \otimes SU(2) \otimes U(1)$.

That the Hamiltonian \hat{H}_u , Eq. (1), global symmetry is $[SO(4) \otimes U(1)]/Z_2$ has direct effects on the 4^L energy and momentum eigenstates of the Hamiltonian \hat{H} in the presence of a chemical potential and magnetic field also given in Eq. (1), as these states refer to 4^L state representations of the group $[SO(4) \otimes U(1)]/Z_2$ in the model full Hilbert space. In the present 1D case the occurrence of the global lattice $U(1)$ symmetry justifies for instance that the spin and charge monodromy matrices of the BA inverse-scattering method have different ABCD and ABCDF forms associated with the spin $SU(2)$ and charge $U(2) = SU(2) \otimes U(1)$ symmetries, respectively. Consistently, the latter matrix is larger than the former and involves more fields [4]. If the model global symmetry was $SO(4) = [SU(2) \otimes SU(2)]/Z_2$, the charge and a spin monodromy matrices would have the same traditional ABCD form, which is that of the spin-1/2 XXX Heisenberg chain [61].

The relation of the global lattice $U(1)$ symmetry beyond $SO(4)$ to the LHB and UHB as defined here for $u > 0$ and all densities results from its generator being the operator that counts the number N_s^R of rotated-electron singly occupied sites or, alternatively, the number $N_\eta^R = L - N_s^R$ of rotated-electron unoccupied sites plus doubly occupied sites. Indeed, for the electronic density ranges (i) $n_e \in [0, 1]$ and (ii) $n_e \in [1, 2]$ the UHB exactly originates from transitions to energy eigenstates with a finite number of (i) rotated-electron doubly occupied sites and (ii) rotated-electron unoccupied sites, respectively.

B. Rotated-electron separation in terms of c pseudoparticles, rotated spins 1/2, and rotated η -spins 1/2

The charge-only and spin-only fractionalized particles that emerge in 1D correlated electronic systems are usually identified with holons and spinons, respectively [62]. Such holons and spinons are in 1D integrable correlated electronic models associated with specific quantum numbers of the exact solutions. The use of holon and spinon representations provides a suitable description of these models low-energy physics. Some of such quantum liquids exotic properties survive at higher energies yet the exponents characterizing the dynamical correlation functions singularities are functions of the momentum and differ significantly from the predictions of the linear Tomonaga-Luttinger liquid theory [38, 41–43]. This applies to the 1D Hubbard model.

Furthermore, a careful analysis of the high-energy dynamical correlation functions reveals that their spectral weights are controlled by the scattering of both spinless fractionalized particles and neutral composite objects whose constituents are spin-1/2 or η -spin 1/2 fractionalized particles. Both such spinless fractionalized particles and composite elementary objects refer to the pseudofermions of the PDT representation used in this paper to study the σ one-electron spectral functions, Eq. (4). Such pseudofermions are identical to the pseudoparticles of Ref. [37] except that their momentum values are slightly shifted by a well defined unitary transformation. The direct relation of the corresponding spinless c pseudoparticles and spin-1/2 or η -spin 1/2 fractionalized particles within the neutral composite pseudoparticles to the rotated electrons whose operators are given in Eq. (8) refers to the above mentioned needed link of the corresponding non-perturbative relation between the electrons and PDT pseudofermions.

For the 1D Hubbard model there is an infinite number of transformations that generate σ rotated electrons from the σ electrons such that σ rotated-electron single occupancy is a good quantum number for $u > 0$ [60]. The pseudoparticle representation and corresponding pseudofermion representation refer though to a specific choice of σ rotated electrons. Those are generated from the σ electrons by a unitary transformation uniquely defined by the BA. Actually, the BA solution performs such a transformation. The corresponding electron - rotated-electron unitary operator \hat{V} in Eq. (8) can be defined by its matrix elements between the model 4^L energy and momentum eigenstates. Fortunately, such matrix elements can be expressed in terms of the following known BA amplitudes of the Bethe states $|l_r, l_{\eta s}^0, u\rangle$ [34, 35],

$$f_{l_r, l_{\eta s}^0, u}(x_1 \sigma_1, \dots, x_{N^0} \sigma_{N^0}) = \langle x_1 \sigma_1, \dots, x_{N^0} \sigma_{N^0} | l_r, l_{\eta s}^0, u \rangle. \quad (11)$$

Such amplitudes are uniquely defined in Eqs. (2.5)-(2.10) of Ref. [34] in terms of BA solution quantities. In them, $|x_1 \sigma_1, \dots, x_{N^0} \sigma_{N^0}\rangle$ denotes a local state in which the $N^0 = L - 2S_\eta$ electrons with spin projection $\sigma_1, \dots, \sigma_{N^0}$ are located at sites of spatial coordinates x_1, \dots, x_{N^0} , respectively. For a LWS their numbers are $N_\uparrow^0 = L/2 - S_\eta + S_s$ and $N_\downarrow^0 = L/2 - S_\eta - S_s$. Due to symmetry, the amplitudes of the non-LWSs $|l_r, l_{\eta s}, u\rangle$ generated from each Bethe state as given in Eq. (3) differ from it by the trivial phase factor $(-1)^{n_\eta}$. Here $n_\eta = S_\eta + S_\eta^z$ is the non-LWS number given in Eq. (2).

For the set of Bethe states corresponding to different finite $u > 0$ values and belonging to the same V tower the amplitudes, Eq. (11), smoothly and continuously behave as a function of u . That the amplitudes $\langle n_\eta; n_s; x_1 \sigma_1, \dots, x_{N^0} \sigma_{N^0} | l_r, l_{\eta s}, u \rangle$ of a non-LWS involving the states $|n_\eta; n_s; x_1 \sigma_1, \dots, x_{N^0} \sigma_{N^0}\rangle$ are given in terms of those of the corresponding Bethe state merely by $(-1)^{n_\eta} \langle x_1 \sigma_1, \dots, x_{N^0} \sigma_{N^0} | l_r, l_{\eta s}^0, u \rangle$ and thus by

$(-1)^{n_\eta} f_{l_r, l_{\eta s}, u}(x_1 \sigma_1, \dots, x_{N^0} \sigma_{N^0})$ follows from except for the phase factor $(-1)^{n_\eta}$ the non-LWS amplitudes being insensitive to the n_η created electrons pairs and their spatial coordinates. These electrons pairs emerge as a result of the application onto the Bethe state of the η -spin off-diagonal generator \hat{S}_η^+ a number of times n_η , as given in Eq. (3). Moreover, such amplitudes are insensitive to the spatial coordinates of the n_s electrons whose spin has been flipped by the n_s spin off-diagonal generators $(\hat{S}_s^+)^{n_s}$, Eq. (3). Such insensitivities are behind denoting the local states $|x'_1 \sigma_{1'}, \dots, x'_{N^0+2n_\eta} \sigma_{(N^0+2n_\eta)'}\rangle$ in which the $N^0 + 2n_\eta$ electrons with spin projection $\sigma_{1'}, \dots, \sigma_{(N^0+2n_\eta)'}$ are located at sites of spatial coordinates $x'_1, \dots, x'_{N^0+2n_\eta}$ by $|n_\eta; n_s; x_1 \sigma_1, \dots, x_{N^0} \sigma_{N^0}\rangle$. They also imply that, as for the Bethe states, for the set of any energy eigenstates corresponding to different finite u values and belonging to the same V tower the general amplitudes $f_{l_r, l_{\eta s}, u}(x_1 \sigma_1, \dots, x_{N^0} \sigma_{N^0}) = \langle n_\eta; n_s; x_1 \sigma_1, \dots, x_{N^0} \sigma_{N^0} | l_r, l_{\eta s}, u \rangle$ smoothly and continuously behave as a function of u .

It then follows from basic quantum mechanics arguments that the electron - rotated-electron unitary operator \hat{V} in Eq. (8) is uniquely defined by the set of the following matrix elements between the energy eigenstates,

$$\langle l_r, l_{\eta s}, u | \hat{V} | l'_r, l'_{\eta s}, u \rangle = \delta_{l_{\eta s}, l'_{\eta s}} \sum_{x=1}^L \dots \sum_{x_{N^0}=1}^L f_{l_r, l_{\eta s}, u}^*(x_1 \sigma_1, \dots, x_{N^0} \sigma_{N^0}) f_{l'_r, l'_{\eta s}, \infty}(x_1 \sigma_1, \dots, x_{N^0} \sigma_{N^0}). \quad (12)$$

Here and throughout this paper $\delta_{l, l'}$ is the usual Kronecker symbol such that $\delta_{l, l'} = 1$ for $l = l' = 0, 1, 2, \dots$ and $\delta_{l, l'} = 0$ for $l \neq l'$ and $f_{l_r, l_{\eta s}, u}(x_1 \sigma_1, \dots, x_{N^0} \sigma_{N^0})$ and $f_{l'_r, l'_{\eta s}, \infty}(x_1 \sigma_1, \dots, x_{N^0} \sigma_{N^0})$ are the amplitudes defined by Eqs. (2.5)-(2.10) of Ref. [34] for $u > 0$ and Eq. (2.23) of Ref. [35] for $u \rightarrow \infty$, respectively. The factor $\delta_{l_{\eta s}, l'_{\eta s}}$ implies that the phase factors $(-1)^{n_\eta}$ always occur in pairs, which gives rise to an overall phase factor $(-1)^{2n_\eta} = 1$. Since the set of $4^L \times 4^L = 4^{2L}$ matrix elements of form, Eq. (12), are between all 4^L energy and momentum eigenstates that span the model full Hilbert space they uniquely define the electron - rotated-electron unitary operator \hat{V} .

That because of symmetries behind the factor $\delta_{l_{\eta s}, l'_{\eta s}}$ many of the matrix elements, Eq. (12), vanish simplifies the quantum problem under consideration. Indeed, the electron - rotated-electron unitary operator \hat{V} commutes with the three generators of both the global η -spin and spin $SU(2)$ symmetry algebras and the charge density operator. As a result, the σ rotated electrons have the same charge, spin 1/2, and η -spin 1/2 degrees of freedom as the σ electrons. Application of the operator \hat{V} onto the σ electron operators merely changes the σ electrons lattice spatial occupancy configurations. On the other hand, from analysis of the relation between (i) the BA quantum numbers and (ii) rotated-electron occupancy configurations, respectively, that generate the finite- u exact energy eigenstates $|l_r, l_{\eta s}, u\rangle = \hat{V}^\dagger |l_r, l_{\eta s}, \infty\rangle$ of any V tower one reaches important physical information.

First, the σ rotated-electron spatial occupancy configurations that generate the finite- u energy eigenstates $|l_r, l_{\eta s}, u\rangle = \hat{V}^\dagger |l_r, l_{\eta s}, \infty\rangle$ of any V tower are exactly the same as the σ electron spatial occupancy configurations of the tower $u \rightarrow \infty$ energy eigenstate $|l_r, l_{\eta s}, \infty\rangle$. Hence for $u > 0$ the number $N_{s, \pm 1/2}^R$ of spin-projection $\pm 1/2$ rotated-electron singly occupied sites, $N_{\eta, +1/2}^R$ of rotated-electron unoccupied sites, and $N_{\eta, -1/2}^R$ of rotated-electron doubly occupied sites are conserved. Such numbers obey the sum rules $N_{s, \pm 1/2}^R + N_{\eta, -1/2}^R = N_{\pm 1/2}$, $N_s^R + 2N_{\eta, -1/2}^R = N$, and $N_s^R + N_\eta^R = L$. The σ rotated-electron numbers values equal those of the σ electrons, so that here $N_{\pm 1/2}$ denotes the number of electrons and rotated electrons of spin projection $\pm 1/2$. On the other hand, for finite u values the numbers $N_s^R = N_{s, +1/2}^R + N_{s, -1/2}^R$ of rotated-electron singly occupied sites and $N_\eta^R = N_{\eta, +1/2}^R + N_{\eta, -1/2}^R$ of rotated-electron doubly occupied plus unoccupied sites are only conserved for rotated electrons.

Second, for $u > 0$ a non-perturbative three degrees of freedom lattice - η -spin - spin separation occurs at all energy scales. Here the lattice - η -spin degrees of freedom separation may be considered as a separation of the charge degrees of freedom. At energy scales lower than $2|\mu|$ one has that $D = N_{\eta, -1/2}^R = 0$ (and $N_{\eta, +1/2}^R = 0$) for $n_e \in [0, 1[$ (and $n_e \in]1, 2]$), so that the η -spin degrees of freedom are hidden and the three degrees of freedom non-perturbative lattice - η -spin - spin separation is seen as the usual two degrees of freedom charge - spin separation. Within the former general separation the (i) lattice global $U(1)$ symmetry, (ii) η -spin global $SU(2)$ symmetry, and (iii) spin global $SU(2)$ symmetry state representations are in each fixed number N_s^R of rotated-electron singly occupied sites subspace generated by the occupancy configurations of (i) $N_c = N_s^R$ spinless c pseudoparticles and corresponding $N_c^h = N_\eta^R$ c pseudoparticle holes whose c effective lattice is identical to the original lattice and thus has $N_s^R + N_\eta^R = L$ sites, (ii) $M_{s, \pm 1/2} = N_{s, \pm 1/2}^R$ spin-1/2 fractionalized particles of spin projection $\pm 1/2$ that we call *rotated spins* 1/2, and (iii) $M_{\eta, \pm 1/2} = N_{\eta, \pm 1/2}^R$ η -spin-1/2 fractionalized particles of η -spin projection $\pm 1/2$ that we call *rotated η -spins* 1/2, respectively. ($+1/2$ and $-1/2$ η -spin projections refer to η -spin degrees of freedom of rotated-electron unoccupied and

doubly occupied sites, respectively.) It then follows that these numbers are such that,

$$\begin{aligned}
M_s &= M_{s,+1/2} + M_{s,-1/2} = N_c, \\
M_\eta &= M_{\eta,+1/2} + M_{\eta,-1/2} = L - N_c = N_c^h, \\
M_{s,+1/2} - M_{s,-1/2} &= -2S_s^z = N_\uparrow - N_\downarrow, \\
M_{\eta,+1/2} - M_{\eta,-1/2} &= -2S_\eta^z = L - N,
\end{aligned} \tag{13}$$

where M_s denotes the number of rotated spins and M_η that of rotated η -spins, which equal those N_c of c pseudoparticles and $N_c^h = L - N_c$ of c pseudoparticle holes, respectively. Consistently with the N_c c pseudoparticles, $M_{\eta,\pm 1/2}$ rotated η -spins of η -spin projection $\pm 1/2$, and $M_{s,\pm 1/2}$ rotated spins of spin projection $\pm 1/2$ under consideration stemming from rotated-electron occupancy configurations degrees of freedom separation, their numbers are fully controlled by those of rotated electrons as follows,

$$\begin{aligned}
N_c &= N_R^s; & N_c^h &= N_R^\eta; & N_c + N_c^h &= N_R^s + N_R^\eta = L, \\
M_{\alpha,\pm 1/2} &= N_{R,\pm 1/2}^\alpha; & M_\alpha &= M_{\alpha,+1/2} + M_{\alpha,-1/2} = N_R^\alpha, & \alpha &= \eta, s.
\end{aligned} \tag{14}$$

Indeed the degrees of freedom of each rotated-electron occupied site decouple into one spinless c pseudoparticle that carries the rotated-electron charge and one rotated spin $1/2$ that carries its spin. On the other hand, the degrees of freedom of each rotated-electron unoccupied and doubly occupied site decouple into one c pseudoparticle hole and one rotated η -spin $1/2$ of projection $+1/2$ and $-1/2$, respectively. Hence the rotated-electron on-site separation refers to two degrees of freedom associated with the lattice global $U(1)$ symmetry and one of the two global $SU(2)$ symmetries, respectively. That the rotated-electron occupancy configurations give rise to the independent occupancy configurations of the c pseudoparticles, rotated spins $1/2$, and rotated η -spins $1/2$ is behind the exotic properties of the corresponding quantum liquid.

Third, from the further analysis of the relation between the BA quantum numbers and the three degrees of freedom separation of the rotated-electron occupancy configurations one finds that such quantum numbers are directly associated with the occupancy configurations of the three types of fractionalized particles that generate all 4^L energy eigenstates, Eq. (3). For the densities ranges $n_e \in [0, 1]$ and $m \in [0, n_e]$ one has that $N_{s,+1/2}^R \geq N_{s,-1/2}^R$ and $N_{\eta,+1/2}^R \geq N_{\eta,-1/2}^R$. For the corresponding exact Bethe states, there is a number $M_{s\text{ sp}} = N_{s,-1/2}^R$ of spin-singlet pairs ($\alpha = s$) and $M_{\eta\text{ sp}} = N_{\eta,-1/2}^R$ of η -spin-singlet pairs ($\alpha = \eta$) within which all $N_{s,-1/2}^R$ rotated spins of projection $-1/2$ are paired with an equal number of rotated spins of projection $+1/2$ and all $N_{\eta,-1/2}^R$ rotated η -spins of projection $-1/2$ are paired with an equal number of rotated η -spins of projection $+1/2$, respectively. Such $M_{\alpha\text{ sp}}$ spin-singlet ($\alpha = s$) and η -spin-singlet ($\alpha = \eta$) pairs are found to be contained in a set of composite αn pseudoparticles. Here $n = 1, \dots, \infty$ gives the number of pairs that refer to their internal structure. One denotes by $N_{\alpha n}$ the number of such αn pseudoparticles in each energy and momentum eigenstate. The sum rule $M_{\alpha\text{ sp}} = \sum_{n=1}^{\infty} n N_{\alpha n}$ is then obeyed.

The remaining $M_\alpha^{un} = N_{\alpha,+1/2}^R - N_{\alpha,-1/2}^R = 2S_\alpha$ unpaired rotated spins ($\alpha = s$) and rotated η -spins ($\alpha = \eta$) have for a Bethe state spin and η -spin projection $+1/2$. For general energy eigenstates the configurations of these $2S_s$ unpaired rotated spins and $2S_\eta$ unpaired rotated η -spins generate the spin and η -spin, respectively, towers of non-LWSs. Specifically, the $2S_s$ unpaired rotated spins and $2S_\eta$ unpaired rotated η -spins of the Bethe states are flipped upon the application of the corresponding $SU(2)$ algebras off-diagonal generators, as given in Eq. (3). Application of such generators leaves the spin ($\alpha = s$) and η -spin ($\alpha = \eta$) singlet configurations of the $M_{\alpha\text{ sp}} = \sum_{n=1}^{\infty} n N_{\alpha n}$ pairs contained in αn pseudoparticles unchanged. Hence for general $u > 0$ energy eigenstates one finds that the number $M_{s,\pm 1/2}^{un}$ of unpaired rotated spins of projection $\pm 1/2$ and $M_{\eta,\pm 1/2}^{un}$ of unpaired rotated η -spins of projection $\pm 1/2$ are good quantum numbers, which read,

$$M_{\alpha,\pm 1/2}^{un} = (S_\alpha \mp S_\alpha^z); \quad M_\alpha^{un} = M_{\alpha,-1/2}^{un} + M_{\alpha,+1/2}^{un} = 2S_\alpha, \quad \alpha = \eta, s. \tag{15}$$

For the $\alpha = \eta, s$ LWSs one has that $M_{\alpha,+1/2}^{un} = M_\alpha^{un} = 2S_\alpha$ and $M_{\alpha,-1/2}^{un} = 0$ for both $\alpha = \eta, s$. The set of $M_{\eta\text{ sp}}$ η -spin-singlet pairs and $M_{s\text{ sp}}$ spin-singlet pairs of an energy eigenstate contains an equal number of rotated η -spins and rotated spins, respectively, of opposite projection. Hence the total numbers $M_{\eta,\pm 1/2}$ of rotated η -spins of projection $\pm 1/2$ and $M_{s,\pm 1/2}$ of rotated spins of projection $\pm 1/2$ read,

$$M_{\alpha,\pm 1/2} = M_{\alpha\text{ sp}} + M_{\alpha,\pm 1/2}^{un}, \quad \alpha = \eta, s. \tag{16}$$

Moreover, by combining the above equations one finds that the set of numbers $\{N_{\alpha n}\}$ of composite αn pseudoparticles of any $u > 0$ energy eigenstate obey the following exact sum rules concerning the number of $M_{\alpha\text{ sp}}$ of spin ($\alpha = s$)

and η -spin ($\alpha = \eta$) singlet pairs of any $u > 0$ energy eigenstate,

$$\begin{aligned} M_{\alpha \text{ sp}} &= \sum_{n=1}^{\infty} n N_{\alpha n} = \frac{1}{2}(L_{\alpha} - 2S_{\alpha}), \quad \alpha = s, \eta, \\ M_{\text{sp}}^{SU(2)} &\equiv \sum_{\alpha=\eta, s} \sum_{n=1}^{\infty} n N_{\alpha n} = \frac{1}{2}(L - 2S_s - 2S_{\eta}), \end{aligned} \quad (17)$$

where $M_{\text{sp}}^{SU(2)}$ denotes the total number of both rotated spins and rotated η -spins pairs.

The BA solution contains different types of quantum numbers whose occupancy configurations are within the pseudoparticle representation described by corresponding occupancy configurations of spinless c pseudoparticles with no internal structure and composite αn pseudoparticles. Complete information on the microscopic details of the latter pseudoparticles internal η -spin ($\alpha = \eta$) and spin ($\alpha = s$) n -pair configurations is encoded within the BA solution and is not needed for the goals and studies of this paper. Indeed, within the present TL the problem concerning a αn pseudoparticle internal degrees of freedom and that associated with its translational degrees of freedom center of mass motion separate. Here we merely provide some general information on the internal degrees of freedom issue, which as further discussed below involves the imaginary part of the BA complex rapidities [5],

$$\Lambda^{\alpha n, l}(q_j) = \Lambda^{\alpha n}(q_j) + i(n+1-2l)u, \quad l = 1, \dots, n, \quad (18)$$

where $\alpha = \eta, s$ and $n = 1, \dots, \infty$. The corresponding number $L_{\alpha n}$ of the set $j = 1, \dots, L_{\alpha n}$ of the αn branch BA quantum numbers $\{q_j\}$ and that L_c of the related set $j = 1, \dots, L_c$ of the c branch BA quantum numbers $\{q_j\}$ are given by,

$$\begin{aligned} L_{\alpha n} &= N_{\alpha n} + N_{\alpha n}^h; \quad N_{\alpha n}^h = 2S_{\alpha} + \sum_{n'=n+1}^{\infty} 2(n'-n)N_{\alpha n'}, \quad \alpha = \eta, s, \quad n = 1, \dots, \infty, \\ L_c &= N_c + N_c^h = N_s^R + N_{\eta}^R = L, \end{aligned} \quad (19)$$

respectively. The real part $\Lambda^{\alpha n}(q_j)$ of the complex rapidities, Eq. (18), is a function of the $j = 1, \dots, L_{\alpha n}$ quantum numbers q_j that has the same value for the whole set $l = 1, \dots, n$ of αn rapidities. It is the rapidity function which for each $u > 0$ energy eigenstate is the solution of the BA equations introduced in Ref. [5] for the TL. Within the pseudoparticle momentum distribution functional notation [37], these equations have the form given in Eqs. (A1) and (A2) of Appendix A where the sets of $j = 1, \dots, L_c$ and $j = 1, \dots, L_{\alpha n}$ of quantum numbers q_j , respectively, read,

$$q_j = \frac{2\pi}{L} I_j^{\beta}, \quad j = 1, \dots, L_{\beta}, \quad \beta = c, \eta n, s n, \quad n = 1, \dots, \infty. \quad (20)$$

These play the role of $\beta = c, \alpha n$ band microscopic momentum values of the $\beta = c, \alpha n$ pseudoparticle branches. For a given energy and momentum eigenstate, the $j = 1, \dots, L_{\beta}$ quantum numbers I_j^{β} on the right-hand side of Eq. (20) are either integers or half-odd integers according to the following boundary conditions [5],

$$\begin{aligned} I_j^{\beta} &= 0, \pm 1, \pm 2, \dots \quad \text{for } I_{\beta} \text{ even}, \\ &= \pm 1/2, \pm 3/2, \pm 5/2, \dots \quad \text{for } I_{\beta} \text{ odd}. \end{aligned} \quad (21)$$

Here the numbers I_{β} are given by,

$$\begin{aligned} I_c &= N_{\text{ps}}^{SU(2)} \equiv \sum_{\alpha=\eta, s} \sum_{n=1}^{\infty} N_{\alpha n}, \\ I_{\alpha n} &= L_{\alpha n} - 1, \quad \alpha = \eta, s, \quad n = 1, \dots, \infty. \end{aligned} \quad (22)$$

From analysis of the BA quantum numbers, one finds that the set of numbers $\{N_{\alpha n}\}$ of composite αn pseudoparticles obey a second exact sum rule in addition to the spin ($\alpha = s$) and η -spin ($\alpha = \eta$) singlet pairs sum rule given in Eq. (17). It is associated with the value of the total number $N_{\alpha \text{ ps}} = \sum_{n=1}^{\infty} N_{\alpha n}$ of composite αn pseudoparticles of all

$n = 1, \dots, \infty$ branches of a $u > 0$ energy eigenstate and reads,

$$\begin{aligned} N_{s\text{ps}} &= \sum_{n=1}^{\infty} N_{sn} = \frac{1}{2}(N_c - N_{s1}^h), \\ N_{\eta\text{ps}} &= \sum_{n=1}^{\infty} N_{\eta n} = \frac{1}{2}(N_c^h - N_{\eta 1}^h), \\ N_{\text{ps}}^{SU(2)} &= \sum_{\alpha=\eta,s} \sum_{n=1}^{\infty} N_{\alpha n} = \frac{1}{2}(L - N_{s1}^h - N_{\eta 1}^h). \end{aligned} \quad (23)$$

Here $N_{\text{ps}}^{SU(2)}$ is the number of both $\alpha = \eta$ and $\alpha = s$ composite αn pseudoparticles of all $n = 1, \dots, \infty$ branches also appearing in Eq. (22) and $N_{\alpha 1}^h$ is that of $\alpha 1$ -band holes, Eq. (19) for $\alpha = \eta, s$ and $n = 1$. The interesting point is that for given fixed N_c and thus $N_c^h = L - N_c$ values that of $N_{\alpha\text{ps}}$ is fully determined by the corresponding value of the number $N_{\alpha 1}^h$ of $\alpha 1$ -band holes.

The $\beta = c, \alpha n$ band successive set $j = 1, \dots, L_\beta$ of momentum values q_j , Eq. (20), have only β pseudoparticle occupancies zero and one and the usual separation, $q_{j+1} - q_j = 2\pi/L$. That they play the role of $\beta = c, \alpha n$ band momentum values is consistent with within our functional representation the momentum eigenvalues of all $u > 0$ energy and momentum eigenstates reading,

$$P = \sum_{j=1}^L q_j N_c(q_j) + \sum_{n=1}^{\infty} \sum_{j=1}^{L_{sn}} q_j N_{sn}(q_j) + \sum_{n=1}^{\infty} \sum_{j=1}^{L_{\eta n}} (\pi - q_j) N_{\eta n}(q_j) + \pi M_{\eta, -1/2}, \quad (24)$$

being thus additive in q_j . Within that representation, the β -band momentum distribution functions $N_\beta(q_j)$ in Eq. (24) and BA equations, Eqs. (A1) and (A2) of Appendix A, read $N_\beta(q_j) = 1$ and $N_\beta(q_j) = 0$ for occupied and unoccupied discrete momentum values, respectively. The momentum contribution $\pi M_{\eta, -1/2}$, which from the use of Eq. (16) can be written as $\pi(M_{\eta\text{sp}} + M_{\eta, -1/2}^{un})$, follows from both the paired and unpaired rotated spins 1/2 and rotated η -spins 1/2 of projection $\pm 1/2$ having a momentum given by,

$$q_{s, \pm 1/2} = q_{\eta, +1/2} = 0; \quad q_{\eta, -1/2} = \pi. \quad (25)$$

On the other hand, the ηn pseudoparticle contribution $(\pi - q_j)$ to the momentum eigenvalue, Eq. (24), refers to its translational degrees of freedom. It is associated with the center of mass motion of that composite n -pair object as a whole. That such a contribution to the momentum eigenvalue reads $(\pi - q_j)$ rather than q_j , as for the c and sn pseudoparticles, follows from the $2n$ -rotated- η -spin configuration of a composite ηn pseudoparticle having an anti-bounding character, as confirmed below in Section II E.

The c band is populated by $N_c = N_s^R$ c pseudoparticles. They occupy N_c discrete momentum values out of the c band $j = 1, \dots, L_c$ such momentum values, where $L_c = L$. Hence the number of c pseudoparticle holes indeed reads $N_c^h = N_\eta^R = L - N_s^R$. On the other hand, the number $L_{\alpha n}$ in Eq. (19) refers to that of αn band $j = 1, \dots, L_{\alpha n}$ momentum values q_j in Eq. (20). For an energy and momentum eigenstate each such bands is populated by a well defined number $N_{\alpha n}$ of αn pseudoparticles, so that the corresponding number $N_{\alpha n}^h$ of αn pseudoparticle holes is that given in Eq. (19).

The set $j = 1, \dots, L_\beta$ of $\beta = c, \alpha n$ bands discrete momentum values q_j whose different occupancy configurations generate the energy and momentum eigenstates and determine the corresponding momentum eigenvalues, Eq. (24), belong to well-defined domains, $q_j \in [q_\beta^-, q_\beta^+]$, where,

$$\begin{aligned} q_c^\pm &= \pm \frac{\pi}{L}(L-1) \approx \pm \pi \text{ for } N_{\text{ps}}^{SU(2)} \text{ odd}; \quad q_c^\pm = \pm \frac{\pi}{L}(L-1 \pm 1) \approx \pm \pi \text{ for } N_{\text{ps}}^{SU(2)} \text{ even}, \\ q_{\alpha n}^\pm &= \pm \frac{\pi}{L}(L_{\alpha n} - 1). \end{aligned} \quad (26)$$

The label l_r in the energy eigenstates $\{|l_r, l_{\eta s}, u\rangle\}$, Eq. (3), can now be defined. It corresponds to a short notation for the following set of BA quantum numbers,

$$l_r = \{I_j^\beta\} \text{ such that } N_\beta(q_j) = 1 \text{ where } q_j = \frac{2\pi}{L} I_j^\beta \text{ for } j = 1, \dots, L_\beta, \beta = c, \eta n, sn, n = 1, \dots, \infty, \quad (27)$$

Ground states are neither populated by composite sn pseudoparticles with $n > 1$ spin-singlet pairs nor by composite ηn pseudoparticles with any number $n = 1, \dots, \infty$ of η -spin-singlet pairs. For electronic densities $n_e \in [0, 1]$ and spin

densities $m \in [0, n_e]$, ground states have no unpaired rotated spins of projection $-1/2$ and no unpaired rotated η -spins of projection $-1/2$. For them the number $M_s^{un} = N_s^R = 2S_s$ of unpaired rotated spins of projection $+1/2$ and the number $M_\eta^{un} = N_\eta^R = 2S_\eta$ of unpaired rotated η -spins of projection $+1/2$ equal those $N_{s1}^h = N_s^R = 2S_s$ of $s1$ pseudoparticle holes and $N_c^h = N_\eta^R = 2S_\eta$ of c pseudoparticle holes, respectively. Indeed, within the pseudoparticle representation the unpaired rotated spins and unpaired rotated η -spins play the role of empty sites of the c effective lattice and squeezed $s1$ effective lattice, respectively, considered in Section II C. Hence they are implicitly accounted for by the pseudoparticle representation.

The ground-state β band pseudoparticle momentum distribution functions are given by,

$$N_c^0(q_j) = \theta(q_j - q_{Fc}^-) \theta(q_{Fc}^+ - q_j); \quad N_{s1}^0(q_j) = \theta(q_j - q_{Fs1}^-) \theta(q_{Fs1}^+ - q_j); \quad N_{\alpha n}^0(q_j) = 0, \quad \alpha n \neq s1, \quad (28)$$

where the distribution $\theta(x)$ reads $\theta(x) = 1$ for $x > 0$ and $\theta(x) = 0$ for $x \leq 0$. For the c and $s1$ bands the momentum distribution functions, Eq. (28), refer to compact and symmetrical occupancy configurations. The corresponding $\beta = c, s1$ Fermi points are associated with the Fermi momentum values $q_{F\beta}^\pm$ in Eq. (28). Accounting for $\mathcal{O}(1/L)$ corrections, they are given in Eqs. (C.4)-(C.11) of Ref. [37]. If within the TL we ignore such corrections, one finds that $N_\beta^0(q_j) = \theta(q_{F\beta} - |q_j|)$ for $\beta = c, s1$ where the Fermi momentum values are given by,

$$q_{Fc} = 2k_F = \pi n_e; \quad q_{Fs1} = k_{F\downarrow} = \pi n_{e\downarrow}. \quad (29)$$

The c pseudoparticles have no internal structure. On the other hand, the imaginary part $i(n+1-2l)u$ of the set of $l = 1, \dots, n$ complex rapidities, Eq. (18), with the same real part $\Lambda^{\alpha n}(q_j)$ refers to the internal degrees of freedom of one composite αn pseudoparticle with $n > 1$ pairs whose center of mass carries αn band momentum q_j . Specifically, for $\alpha = s$ the imaginary part of such $l = 1, \dots, n$ rapidities is associated with a corresponding set $l = 1, \dots, n$ of spin-singlet pairs of rotated spins $1/2$ and the binding of these pairs within the composite sn pseudoparticle. For $\alpha = \eta$ it is rather associated with a set $l = 1, \dots, n$ of η -spin-singlet pairs of rotated η -spins $1/2$ and the anti-binding of these pairs within the composite ηn pseudoparticle. Each such $l = 1, \dots, n$ rapidities thus refers to one of the $l = 1, \dots, n$ singlet pairs bound and anti-bound within the composite sn and ηn pseudoparticle, respectively. For $n = 1$ the rapidity imaginary part vanishes. Indeed, the $\alpha 1$ pseudoparticle internal degrees of freedom refer to a single singlet pair of rotated spins $1/2$ ($\alpha = s$) or rotated η -spins $1/2$ ($\alpha = \eta$).

Below in Section II E the form of the composite sn and ηn pseudoparticle energy dispersions is used to extract valuable information on the bounding and anti-bounding character of their $2n = 2, 4, \dots$ paired rotated spins and paired rotated η -spins configuration, respectively.

C. The c pseudoparticle, rotated spin, and rotated η -spin operators in terms of σ rotated-electron operators

That the c pseudoparticles, rotated spins $1/2$, and rotated η -spins $1/2$ naturally emerge from the σ rotated-electron onsite occupancy configurations separation allows the introduction of local operators for these fractionalized particles in terms of the local rotated-electron creation and annihilation operators, Eq. (8).

The simplest case refers to the $l = z, \pm$ local operators associated with the rotated spins $1/2$ ($\alpha = s$) and rotated η -spins $1/2$ ($\alpha = \eta$), which read,

$$\begin{aligned} \tilde{S}_{j,\alpha}^l &= \hat{V}^\dagger \hat{S}_{j,\alpha}^l \hat{V}, \quad l = z, \pm, \quad \alpha = \eta, s, \\ \tilde{S}_{j,\alpha}^\pm &= \tilde{S}_{j,\alpha}^x \pm i \tilde{S}_{j,\alpha}^y, \quad \alpha = \eta, s, \end{aligned} \quad (30)$$

where $\hat{S}_{j,\alpha}^l$ are the usual unrotated $l = z, \pm$ local spin ($\alpha = s$) and η -spin ($\alpha = \eta$) operators. The $l = z, \pm$ local operators $\tilde{S}_{j,\alpha}^l$, Eq. (30), have in terms of creation and annihilation σ rotated-electron operators, Eq. (8), exactly the same expressions as the corresponding unrotated $l = z, \pm$ local operators $\hat{S}_{j,\alpha}^l$ in terms of creation and annihilation σ electron operators.

Specifically, the spin operators $\tilde{S}_{j,s}^l$, which act onto sites singly occupied by σ rotated electrons, read $\tilde{S}_{j,s}^- = (\tilde{S}_{j,s}^+)^{\dagger} = \tilde{c}_{j,\uparrow}^{\dagger} \tilde{c}_{j,\downarrow}$ and $\tilde{S}_{j,s}^z = (\tilde{n}_{j,\downarrow} - 1/2)$. Similarly, the η -spin operators $\tilde{S}_{j,\eta}^l$, which act onto sites unoccupied by rotated electrons and sites doubly occupied by rotated electrons, are given by $\tilde{S}_{j,\eta}^- = (\tilde{S}_{j,\eta}^+)^{\dagger} = (-1)^j \tilde{c}_{j,\uparrow} \tilde{c}_{j,\downarrow}$ and $\tilde{S}_{j,\eta}^z = (\tilde{n}_{j,\downarrow} - 1/2)$.

Below the c pseudoparticle creation operator $f_{j,c}^{\dagger}$ and annihilation operator $f_{j,c}$ on the lattice site $j = 1, \dots, L$ are uniquely defined in terms of the local rotated-electron creation and annihilation operators, Eq. (8). (The c effective lattice considered below is identical to the original lattice.) The c pseudoparticles have inherently emerged from the σ rotated electrons to the sites singly occupied by the latter being occupied by c pseudoparticles and those unoccupied and doubly occupied by rotated electrons being unoccupied by c pseudoparticles. Hence the c pseudoparticle local

density operator $\tilde{n}_{j,c} \equiv f_{j,c}^\dagger f_{j,c}$ and the corresponding operator $(1 - \tilde{n}_{j,c})$ are the natural projectors onto the subset of $N_R^s = N_c$ original-lattice sites singly occupied by rotated electrons and onto the subset of $N_R^\eta = N_c^h = L - N_c$ original-lattice sites unoccupied and doubly occupied by rotated electrons, respectively. It then follows that the $\alpha = s, \eta$ and $l = z, \pm$ local operators $\tilde{S}_{j,\alpha}^l$, Eq. (30), can be written as,

$$\tilde{S}_{j,s}^l = \tilde{n}_{j,c} \tilde{q}_j^l; \quad \tilde{S}_{j,\eta}^l = (1 - \tilde{n}_{j,c}) \tilde{q}_j^l, \quad l = z, \pm, \quad (31)$$

respectively, where the $l = z, \pm$ local ηs quasi-spin operators,

$$\tilde{q}_j^l = \tilde{S}_{j,s}^l + \tilde{S}_{j,\eta}^l, \quad l = \pm, z, \quad (32)$$

such that $\tilde{q}_j^\pm = \tilde{q}_j^x \pm i \tilde{q}_j^y$, have the following expression in terms of σ rotated-electron creation and annihilation operators,

$$\tilde{q}_j^- = (\tilde{q}_j^+)^\dagger = (\tilde{c}_{j,\uparrow}^\dagger + (-1)^j \tilde{c}_{j,\uparrow}) \tilde{c}_{j,\downarrow}; \quad \tilde{q}_j^z = (\tilde{n}_{j,\downarrow} - 1/2). \quad (33)$$

The $N_c c$ pseudoparticles live on the $N_R^s = N_c$ sites singly occupied by the rotated electrons, so that their occupancy configurations refer to the lattice degrees of freedom associated with the relative positions of the $M_s = N_R^s = N_c$ sites occupied by rotated spins 1/2 and $M_\eta = N_R^\eta = N_c^h = L - N_c$ sites occupied by rotated η -spins 1/2. The corresponding three degrees of freedom separation of the σ rotated-electron occupancy configurations then implies that their operators, Eq. (8), can be written as,

$$\begin{aligned} \tilde{c}_{j,\uparrow}^\dagger &= \left(\frac{1}{2} - \tilde{S}_{j,s}^z - \tilde{S}_{j,\eta}^z \right) f_{j,c}^\dagger + (-1)^j \left(\frac{1}{2} + \tilde{S}_{j,s}^z + \tilde{S}_{j,\eta}^z \right) f_{j,c}; & \tilde{c}_{j,\uparrow} &= (\tilde{c}_{j,\uparrow}^\dagger)^\dagger, \\ \tilde{c}_{j,\downarrow}^\dagger &= (\tilde{S}_{j,s}^+ + \tilde{S}_{j,\eta}^+)(f_{j,c}^\dagger + (-1)^j f_{j,c}), & \tilde{c}_{j,\downarrow} &= (\tilde{c}_{j,\downarrow}^\dagger)^\dagger. \end{aligned} \quad (34)$$

The local c pseudoparticle operators $f_{j,c}^\dagger$ and $f_{j,c}$ appearing here are then *uniquely* defined for $u > 0$ in terms of σ rotated-electron creation and annihilation operators, Eq. (8), by combining the inversion of the relations, Eq. (34), with the expressions of the $l = z, \pm$ local operators $\tilde{S}_{j,\alpha}^l$ associated with the rotated spins 1/2 ($\alpha = s$) and rotated η -spins 1/2 ($\alpha = \eta$), Eq. (30), provided in Eqs. (31)-(33), which gives,

$$f_{j,c}^\dagger = (f_{j,c})^\dagger = \tilde{c}_{j,\uparrow}^\dagger (1 - \tilde{n}_{j,\downarrow}) + (-1)^j \tilde{c}_{j,\uparrow} \tilde{n}_{j,\downarrow}; \quad \tilde{n}_{j,c} = f_{j,c}^\dagger f_{j,c}, \quad j = 1, \dots, L, \quad (35)$$

where $\tilde{n}_{j,\sigma}$ is the σ rotated-electron local density operator given in Eq. (8).

The unitarity of the electron - rotated-electron transformation implies that the rotated-electron operators $\tilde{c}_{j,\sigma}^\dagger$ and $\tilde{c}_{j,\sigma}$, Eqs. (8) and (34), have the same anticommutation relations as the corresponding electron operators $c_{j,\sigma}^\dagger$ and $c_{j,\sigma}$, respectively. Straightforward manipulations based on Eqs. (30)-(35) then lead to the following algebra for the local c pseudoparticle creation and annihilation operators,

$$\{f_{j,c}^\dagger, f_{j',c}\} = \delta_{j,j'}; \quad \{f_{j,c}^\dagger, f_{j',c}^\dagger\} = \{f_{j,c}, f_{j',c}\} = 0. \quad (36)$$

Furthermore, the local c pseudoparticle operators and the $l = z, \pm$ local rotated quasi-spin operators \tilde{q}_j^l , Eq. (33), commute with each other and the latter $l = z, \pm$ operators and corresponding rotated η -spin ($\alpha = \eta$) and rotated spin ($\alpha = s$) operators $\tilde{S}_{j,\alpha}^l$, Eqs. (30) and (31), obey the usual $SU(2)$ operator algebra.

The c pseudoparticle and ηs quasi-spin operator algebras refer to the whole Hilbert space. On the other hand, those of the rotated η -spin and rotated spin operators correspond to well-defined subspaces spanned by energy eigenstates whose value of the number $N_s^R = N_c$ of rotated-electron singly occupied sites and thus of c pseudoparticles is fixed. This ensures that the value of the corresponding rotated η -spin number $M_\eta = N_\eta^R = L - N_c$ and rotated spin number $M_s = N_s^R = N_c$ is fixed as well.

The degrees of freedom separation, Eq. (34), is such that the c pseudoparticle operators, Eq. (35), rotated-spin 1/2 and rotated- η -spin 1/2 operators, Eq. (31), and the related ηs quasi-spin operators, Eqs. (32) and (33), emerge from the σ rotated-electron operators by an exact local transformation that *does not* introduce constraints.

That as given in Eq. (28) ground states are neither populated by composite ηn pseudoparticles nor by composite sn pseudoparticles with $n > 1$ spin-singlet pairs plays an important role in the PDT. The $s1$ pseudoparticle translational degrees of freedom are associated with its center of mass motion and corresponding $s1$ band momentum q_j . The PDT involves $s1$ pseudoparticle creation and annihilation operators associated with such translational degrees of freedom.

As mentioned above, for $u > 0$ the c pseudoparticles live on a c effective lattice identical to the original lattice that has $j = 1, \dots, L$ sites and length L . On the other hand, the $s1$ pseudoparticles live in the TL on a squeezed $s1$ effective

lattice [33, 36, 63] whose $j = 1, \dots, L_{s1}$ sites number L_{s1} equals that of $s1$ band discrete momentum values, Eq. (19) for $\alpha n = s1$. The $s1$ effective lattice has length L . Its spacing is in general larger than a and given by,

$$a_{s1} = \frac{N_a}{L_{s1}} a, \quad (37)$$

which ensures that indeed $L = L_{s1} a_{s1}$. (Except in Eq. (37), in this paper we use units of lattice spacing a one, so that the lattice length L equals the number of lattice sites N_a .)

As for the local creation and annihilation c pseudoparticle operators, Eq. (36), the $s1$ pseudoparticle translational degrees of freedom center of mass motion are described by operators $f_{j,s1}^\dagger$ (and $f_{j,s1}$) that create (and annihilate) one $s1$ pseudoparticle at the $s1$ effective lattice site $x_j = a_{s1} j$ where $j = 1, \dots, L_{s1}$. Such local $s1$ pseudoparticle creation and annihilation operators obey a fermionic algebra, consistently with the $\beta = c, s1$ band momentum value q_j having only occupancies zero and one.

The $s1$ pseudoparticle operator representation is valid for the 1D Hubbard model in subspaces spanned by energy eigenstates with fixed L_{s1} value, Eq. (19) for $\alpha n = s1$. That in such subspaces the local $s1$ pseudoparticle operators obey a fermionic algebra, can be confirmed in terms of their statistical interactions [64]. This is a problem that we address here very briefly. The local $s1$ pseudoparticle creation and annihilation operators may be written as,

$$f_{j,s1}^\dagger = e^{i\phi_{j,s1}} g_{j,s1}^\dagger; \quad f_{j,s1} = (f_{j,s1}^\dagger)^\dagger, \quad j = 1, \dots, L_{s1}, \quad (38)$$

where $\phi_{j,s1} = \sum_{j' \neq j} f_{j',s1}^\dagger$ and the operator $g_{j,s1}^\dagger$ obeys a hard-core bosonic algebra. This algebra is justified by the corresponding statistical interaction vanishing for the model in subspaces spanned by energy eigenstates with fixed L_{s1} value, Eq. (19) for $\alpha n = s1$. The $s1$ effective lattice has been constructed inherently to that algebra being of hard-core type for the operators $g_{j,s1}^\dagger$ and $g_{j,s1}$. Therefore, through a Jordan-Wigner transformation, $f_{j,s1}^\dagger = e^{i\phi_{j,s1}} g_{j,s1}^\dagger$ [65], the operators $f_{j,s1}^\dagger$ and $f_{j,s1} = (f_{j,s1}^\dagger)^\dagger$ in Eq. (38) obey indeed a fermionic algebra,

$$\{f_{j,s1}^\dagger, f_{j',s1}\} = \delta_{j,j'}; \quad \{f_{j,s1}^\dagger, f_{j',s1}^\dagger\} = \{f_{j,s1}, f_{j',s1}\} = 0. \quad (39)$$

Each of the N_{s1} occupied $s1$ effective lattice sites corresponds to a spin-singlet pair that involves two original lattice sites occupied by rotated spins 1/2 of opposite spin projection. For the densities $n_e \in [0, 1[$ and $m \in [0, n_e]$ the line shape in the vicinity of the singular features of the σ one-electron spectral functions, Eq. (4), studied in Sections III and IV involves ground state transitions to excited energy eigenstates for which $N_{sn} = 0$ for $n > 1$. For both the ground states and such excited states the number of N_{s1}^h unoccupied $s1$ effective lattice sites, Eq. (19) for $\alpha n = s1$, reads $N_{s1}^h = 2S_s$. Indeed for such states the $s1$ effective lattice unoccupied sites refer to the $M_s^{un} = M_{s,+1/2}^{un} = 2S_s$ sites occupied in the original lattice by the unpaired rotated spins 1/2. Such unpaired rotated spins 1/2 are used within the $s1$ pseudoparticle motion as unoccupied sites with which they interchange position. Hence they are implicitly accounted for by the pseudoparticle representation.

The $\beta = c, s1$ pseudoparticle operators labelled by the $\beta = c, s1$ band momentum values defined in Eqs. (20) and (21), which are the quantum numbers of the exact BA solution whose occupancy configurations generate the energy eigenstates considered in the studies of this paper, play a key role in these studies and read,

$$f_{q_j,\beta}^\dagger = \frac{1}{\sqrt{L}} \sum_{j'=1}^{L_\beta} e^{i q_j x_{j'}} f_{j',\beta}^\dagger; \quad f_{q_j,\beta} = (f_{q_j,\beta}^\dagger)^\dagger, \quad j = 1, \dots, L_\beta, \quad \beta = c, s1. \quad (40)$$

Besides acting within subspaces spanned by energy eigenstates with fixed L_{s1} values, the $s1$ pseudofermion operators labelled by momentum q_j also appear in the expressions of the shake-up effects generators that transform such subspaces quantum number values into each other.

The (k, ω) -plane line shapes near the singular features of the σ one-electron LHB and UHB addition spectral functions, Eq. (9), studied in Sections III and IV for $u > 0$ and densities $n_e \in [0, 1[$ and $m \in [0, n_e]$ are determined by transitions to excited energy and momentum eigenstates with $N_{\eta 1} = 0$ and $N_{\eta 1} = 1$, respectively. Such states are not populated by composite αn pseudoparticles with $n > 1$ pairs and have no unpaired rotated spins of projection $-1/2$ and no unpaired rotated η -spins of projection $-1/2$.

Hence and as further discussed in Section III, only the c and $s1$ pseudofermion operator representation generated from the $\beta = c, s1$ pseudoparticle operators, Eq. (40), is needed to study such (k, ω) -plane line shapes. The unpaired rotated spins of projection $+1/2$ and unpaired rotated η -spins of projection $+1/2$ are accounted for within both the pseudoparticle and pseudofermion representations as unoccupied sites of the $s1$ and c effective lattices, respectively. On the other hand, the effects under σ one-electron UHB addition of the creation of one $\eta 1$ pseudofermion are simpler to be accounted for than those stemming from the c and $s1$ pseudofermion processes and fortunately do not require the explicit use of the $\eta 1$ pseudofermion operator representation.

D. Needed quantities associated with the β pseudoparticle quantum liquid

For the densities $n_e \in [0, 1[$ and $m \in [0, n_e]$ considered in this paper for which ground states are LWSs of both the spin and η -spin $SU(2)$ symmetry algebras, a *particle subspace* (PS) is spanned by one such ground states and the set of excited energy eigenstates generated from it by a finite number of β pseudoparticle processes. For these excited energy eigenstates, the deviation densities $\delta N_\beta/L$, $\delta S_s/L$, and $\delta S_{\eta/L}$ vanish as $L \rightarrow \infty$. For a PS there are though no restrictions on the value of the excitation energy and excitation momentum.

It is often convenient within the TL to replace the $\beta = c, \alpha n$ band discrete momentum values q_j , Eq. (20), such that $q_{j+1} - q_j = 2\pi/L$, by a corresponding continuous momentum variable, q . It belongs to a domain $q \in [q_\beta^-, q_\beta^+]$ whose limiting momentum values q_β^\pm are given in Eq. (26). For the $\beta = \alpha n$ bands the relation $q_{\alpha n}^- = -q_{\alpha n}^+$ is exact, as given in that equation. Ignoring $1/L$ corrections as $L \rightarrow \infty$, one finds $q_\beta^\pm \approx \pm q_\beta$ where for all $\beta = c, \alpha n$ bands q_β has simple expressions for the ground states and their PS excited energy eigenstates. For the present densities ranges they read [37],

$$q_c = \pi; \quad q_{s1} = k_{F\uparrow}; \quad q_{sn} = (k_{F\uparrow} - k_{F\downarrow}) = \pi m, \quad n > 1; \quad q_{\eta n} = (\pi - 2k_F) = \pi(1 - n_e). \quad (41)$$

The $\beta = c, \alpha n$ momentum band distribution functions of the PS excited energy eigenstates are of the general form $N_\beta(q_j) = N_\beta^0(q_j) + \delta N_\beta(q_j)$ where the ground-state β band pseudoparticle momentum distribution functions $N_\beta^0(q_j)$ are given in Eq. (28). Several physical quantities are then expressed as functionals of the corresponding $\beta = c, \alpha n$ momentum band distribution function deviations,

$$\delta N_\beta(q_j) = N_\beta(q_j) - N_\beta^0(q_j), \quad j = 1, \dots, L_\beta, \quad \beta = c, \alpha n, \quad n = 1, \dots, \infty. \quad (42)$$

Under transitions from a ground state to a PS excited energy eigenstate, there may occur a shakeup effect associated with the overall β -band discrete momentum shifts, $q_j \rightarrow q_j + 2\pi \Phi_\beta^0/L$, that follow from the boundary conditions change in Eq. (21). Here Φ_β^0 reads,

$$\begin{aligned} \Phi_c^0 &= 0; & \delta N_{ps}^{SU(2)} & \text{even}; & \Phi_c^0 &= \pm \frac{1}{2}; & \delta N_{ps}^{SU(2)} & \text{odd}; \\ \Phi_{\alpha n}^0 &= 0; & \delta N_c + \delta N_{\alpha n} & \text{even}; & \Phi_{\alpha n}^0 &= \pm \frac{1}{2}; & \delta N_c + \delta N_{\alpha n} & \text{odd}, \quad \alpha = \eta, s, \quad n = 1, \dots, \infty, \end{aligned} \quad (43)$$

where $\delta N_{ps}^{SU(2)}$ is the deviation in the number $N_{ps}^{SU(2)}$ in Eq. (23).

Within the continuum q representation, the deviation values $\delta N_\beta(q_j) = -1$ and $\delta N_\beta(q_j) = +1$, Eq. (42), become $\delta N_\beta(q) = -(2\pi/L)\delta(q - q_j)$ and $\delta N_\beta(q) = +(2\pi/L)\delta(q - q_j)$, respectively. Here and throughout this paper, $\delta(x)$ denotes the usual Dirac delta-function distribution. According to Eqs. (20) and (21), under a transition to an excited energy eigenstate the β band discrete momentum values $q_j = (2\pi/L)I_j^\beta$ may undergo a collective shift, $(2\pi/L)\Phi_\beta^0 = \pm\pi/L$. For q at the $\beta = c, s1$ and $\iota = \pm 1$ Fermi points, $\iota q_{F\beta}$, such an effect is captured within the continuum representation by additional deviations, $\pm(\pi/L)\delta(q - \iota q_{F\beta})$. For transitions to an excited energy eigenstate for which $\delta L_{\alpha n} \neq 0$, the removal or addition of BA αn band discrete momentum values occurs in the vicinity of the band edges $q_{\alpha n}^- = -q_{\alpha n}^+$, Eq. (26). Those are zero-momentum and zero-energy processes.

The PS energy functionals are derived from the use in the TBA equations, Eqs. (A1)-(A2) of Appendix A, and general energy spectra, Eq. (A4) of that Appendix, of distribution functions of general form $N_\beta(q_j) = N_\beta^0(q_j) + \delta N_\beta(q_j)$ for the excited energy eigenstates. The combined and consistent solution of such equations and spectra up to second order in the deviations, Eq. (42), leads to [55],

$$\delta E = \sum_{\beta} \sum_{j=1}^{L_\beta} \varepsilon_\beta(q_j) \delta N_\beta(q_j) + \frac{1}{L} \sum_{\beta} \sum_{\beta'} \sum_{j=1}^{L_\beta} \sum_{j'=1}^{L_{\beta'}} \frac{1}{2} f_{\beta\beta'}(q_j, q_{j'}) \delta N_\beta(q_j) \delta N_{\beta'}(q_{j'}) + \sum_{\alpha=\eta, s} \varepsilon_{\alpha, -1/2} M_{\alpha, -1/2}^{un}, \quad (44)$$

where for the present densities ranges the unpaired rotated η -spin ($\alpha = \eta$) and unpaired rotated spin ($\alpha = s$) energies relative to the ground state zero-energy level read,

$$\varepsilon_{\alpha, -1/2} = 2\mu_\alpha; \quad \varepsilon_{\alpha, +1/2} = 0, \quad \alpha = \eta, s, \quad (45)$$

and the energy scales $2\mu_\alpha$ are given by,

$$2\mu_\eta = 2|\mu|; \quad 2\mu_s = 2\mu_B |h|, \quad (46)$$

for general electronic and spin densities and by $2\mu_\eta = 2\mu$ and $2\mu_s = 2\mu_B h$ for the densities ranges $n_e \in [0, 1[$ and $m \in [0, n_e]$ for which Eq. (45) applies. For the $n_e = 1$ Mott-Hubbard insulator phase the unpaired rotated η -spin energy rather reads $\varepsilon_{\eta, \mp 1/2} = (\mu_u \pm \mu)$ for $\mu \in [-\mu_u, \mu_u]$. The $n_e = 1$ Mott-Hubbard gap $2\mu_u$ appearing here whose limiting behaviors are given in Eq. (5) is behind the spectra of the one-electron and charge excitations of the half-filled 1D Hubbard model being gapped [1, 2, 54].

Furthermore, in Eq. (44) the $\beta = c, \alpha n$ band energy dispersions $\varepsilon_\beta(q_j)$ are given by,

$$\varepsilon_\beta(q_j) = E_\beta(q_j) + \frac{t}{\pi} \int_{-Q}^Q dk 2\pi \bar{\Phi}_{c,\beta} \left(\frac{\sin k}{u}, \frac{\Lambda_0^\beta(q_j)}{u} \right) \sin k, \quad j = 1, \dots, L_\beta. \quad (47)$$

Here $\Lambda_0^\beta(q_j)$ is a ground-state rapidity function and $E_\beta(q_j)$ is for $\beta = c, \eta n, sn$ the energy spectrum, Eq. (A5) of Appendix A, with the rapidity functions in their expressions given by the ground-state rapidity functions $k_0^c(q_j)$ and $\Lambda_0^\beta(q_j)$. These functions are the solution of Eqs. (A1) and (A2) of that Appendix for the β -band ground-state distribution function distributions, Eq. (28). The parameter Q also appearing in Eq. (47) and related parameters B , r_c^0 , and r_s^0 read,

$$Q \equiv k_c^0(2k_F); \quad B \equiv \Lambda_0^{s1}(k_{F\downarrow}); \quad r_c^0 = \frac{\sin Q}{u}; \quad r_s^0 = \frac{B}{u}. \quad (48)$$

Furthermore, the rapidity dressed phase shift $2\pi \bar{\Phi}_{c,\beta}(r, r')$ in Eq. (47) is a particular case of the more general rapidity dressed phase shifts $2\pi \bar{\Phi}_{\beta,\beta'}(r, r')$ uniquely defined by the set of integral equations given in Eqs. (A8)-(A22) of Appendix A. The general expression of the f functions in the second-order terms of the energy functional, Eq. (44), is provided in Eq. (A24) of that Appendix and involves the related momentum dressed phase shifts $2\pi \Phi_{\beta,\beta'}(q_j, q_{j'})$,

$$2\pi \Phi_{\beta,\beta'}(q_j, q_{j'}) = 2\pi \bar{\Phi}_{\beta,\beta'}(r, r'); \quad r = \Lambda_0^\beta(q_j)/u; \quad r' = \Lambda_0^{\beta'}(q_{j'})/u. \quad (49)$$

Such f function expression also involves the β band group velocities $v_\beta(q_j)$ that within the TL continuum q representation are given by,

$$v_\beta(q) = \frac{\partial \varepsilon_\beta(q)}{\partial q}, \quad \beta = c, \eta n, sn, \quad n = 1, \dots, \infty; \quad v_\beta \equiv v_\beta(q_{F\beta}), \quad \beta = c, s1, \quad (50)$$

where the β band energy dispersions are given in Eq. (47).

An overall dressed phase shift functional involving the momentum dressed phase shifts, Eq. (49), that within the PDT plays an active role in the control of the (k, ω) -plane σ one-electron spectral weight distributions is given by,

$$2\pi \Phi_\beta(q_j) = \sum_{\beta'} \sum_{j'=1}^{N_{\alpha\beta'}} 2\pi \Phi_{\beta,\beta'}(q_j, q_{j'}) \delta N_{\beta'}(q_{j'}), \quad j = 1, \dots, L_\beta, \quad \beta = c, s1, \quad (51)$$

where the summation $\sum_{\beta'}$ refers to $\beta' = c, s1$ for σ one-electron removal and LHB addition and to $\beta' = c, s1, \eta 1$ for σ one-electron UHB addition and the deviation $\delta N_{\beta'}(q_{j'})$ is defined in Eq. (42).

The functional energy spectrum, Eq. (44), describes the 1D Hubbard model as a quantum liquid of c , ηn , and sn pseudoparticles that have residual interactions associated with the f functions, Eqs. (A24). While the general energy spectrum, Eq. (A4) of Appendix A, gives the energy eigenvalues, that given in Eq. (44) rather provides the excited-state energy eigenvalues minus the ground state energy. The second term of the energy dispersion, Eq. (47), and the f -function terms in Eq. (44) are absent from Eq. (A4) of Appendix A and stem from such energies difference. This is why that energy dispersion term and the f -function expressions involve dressed phase shifts, Eq. (49). Indeed those emerge under the transitions from the ground state to energy eigenstates of excitation energy, Eq. (44).

As found in Sections III and IV, the spectra of the σ one-electron spectral functions near their singular features are expressed in terms of the c and $s1$ band energy dispersions, Eq. (47) for $\beta = c, s1$, the definition of a particular type of such features called a boundary line involves β pseudoparticle group velocities, Eq. (50), and the exponents that control the line shape in the vicinity of another type of singular features are expressed in terms of momentum dressed phase shifts, Eq. (49). Hence in Appendix B useful limiting behaviors of all such quantities are provided.

E. Bounding and anti-bounding character of the composite αn pseudoparticle $2n = 2, 4, \dots$ rotated spins $1/2$ ($\alpha = s$) and rotated η -spins $1/2$ ($\alpha = \eta$) configuration

Analysis of the form of the composite αn pseudoparticle energy dispersions, Eq. (47) for $\beta = \alpha n$, provides valuable information on the bounding and anti-bounding character of its $2n = 2, 4, \dots$ paired rotated spins $1/2$ ($\alpha = s$) and paired rotated η -spins $1/2$ ($\alpha = \eta$) singlet configuration, respectively.

Consistently with Eq. (45) for the particular case of densities $n_e \in [0, 1[$ and $m \in [0, n_e]$, for general electronic densities $n_e \neq 1$ and all corresponding spin densities m the energy of two unpaired rotated η -spins ($\alpha = \eta$) and of two unpaired rotated spins ($\alpha = s$) of opposite projection reads,

$$2\mu_\alpha = \varepsilon_{\alpha, -1/2} + \varepsilon_{\alpha, +1/2}, \quad \alpha = \eta, s, \quad (52)$$

where the energy scale $2\mu_\alpha$ is given in Eq. (46). For $n_e = 1$ and $m \in [-1, 1]$ this expression remains being valid for $\alpha = s$ yet rather involves the Mott-Hubbard gap, Eq. (5), and is replaced by $2\mu_u = \varepsilon_{\eta, -1/2} + \varepsilon_{\eta, +1/2}$ for $\alpha = \eta$. The bare η -spin-triplet ($\alpha = \eta$) and spin-triplet ($\alpha = s$) pair energy, Eq. (52), also applies to a η -spin-singlet ($\alpha = \eta$) and spin-singlet ($\alpha = s$) pair in case that the corresponding configuration has no bounding or anti-bounding character.

The αn pseudoparticle energy dispersion, Eq. (47) for $\beta = \alpha n$, may be written as,

$$\varepsilon_{\alpha n}(q_j) = \varepsilon_{\alpha n}^0(q_j) + n 2\mu_\alpha, \quad \alpha = \eta, s, \quad n = 1, \dots, \infty. \quad (53)$$

The term $n 2\mu_\alpha$ in this energy dispersion is merely additive in the bare energy $2\mu_\alpha$, Eq. (52). On the other hand, $\varepsilon_{\alpha n}^0(q_j)$ is a bounding or anti-bounding energy if $\varepsilon_{\alpha n}^0(q_j) < 0$ or $\varepsilon_{\alpha n}^0(q_j) > 0$, respectively. The use of such a criterion reveals that the sn pseudoparticles $2n$ rotated spins configuration has a bounding character, since $\varepsilon_{s1}^0(q_j) < 0$ for $|q_j| < q_{sn}$. The ηn pseudoparticles $2n$ rotated η -spins configuration has in turn an anti-bounding character because $\varepsilon_{\eta n}^0(q_j) > 0$ for $|q_j| < q_{\eta n}$.

Interestingly, $\varepsilon_{\alpha n}^0(\pm q_{\alpha n}) = 0$ so that at the αn band limiting values $q_j = \pm q_{\alpha n}$ given in Eq. (41) one has that the energy, Eq. (53), becomes additive in the bare energy $2\mu_\alpha$ of two unpaired rotated η -spins ($\alpha = \eta$) and of two unpaired rotated spins ($\alpha = s$) of opposite projection, $\varepsilon_{\alpha n}(\pm q_{\alpha n}) = n 2\mu_\alpha$. As discussed below in Sec. IV C, this is due to a symmetry that is behind the σ one-electron UHB addition singular spectral features being for $n_e \in [0, 1[$ and under the transformations $k \rightarrow \pi - k$ and $\omega \rightarrow 2\mu - \omega$ similar to those of the corresponding $\bar{\sigma}$ one-electron removal singular spectral features.

On the other hand, the c pseudoparticle energy dispersion, Eq. (47) for $\beta = c$, can be written as,

$$\varepsilon_c(q_j) = \varepsilon_c^0(q_j) + \mu_\eta - \mu_s. \quad (54)$$

The magnetic-field energy scale $2\mu_B h = 2\mu_B h(m)$ dependence on the spin density $m \in [0, n_e]$ and the energy scale $2\mu = 2\mu(n_e)$ associated with the chemical potential μ dependence on the electronic density $n_e \in [0, 1[$ are fully determined by the $s1$ band energy dispersion $\varepsilon_{s1}^0(q_j)$ at $q_j = q_{Fs1} = k_{F\downarrow}$ in Eq. (53) for $\alpha n = s1$ and the c band energy dispersion $\varepsilon_c^0(q_j)$ at $q_j = q_{Fc} = 2k_F$ in Eq. (54), respectively, as follows [55],

$$\begin{aligned} 2\mu_B h(m) &= -\varepsilon_{s1}^0(q_{Fs1}) \in [0, 2\mu_B h_c] \\ &\quad \text{for } q_{Fs1} = k_{F\downarrow} = \frac{\pi}{2}(n_e - m) \text{ where } m \in [0, n_e] \text{ at fixed } n_e, \\ 2\mu(n_e) &= -2\varepsilon_c^0(q_{Fc}) - \varepsilon_{s1}^0(q_{Fs1}) \in [2\mu_u, (U + 4t)] \\ &\quad \text{for } q_{Fc} = 2k_F = \pi n_e \text{ and } q_{Fs1} = \frac{\pi}{2}(n_e - m) \text{ where } n_e \in [0, 1[\text{ at fixed } m < n_e, \end{aligned} \quad (55)$$

where $2\mu_B h(0) = 0$, $2\mu_B h(n_e) = 2\mu_B h_c$ is the magnetic energy scale, Eq. (6), $2\mu(0) = (U + 4t)$, and $\lim_{n_e \rightarrow 1} 2\mu(n_e) = 2\mu_u$ is the Mott-Hubbard gap, Eq. (5).

III. THE PSEUDOFERMION DYNAMICAL THEORY MICROSCOPIC PROCESSES THAT ACCOUNT FOR THE σ ONE-ELECTRON SPECTRAL WEIGHTS

The main goal of this section is to provide information beyond that of Refs. [38, 39] on the microscopic processes that control the σ one-electron spectral weights at finite magnetic field. This includes how the PDT accounts through such processes for the matrix elements of the σ electron creation or annihilation operators between the initial ground state and the excited energy eigenstates. To accomplish that aim, we start by briefly introducing in Section III A the pseudofermion representation to be used for these matrix elements. In Section III B the σ one-electron problem is expressed in terms of pseudofermion operators. The matrix elements of the σ electron creation or annihilation operators and the expression of the corresponding σ one-electron spectral functions in terms of $\beta = c, s1$ pseudofermion spectral functions are the issues addressed in Section III C. In Section III D the effects of the small higher-order pseudofermion contributions to the σ one-electron spectral weight are discussed. Section III E addresses the involved state summations problem and the analytical expressions obtainable near σ one-electron singular spectral features. Finally, the validity of the expressions for the line shape near such features is the subject of Section III F.

A. Pseudofermion representation to be used for the σ electron operators matrix elements

For the 1D Hubbard model at a finite magnetic field in a PS as defined in Section IID, the c and $s1$ rapidity functions of the excited energy eigenstates can be expressed in terms of those of the corresponding initial ground state as given in Eq. (A7) of Appendix A. The set of $j = 1, \dots, L_\beta$ values $\bar{q}_j = \bar{q}(q_j)$ in such excited energy eigenstates rapidity expressions $\Lambda^c(q_j) = \Lambda_0^c(\bar{q}(q_j))$ and $\Lambda^{s1}(q_j) = \Lambda_0^{s1}(\bar{q}(q_j))$ are the $\beta = c, s1$ band discrete *canonical momentum* values. They are given by,

$$\bar{q}_j = \bar{q}(q_j) = q_j + \frac{2\pi \Phi_\beta(q_j)}{L} = \frac{2\pi}{L} \left(I_j^\beta + \Phi_\beta(q_j) \right), \quad j = 1, \dots, L_\beta, \quad \beta = c, s1. \quad (56)$$

Here $2\pi \Phi_\beta(q_j)$ stands for the dressed phase-shift functional, Eq. (51), in units of 2π . The discrete canonical momentum values, Eq. (56), have spacing $\bar{q}_{j+1} - \bar{q}_j = 2\pi/L + \text{h.o.}$, where h.o. stands for contributions of second order in $1/L$.

We call a $\beta = c, s1$ *pseudofermion* each of the N_β occupied β -band discrete canonical momentum values \bar{q}_j [38, 39]. We call a β *pseudofermion hole* the remaining N_β^h unoccupied β -band discrete canonical momentum values \bar{q}_j of a PS energy eigenstate. There is a pseudofermion representation for each ground state and its PS. This holds for all electronic and spin densities.

The $\beta = c, s1$ pseudofermion creation and annihilation operators are generated from the corresponding $\beta = c, s1$ pseudoparticle creation and annihilation operators, Eq. (40), as follows,

$$\begin{aligned} \bar{f}_{\bar{q}_j, \beta}^\dagger &= f_{q_j + 2\pi \Phi_\beta(q_j)/L, \beta}^\dagger = \left(\hat{S}_\beta^\Phi \right)^\dagger f_{q_j, \beta}^\dagger \hat{S}_\beta^\Phi; & \bar{f}_{\bar{q}_j, \beta} &= \left(\bar{f}_{\bar{q}_j, \beta}^\dagger \right)^\dagger, \\ \hat{S}_\beta^\Phi &= e^{\sum_{j=1}^{L_\beta} f_{q_j + 2\pi \Phi_\beta(q_j)/L, \beta}^\dagger f_{q_j, \beta}}; & \left(\hat{S}_\beta^\Phi \right)^\dagger &= e^{\sum_{j=1}^{L_\beta} f_{q_j}^\dagger f_{q_j - 2\pi \Phi_\beta(q_j)/L, \beta}}, \end{aligned} \quad (57)$$

where and \hat{S}_β^Φ is the β pseudoparticle - β pseudofermion unitary operator. By combining Eq. (35) with Eq. (59) for $\beta = c$, the c pseudofermion operator given here can be formally expressed in terms of rotated-electron operators as,

$$\bar{f}_{\bar{q}_j, c}^\dagger = \frac{1}{\sqrt{L}} \sum_{j'=1}^L e^{+i\bar{q}_j j'} \left(\tilde{c}_{j', \uparrow}^\dagger (1 - \tilde{n}_{j', \downarrow}) + (-1)^{j'} \tilde{c}_{j', \uparrow} \tilde{n}_{j', \downarrow} \right); \quad \bar{f}_{\bar{q}_j, c} = \left(\bar{f}_{\bar{q}_j, c}^\dagger \right)^\dagger. \quad (58)$$

As in the case of the corresponding $\beta = c, s1$ pseudoparticle operators, the canonical-momentum $\beta = c, s1$ pseudofermion operators, Eq. (57), are related to local $\beta = c, s1$ pseudofermion operators $\bar{f}_{j', \beta}^\dagger$ and $\bar{f}_{j', \beta}$ that create and annihilate, respectively, one $\beta = c, s1$ pseudofermion at the $\beta = c, s1$ effective lattice site $x_{j'} = a_\beta j'$ where $j' = 1, \dots, L_\beta$. The relation reads,

$$\bar{f}_{\bar{q}_j, \beta}^\dagger = \frac{1}{\sqrt{L}} \sum_{j'=1}^{L_{s1}} e^{i\bar{q}_j x_{j'}} \bar{f}_{j', \beta}^\dagger; \quad \bar{f}_{\bar{q}_j, \beta} = \frac{1}{\sqrt{L}} \sum_{j'=1}^{L_{s1}} e^{-i\bar{q}_j x_{j'}} \bar{f}_{j', \beta}, \quad j = 1, \dots, L_\beta, \quad \beta = c, s1. \quad (59)$$

Indeed, the c and $s1$ pseudofermions also live in the c effective lattice, which is identical to the original lattice, and in the squeezed $s1$ effective lattice, respectively. As the c pseudoparticles, the c pseudofermions have no internal structure, whereas the $s1$ pseudofermions have the same internal structure as the corresponding $s1$ pseudoparticles. They only differ in their discrete momentum values, which rather refer to the translational degrees of freedom associated with their center of mass motion.

In the present pseudofermion operator representation a PS ground state has the simple form,

$$|GS\rangle = \prod_{\bar{q} = -k_{F\downarrow}}^{k_{F\downarrow}} \prod_{\bar{q}' = -\pi}^{\pi} \bar{f}_{\bar{q}, s1}^\dagger \bar{f}_{\bar{q}', c}^\dagger |0\rangle = \prod_{j=1}^{N_\downarrow} \prod_{j'=1}^L \bar{f}_{\bar{q}_j, s1}^\dagger \bar{f}_{\bar{q}_{j'}, c}^\dagger |0\rangle. \quad (60)$$

That representation has been inherently constructed to $\bar{q} = q$ for a PS ground state, so that here the $s1$ and c band momentum values $\bar{q} = q = \bar{q}_j = q_j$ and $\bar{q}' = q' = \bar{q}_{j'} = q_{j'}$, respectively, are those of the corresponding $s1$ and c pseudoparticle occupied ground-state Fermi seas. Moreover, $|0\rangle$ stands in Eq. (60) for the electron and rotated-electron vacuum and the ground-state generator has been written in terms of $s1$ and c pseudofermion creation operators, Eqs. (57) and (59).

The c pseudofermions as defined here refer to an extension to finite u of the usual $u \rightarrow \infty$ spinless fermions [32, 33]. Indeed, in the $u \rightarrow \infty$ limit the momentum rapidity function of the ground state $k_0^c(q_j)$ simplifies to $k_0^c(q_j) = q_j$.

Hence, according to Eq. (A7) of Appendix A, for the PS excited energy eigenstates associated with the initial ground state under consideration such a function reads, $k^c(q_j) = \bar{q}_j$. The $u \rightarrow \infty$ spinless fermions of Refs. [32, 33] have been constructed inherently to carry the momentum rapidly $k_j = k^c(q_j) = \bar{q}_j$. This reveals that such spinless fermions are the c pseudofermions as defined here in the $u \rightarrow \infty$ limit. Indeed, the relations $\bar{f}_{\bar{q}_j, c}^\dagger = \hat{V}^\dagger b_{k_j}^\dagger \hat{V}$ and $\bar{f}_{\bar{q}_j, c} = \hat{V}^\dagger b_{k_j} \hat{V}$ hold where \hat{V} is the electron - rotated-electron unitary operator defined in terms of its matrix elements in Eq. (12) and $b_{k_j}^\dagger$ and b_{k_j} stand for the $u \rightarrow \infty$ spinless fermions creation and annihilation operators that appear in the anti-commutators given in the first equation of Section IV of Ref. [33].

The one-to-one correspondence between a canonical momentum value \bar{q}_j and the corresponding bare momentum value q_j as defined in Eq. (56) enables the expression of several \bar{q}_j -dependent pseudofermion quantities in terms of the corresponding bare momentum q_j . This applies to the dressed phase shift $2\pi \Phi_{\beta, \beta'}(q_j, q_{j'})$, Eq. (49). Within the pseudofermion representation it has a precise physical meaning: $2\pi \Phi_{\beta, \beta'}(q_j, q_{j'})$ (and $-2\pi \Phi_{\beta, \beta'}(q_j, q_{j'})$) is the phase shift acquired by a β pseudofermion or β pseudofermion hole of canonical momentum $\bar{q}_j = \bar{q}(q_j)$ upon scattering off a β' pseudofermion (and β' pseudofermion hole) of canonical momentum value $\bar{q}_{j'} = \bar{q}(q_{j'})$ created under a transition from the ground state to a PS excited energy eigenstate. Hence the important functional $2\pi \Phi_\beta(q_j)$, Eq. (51), in the $\beta = c, s1$ canonical momentum expression $\bar{q}_j = q_j + \frac{2\pi}{L} \Phi_\beta(q_j)$, Eq. (56), is the phase shift acquired by a β pseudofermion or β pseudofermion hole of canonical momentum value $\bar{q}_j = \bar{q}(q_j)$ upon scattering off the set of β' pseudofermions and β' pseudofermion holes created under a transition from the ground state to a PS excited energy eigenstate. Hence the β pseudofermion phase shift $2\pi \Phi_\beta(q_j)$ has a specific value for each ground-state - excited-state transition.

The line shape near the σ one-electron UHB addition spectral function singular features involves the creation of a single $\eta1$ pseudoparticle at one of the $\eta1$ band limiting momentum values $q_j = \pm q_{\eta1} = \pm(\pi - 2k_F)$, Eq. (41). $\eta1$ band canonical momentum values $\bar{q}_j = q_j + 2\pi \Phi_{\eta1}(q_j)/L$ can be introduced, as in Eq. (56) for the $\beta = c, s1$ bands. Interestingly, one finds that $2\pi \Phi_{\eta1}(q_j) = 0$ at the $\eta1$ band limiting momentum values $q_j = \pm(\pi - 2k_F)$, so that $\bar{q}_j = q_j$. This reveals that a $\eta1$ pseudoparticle and a $\eta1$ pseudofermion of momenta $\pm(\pi - 2k_F)$ are the same quantum object. Such an invariance under the $\eta1$ pseudoparticle - $\eta1$ pseudofermion unitary transformation follows from symmetries related to the anti-bounding energy $\varepsilon_{\eta1}^0(q_j)$ on the right-hand side of Eq. (53) for $\alpha n = \eta1$ vanishing at $q_j = \pm q_{\eta1} = \pm(\pi - 2k_F)$. As the unpaired rotated spins and unpaired rotated η -spins, the $\eta1$ pseudofermions of momentum $\pm q_{\eta1} = \pm(\pi - 2k_F)$ do not acquire a phase shift under the transitions from the ground state to the PS excited energy eigenstates.

One can introduce a creation operator $f_{q_j, \eta1}^\dagger$ for the $\eta1$ pseudoparticles that at $q_j = \iota(\pi - 2k_F)$ is identical to the corresponding $\eta1$ pseudofermion creation operator,

$$\bar{f}_{\bar{q}_j, \eta1}^\dagger = f_{q_j, \eta1}^\dagger \text{ at } \bar{q}_j = q_j = \iota(\pi - 2k_F), \quad \iota = \pm 1, \quad (61)$$

where in the present case $\bar{f}_{\bar{q}_j, \eta1}^\dagger$ creates one $\eta1$ pseudofermion at the canonical momentum values $\bar{q}_j = \pm(\pi - 2k_F)$. Although such a $\eta1$ pseudofermion does not acquire phase shifts of its own, under its creation within a transition from the ground state to an excited energy eigenstate the $\beta = c, s1$ pseudofermions of canonical momentum \bar{q}_j acquire a phase shift $2\pi \Phi_{\beta, \eta1}(q_j, \pm(\pi - 2k_F))$, Eq. (49) for $\beta' = \eta1$ and $q_{j'} = \pm(\pi - 2k_F)$. After some manipulations relying on the use of Eqs. (A9) and (A15) of Appendix A for $\eta n = \eta1$, one finds that it can be written as,

$$2\pi \Phi_{\beta, \eta1}(q_j, \pm(\pi - 2k_F)) = \pm \frac{1}{2} (\delta_{\beta, c} 2\pi + 2\pi \Phi_{\beta, c}(q_j, 2k_F) - 2\pi \Phi_{\beta, c}(q_j, -2k_F)), \quad \beta = c, s1, \quad \iota = \pm 1. \quad (62)$$

Hence except for the factor 1/2 creation of one $\eta1$ pseudofermion at the canonical momentum values $\pm(\pi - 2k_F)$ is felt by a $\beta = c, s1$ pseudofermion as the creation and annihilation of two c pseudofermions at opposite Fermi points.

The exponents that control the σ one-electron spectral weight in the (k, ω) -plane vicinity of a type of singular features called branch lines are found below in Section III C to involve both the two-pseudofermion phase shifts $2\pi \Phi_{c, \beta}(\pm 2k_F, q_j)$ and $2\pi \Phi_{s1, \beta}(\pm k_{F\downarrow}, q_j)$ where $\beta = c, s1$ and the following related $j = 0, 1$ parameters,

$$\xi_{\beta, \beta'}^j = \delta_{\beta, \beta'} + \sum_{\iota = \pm 1} (\iota)^j \Phi_{\beta, \beta'}(q_{F\beta}, \iota q_{F\beta'}), \quad \beta, \beta' = c, s1, \quad j = 0, 1. \quad (63)$$

For the particular case of $\beta = \beta'$ and $\iota = 1$ in Eq. (63), the present notation assumes that the two $\beta = c, s1$ Fermi momenta in the argument of the β pseudofermion phase shift, $2\pi \Phi_{\beta, \beta}(q_{F\beta}, q_{F\beta})$, differ by $2\pi/L$. (For identical momentum values one has that $2\pi \Phi_{\beta, \beta}(q_j, q_j) = 0$.)

The two-pseudofermion phase-shift related anti-symmetrical $\xi_{\beta, \beta'}^1$ and symmetrical $\xi_{\beta, \beta'}^0$ parameters, Eq. (63), that naturally emerge from the pseudofermion representation are actually the entries of the low-energy conformal-field

theory dressed-charge matrix and of the transposition of its inverse matrix [14, 29, 39, 55],

$$Z^1 = \begin{bmatrix} \xi_{cc}^1 & \xi_{cs1}^1 \\ \xi_{s1c}^1 & \xi_{s1s1}^1 \end{bmatrix}; \quad Z^0 = ((Z^1)^{-1})^T = \begin{bmatrix} \xi_{cc}^0 & \xi_{cs1}^0 \\ \xi_{s1c}^0 & \xi_{s1s1}^0 \end{bmatrix}, \quad (64)$$

respectively. (Here the dressed-charge matrix definition of Ref. [14] has been used, which is the transposition of that of Ref. [29].) The limiting behaviors of the parameters, Eq. (63), which are the entries of the matrices, Eq. (64), are given in Appendix B.

Moreover, from the combined use of Eqs. (62) and (63) one finds,

$$\Phi_{\beta,\eta 1}(\iota q_{F\beta}, \iota'(\pi - 2k_F)) = \iota' \frac{\xi_{\beta c}^1}{2}, \quad \beta = c, s1, \quad \iota, \iota' = \pm 1. \quad (65)$$

For the PS excited energy eigenstates with densities $n_e \in [0, 1[$ and $m \in [0, n_e]$ associated with the line shape near the σ one-electron spectral functions singularities the αn pseudofermion numbers have values given by $N_{\alpha n} = 0$ for $n > 1$ and $N_{\eta 1} = 0, 1$ where when $N_{\eta 1} = 1$ the $\eta 1$ pseudofermion has canonical momentum $\pm(\pi - 2k_F)$. For the PSs spanned by these excited energy eigenstates and corresponding ground states the pseudoparticle representation general PS energy functional, Eq. (44), simplifies to,

$$\delta E = \sum_{\beta=c,s1} \sum_{j=1}^{L_\beta} \varepsilon_\beta(q_j) \delta N_\beta(q_j) + \frac{1}{L} \sum_{\beta=c,s1} \sum_{\beta'=c,s1,\eta 1} \sum_{j=1}^{L_\beta} \sum_{j'=1}^{L_{\beta'}} \frac{1}{2} f_{\beta\beta'}(q_j, q_{j'}) \delta N_\beta(q_j) \delta N_{\beta'}(q_{j'}) + 2\mu N_{\eta 1}. \quad (66)$$

Upon expressing this functional in the pseudofermion representation, which involves the $\beta = c, s1$ bands discrete canonical momentum values $\bar{q}_j = \bar{q}(q_j)$, Eq. (56), one finds after some algebra that it reads up to $\mathcal{O}(1/L)$ order,

$$\delta E = \sum_{\beta=c,s1} \sum_{j=1}^{L_\beta} \varepsilon_\beta(\bar{q}_j) \delta N_\beta(\bar{q}_j) + 2\mu N_{\eta 1}. \quad (67)$$

Here the $\beta = c, s1$ pseudofermion energy dispersions $\varepsilon_\beta(\bar{q}_j)$ have exactly the same form as those given in Eq. (47) with the momentum q_j replaced by the corresponding canonical momentum, $\bar{q}_j = \bar{q}(q_j)$.

If in Eq. (67) one expands the $\beta = c, s1$ band canonical momentum $\bar{q}_j = q_j + 2\pi \Phi_\beta(q_j)/L$ around q_j and considers all energy contributions up to $\mathcal{O}(1/L)$ order, one arrives after some algebra to the energy functional, Eq. (66), which includes terms of second order in the deviations $\delta N_\beta(q_j)$. Their absence from the corresponding energy spectrum, Eq. (67), follows from the functional $2\pi \Phi_\beta(q_j)$, Eq. (51), being incorporated in the $\beta = c, s1$ band canonical momentum, Eq. (56).

In contrast to the equivalent energy functional, Eq. (66), that in Eq. (67) has no energy interaction terms of second-order in the deviations $\delta N_\beta(\bar{q}_j)$. Indeed the $\beta = c, s1$ pseudofermions have no such interactions up to $\mathcal{O}(1/L)$ order. Within the present TL, only finite-size corrections up to that order are relevant. The property that the excitation energy spectrum, Eq. (67), has no pseudofermion energy interactions is found below to simplify the expression of the σ one-electron spectral functions in terms of a sum of convolutions of c and $s1$ pseudofermion spectral functions whose spectral weights are expressed as Slater determinants of pseudofermion operators.

B. The σ one-electron problem expressed in terms of pseudofermion operators

Within the PDT of Refs. [38, 39] the $\beta = c, s1$ pseudofermion phase shifts determine the dynamical correlation functions spectral-weight distributions. Here we provide information beyond that given in these references about how that dynamical theory accounts for the matrix elements $\langle \nu^- | c_{k,\sigma} | GS \rangle$ and $\langle \nu^+ | c_{k,\sigma}^\dagger | GS \rangle$ in the spectral functions, Eq. (4). For such spectral functions the elementary processes that generate the excited energy eigenstates from ground states with densities in the ranges $n_e \in [0, 1[$ and $m \in [0, n_e]$ can be classified into three (A)-(C) classes:

(A) High-energy and finite-momentum elementary $\beta = c, s1$ pseudofermion processes. Specifically, creation or annihilation of one or a finite number of $\beta = c, s1$ pseudofermions with canonical momentum values $\bar{q}_j \neq \pm \bar{q}_{F\beta}$;

(B) Finite-momentum processes of excitation energy zero or 2μ that change the number of $\beta = c, s1$ pseudofermions at the $\iota = +1$ right and $\iota = -1$ left $\beta = c, s1$ Fermi points. The processes contributing to the line shape near the σ one-electron UHB spectral function singular features involve creation of one $\eta 1$ pseudofermion at a $\eta 1$ band limiting

canonical momentum $q_{\eta 1}^{\pm} = \pm(\pi - 2k_F)$, Eq. (26) for $\alpha n = \eta 1$, which involves a finite-energy 2μ . This is the minimal energy for creation of one rotated-electron doubly occupied site and stems from the first term of the spectrum $E_{\eta 1}(q_j)$, Eq. (A5) of Appendix A for $\alpha n = \eta 1$, in the $\eta 1$ energy dispersion $\varepsilon_{\eta 1}(q_j)$, Eqs. (47) and (53) for $\beta = \eta 1$;

(C) Low-energy and small-momentum elementary pseudofermion particle-hole processes in the vicinity of the $\beta = c, s1$ bands right ($\iota = +1$) and left ($\iota = -1$) Fermi points, relative to the excited-state $\beta = c, s1$ pseudofermion momentum occupancy configurations generated by the above elementary processes (A) and (B).

The creation of one $\eta 1$ pseudofermion associated with the σ one-electron UHB addition singular spectral features refers to transitions from ground states with densities $n_e < 1$. At $n_e = 1$ the σ one-electron UHB involves instead ground-state transitions to excited energy eigenstates populated by one unpaired rotated η -spin 1/2 of η -spin projection $-1/2$. This also amounts for creation of one rotated-electron doubly occupied site.

The first two steps to express in the pseudofermion representation the matrix elements $\langle \nu^- | c_{k,\sigma} | GS \rangle$ and $\langle \nu^+ | c_{k,\sigma}^\dagger | GS \rangle$ in the spectral functions, Eq. (4), of a σ electron operator between the ground state and the excited energy eigenstates are (i) to express the σ electron creation or annihilation operator in terms of σ rotated electron creation and annihilation operators, Eq. (8), and (ii) to express the latter operators in terms of rotated spin 1/2 operators, rotated η -spin 1/2 operators, and c pseudofermion operators. This is accomplished by use of the σ rotated electron creation and annihilation operators expressions in terms of rotated spin 1/2 operators, rotated η -spin 1/2 operators, and c pseudoparticle operators, Eqs. (34) and (70), accounting for the relation between the c pseudoparticle and c pseudofermion operators, Eq. (57) for $\beta = c$.

The momentum k dependent σ electron operators in the spectral functions Lehmann representation, Eq. (4), are related to the corresponding local operators as,

$$c_{k,\sigma} = \frac{1}{\sqrt{L}} \sum_{j=1}^L e^{ikx_j} c_{j,\sigma}; \quad c_{k,\sigma}^\dagger = (c_{k,\sigma})^\dagger, \quad \sigma = \uparrow, \downarrow. \quad (68)$$

To write the operators $c_{k,\sigma}$ and $c_{k,\sigma}^\dagger$ in terms of σ rotated electron creation and annihilation operators, Eq. (8), we use of the Baker-Campbell-Hausdorff formula to rewrite the relation, Eq. (8), as follows,

$$\begin{aligned} c_{k,\sigma} &= \sum_{i=0}^{\infty} c_{k,\sigma,i} = \tilde{c}_{k,\sigma} + \frac{1}{1!} [\tilde{c}_{k,\sigma}, \tilde{S}] + \frac{1}{2!} [[\tilde{c}_{k,\sigma}, \tilde{S}], \tilde{S}] + \dots; \quad c_{k,\sigma}^\dagger = (c_{k,\sigma})^\dagger, \quad \sigma = \uparrow, \downarrow, \\ c_{k,\sigma,i} &= [\tilde{c}_{k,\sigma}, \tilde{S}]_i = \frac{1}{i!} [[\tilde{c}_{k,\sigma}, \tilde{S}]_{i-1}, \tilde{S}], \quad i = 1, \dots, \infty; \quad [\tilde{c}_{k,\sigma}, \tilde{S}]_0 = \tilde{c}_{k,\sigma} = \hat{V}^\dagger c_{k,\sigma} \hat{V}, \\ \hat{V} &= e^{\hat{S}} = e^{\tilde{S}}. \end{aligned} \quad (69)$$

Here the operator $\tilde{S} = \hat{S}$ commutes with \hat{V} and thus has the same expression in terms of creation and annihilation σ rotated-electron operators and σ electron operators, respectively, and the momentum operators $\tilde{c}_{k,\sigma}^\dagger = \hat{V}^\dagger c_{k,\sigma}^\dagger \hat{V}$ and $\tilde{c}_{k,\sigma} = \hat{V}^\dagger c_{k,\sigma} \hat{V}$ can be written in terms of the local operators $\tilde{c}_{j,\sigma}^\dagger$ and $\tilde{c}_{j,\sigma}$, respectively, in Eqs. (8) and (34) as,

$$\tilde{c}_{k,\sigma}^\dagger = \frac{1}{\sqrt{L}} \sum_{j=1}^L e^{ikx_j} \tilde{c}_{j,\sigma}^\dagger; \quad \tilde{c}_{k,\sigma} = (\tilde{c}_{k,\sigma}^\dagger)^\dagger, \quad \sigma = \uparrow, \downarrow. \quad (70)$$

The next step of our program consists in rewriting the rotated-electron expression $c_{k,\sigma} = \sum_{i=0}^{\infty} c_{k,\sigma,i}$ within a related uniquely defined β pseudofermion representation as,

$$c_{k,\sigma} = \sum_{i'=0}^{\infty} \hat{g}_{i'}(k) \hat{c}_\odot. \quad (71)$$

The new index $i' = 0, 1, \dots, \infty$ refers here to β pseudofermions processes and \hat{c}_\odot is a generator that transforms the initial ground state $|GS\rangle$ into a state with the same electron and rotated-electron numbers N_\uparrow and N_\downarrow and compact symmetrical c and $s1$ bands momentum occupancies as the ground state of the final PS, which we call $|GS_f\rangle$. The only difference between the states $\hat{c}_\odot|GS\rangle$ and $|GS_f\rangle$ is their c and $s1$ band discrete momentum values being those of the initial ground state, $\bar{q}' = q'$, and of the excited-energy eigenstate $\sum_{i'=0}^{\infty} \hat{g}_{i'}(k)|GS_f\rangle$, $\bar{q} \neq q$, respectively.

Each term of index $i' = 0, 1, \dots, \infty$ in Eq. (71) may have contributions from several terms of different index $i = 0, 1, \dots, \infty$ in $c_{k,\sigma} = \sum_{i=0}^{\infty} c_{k,\sigma,i}$, Eq. (69). Fortunately, one can compute the operational form in terms of β pseudofermion operators of the leading $i' = 0, 1, \dots, \infty$ orders of $c_{k,\sigma} = \sum_{i'=0}^{\infty} \hat{g}_{i'}(k) \hat{c}_{\odot}$ from the transformation laws of the ground state $|GS\rangle$, Eq. (60), upon acting onto it the related operators $c_{k,\sigma,i}$ in the expression $c_{k,\sigma} = \sum_{i=0}^{\infty} c_{k,\sigma,i}$.

The 1D Hubbard model is a non-perturbative quantum problem in terms of σ electron processes. This is behind the computation of the σ one-electron spectral functions, Eq. (4), being a very complex many-electron problem. On the other hand, a property that plays key role in our study follows from expressing the σ electron operator $c_{k,\sigma}$ in the terms of pseudofermion operators as $c_{k,\sigma} = \sum_{i'=0}^{\infty} \hat{g}_{i'}(k) \hat{c}_{\odot}$, Eq. (71), rendering the computation of the σ one-electron spectral functions, Eq. (4), a perturbative problem.

Note that both the expressions $c_{k,\sigma} = \sum_{i=0}^{\infty} c_{k,\sigma,i}$ and $c_{k,\sigma} = \sum_{i'=0}^{\infty} \hat{g}_{i'}(k) \hat{c}_{\odot}$ are not small-parameter expansions. Consistently, the perturbative character of the β pseudofermions processes refers to the spectral weight contributing to the spectral functions being dramatically suppressed upon increasing the number of corresponding elementary processes of classes (A) and (B). Those are generated by application onto the ground state, Eq. (60), of operators in $\sum_{i'=0}^{\infty} \hat{g}_{i'}(k) \hat{c}_{\odot}$ with an increasingly large value of the index $i' = 0, 1, \dots, \infty$.

The perturbative character of the 1D Hubbard model upon expressing the σ electron creation or annihilation operators in the spectral functions, Eq. (4), in terms of c pseudofermion operators, rotated spins 1/2 operators and corresponding sn pseudofermion operators, and rotated η -spins 1/2 operators and corresponding ηn pseudofermion operators, follows from the exact energy eigenstates being generated by occupancy configurations of these elementary objects. The non-perturbative character of the problem in terms of electrons results from their relation to the above elementary objects having as well a non-perturbative nature, qualitatively different from that of the electrons to the quasiparticles of a Fermi liquid.

For simplicity, in the following we denote the $i' = 0$ operator $\hat{g}_0(k)$ associated with the σ one-electron operator $c_{k,\sigma}$ (or $c_{k,\sigma}^{\dagger}$) by $\hat{g}(k)$. Such a $i' = 0$ leading-order operator term in the one- or two-electron operator expression,

$$c_{k,\sigma} = \left(\hat{g}(k) + \sum_{i'=1}^{\infty} \hat{g}_{i'}(k) \right) \hat{c}_{\odot}, \quad (72)$$

plays a key role in our study.

The leading-order operators $\hat{g}(k) \hat{c}_{\odot}$ are selected inherently to all the singular spectral features in the σ one-electron spectral functions, Eq. (4), being produced by their application onto the ground state. The corresponding leading-order pseudofermion processes (A) and (B) that after being dressed by low-energy and small-momentum elementary $\beta = c, s1$ pseudofermion particle-hole processes (C) in the vicinity of their right ($\iota = +1$) and left ($\iota = -1$) Fermi points control the line shape near the singular features of the σ one-electron spectral functions, Eq. (4), are the following:

(1) Removal of one \uparrow electron and thus of one \uparrow rotated electron is a process that involves annihilation of one c pseudofermion and one unpaired rotated spin 1/2 of projection \uparrow , so that $\delta N_c = -1$. That unpaired rotated spin 1/2 recombines with the annihilated c pseudofermion within the removed \uparrow rotated electron. The annihilation of the unpaired rotated spin 1/2 leaves the number N_{s1} $s1$ pseudofermions unchanged and leads to a deviation $\delta N_{s1}^h = -1$ in the number of $s1$ band holes.

(2) LHB addition of one \uparrow electron and thus of one \uparrow rotated electron is a process that involves creation of one c pseudofermion and one unpaired rotated spin 1/2 of projection \uparrow , so that $\delta N_c = 1$. The creation of the unpaired rotated spin 1/2 leaves the number N_{s1} $s1$ pseudofermions unchanged and gives rise to a deviation $\delta N_{s1}^h = 1$ in the number of $s1$ band holes.

(3) UHB addition of one \uparrow electron and thus of one \uparrow rotated electron is a process that involves annihilation of one c pseudofermion and one $s1$ pseudofermion and creation of one $\eta 1$ pseudofermion and one unpaired rotated spin 1/2 of projection \uparrow , so that $\delta N_c = -1$, $\delta N_{s1} = -1$, and $\delta N_{\eta 1} = 1$. The $s1$ pseudofermion annihilation occurs through its spin-singlet pair breaking. The rotated spin 1/2 of projection \downarrow emerging from such a pair breaking recombines with the annihilated c pseudofermion within one \downarrow rotated electron. Such a \downarrow rotated electron then pairs with the created \uparrow rotated electron onto a doubly occupied site. The rotated η -spin 1/2 of projection $-1/2$ that describes the η -spin degrees of freedom of such a doubly occupied site combines with one ground-state unpaired rotated η -spin 1/2 of projection $+1/2$ within the $\eta 1$ pseudofermion η -spin singlet pair. The creation of one unpaired rotated spin 1/2 is accounted for by the deviation $\delta N_{s1}^h = 1$ in the number of $s1$ band holes.

(4) Removal of one \downarrow electron and thus of one \downarrow rotated electron is a process that involves annihilation of one

c pseudofermion and one $s1$ pseudofermion and creation of one unpaired rotated spin 1/2 of projection \uparrow , so that $\delta N_c = -1$ and $\delta N_{s1} = -1$. The $s1$ pseudofermion annihilation spin-singlet pair breaking gives rise to one rotated spin 1/2 of projection \downarrow that recombines with the annihilated c pseudofermion within the removed \downarrow rotated electron. The created rotated spin 1/2 of projection \uparrow is that left over by the pair breaking. Its creation is accounted for by the deviation $\delta N_{s1}^h = 1$ in the number of $s1$ band holes.

(5) LHB addition of one \downarrow electron and thus of one \downarrow rotated electron is a process that involves the creation of one c pseudofermion and one $s1$ pseudofermion and annihilation of one unpaired rotated spin 1/2 of projection \uparrow , so that $\delta N_c = 1$ and $\delta N_{s1} = 1$. The $s1$ pseudofermion creation involves a spin-singlet pair formation. The annihilated unpaired rotated spin 1/2 of projection \uparrow combines with the rotated spin 1/2 of projection \downarrow of the created \downarrow rotated electron within such a $s1$ pseudofermion spin-singlet pair. The annihilation of the unpaired rotated spin 1/2 of projection \uparrow is accounted for by the deviation $\delta N_{s1}^h = -1$ in the number of $s1$ band holes.

(6) UHB addition of one \downarrow electron and thus of one \downarrow rotated electron is a process that involves the annihilation of one c pseudofermion and one unpaired rotated spin 1/2 of projection \uparrow and creation of one $\eta1$ pseudofermion, so that $\delta N_c = -1$ and $\delta N_{\eta1} = 1$. The annihilated unpaired rotated spin 1/2 recombines with the annihilated c pseudofermion within one \uparrow rotated electron. Such a \uparrow rotated electron then pairs with the created \downarrow rotated electron onto a doubly occupied site. The rotated η -spin 1/2 of projection $-1/2$ that describes the η -spin degrees of freedom of such a doubly occupied site combines with one ground-state unpaired rotated η -spin 1/2 of projection $+1/2$ within the $\eta1$ pseudofermion η -spin singlet pair. The annihilation of one unpaired rotated spin 1/2 leaves the number N_{s1} $s1$ pseudofermions unchanged and gives rise to a deviation $\delta N_{s1}^h = -1$ in the number of $s1$ band holes.

The above elementary processes involving $s1$ pseudofermion annihilation pair breaking and $s1$ pseudofermion creation pair formation are behind the squeezed $s1$ effective lattice and corresponding $s1$ momentum band being exotic, since their number of sites and discrete momentum values, respectively, which both are given by $L_{s1} = N_{s1} + N_{s1}^h$, has different values for different subspaces. Hence within the $s1$ pseudofermion operator algebra, one distinguishes the $s1$ -band holes created and annihilated under processes within which one $s1$ pseudofermion is annihilated and created, respectively, from the $s1$ -band holes created and annihilated upon changing the number $L_{s1} = N_{s1} + N_{s1}^h$ of squeezed $s1$ effective lattice sites, which equals that of $s1$ -band discrete momentum values. (For $S_s > 0$ states such exotic L_{s1} variations only lead to N_{s1}^h variations.)

The former processes are described by application of the operators $\bar{f}_{\bar{q},s1}$ and $\bar{f}_{\bar{q},s1}^\dagger$, respectively, onto the initial state. On the other hand, the latter N_{s1}^h variations that do not conserve $L_{s1} = N_{s1} + N_{s1}^h$ result from vanishing energy and vanishing momentum processes within which discrete momentum values are added to and removed from one of the $s1$ band limiting momentum values q_{s1}^\pm , Eq. (26) for $\alpha n = s1$. Whether such an addition or removal occurs at the left limiting momentum q_{s1}^- or at right limiting momentum q_{s1}^+ is uniquely defined, since the process must leave invariant the $s1$ band symmetrical relation $q_{s1}^+ = -q_{s1}^-$ for the final state.

Specifically, in the case of the (i) \uparrow one-electron removal processes (1) and \downarrow one-electron UHB addition processes (6) and (ii) \uparrow one-electron LHB addition processes (1) a single discrete momentum value is (i) removed from and (ii) added to, respectively, the $s1$ band limiting momentum values. Such vanishing energy and vanishing momentum processes are implicitly accounted for by the pseudofermion representation through the $s1$ band discrete momentum values of the final states, which are uniquely defined.

In the following we use the transformation laws of the ground state, Eq. (60), upon acting onto it with the $i = 0, 1, \dots, \infty$ operators on the right-hand side of the equation, $c_{k,\sigma} = \sum_{i=0}^{\infty} c_{k,\sigma,i}$ (and $c_{k,\sigma}^\dagger = \sum_{i=0}^{\infty} c_{k,\sigma,i}^\dagger$), for the σ electron annihilation (and creation) operators whose first terms are given in Eq. (69) to derive the expression of the corresponding leading-order operators $\hat{g}(k) \hat{c}_\sigma$, Eq. (72), in terms of c and $s1$ pseudofermion operators for the processes (1), (2), (4), and (5) and in terms of c , $s1$, and $\eta1$ pseudofermion operators for the σ one-electron UHB addition processes (3) and (6).

Within our study of the line shape near the σ one-electron spectral weight singular features the expression of the σ electron creation and annihilation operators in terms of pseudofermion operators can be approximated by the corresponding leading-order term, $\hat{g}(k) \hat{c}_\sigma$. In the case of the \uparrow one-electron removal processes (1) one finds the following leading-order expression,

$$\begin{aligned}
c_{k,\uparrow} &\approx \hat{g}_\uparrow(k) \hat{c}_\uparrow, \\
\hat{c}_\sigma &= \bar{f}_{\pm 2k_F, c}; \quad \Phi_c^0 = 0; \quad \Phi_{s1}^0 = \iota/2, \quad \iota = \pm 1, \\
\hat{g}_\iota(k) &= \bar{f}_{\bar{q}(\pm 2k_F), c}^\dagger \bar{f}_{\bar{q}(\iota k_F \downarrow), s1} \sum_{q=-2k_F}^{2k_F} \Theta(k_F \downarrow - |k+q|) \bar{f}_{\bar{q}(q), c} \bar{f}_{\bar{q}(k+q), s1}^\dagger,
\end{aligned} \tag{73}$$

where the shift parameters Φ_β^0 whose value results from the ground-state transition to the excited energy eigenstates are those in Eq. (43) for $\beta = c, s1$, $\bar{q}(q) = q + 2\pi \Phi_\beta(q)/L$, and the capital- Θ distribution $\Theta(x)$ is given here and in the following by $\Theta(x) = 1$ for $x \geq 0$ and $\Theta(x) = 0$ for $x < 0$. The momentum $\mp k_{F\downarrow}$ resulting from the $s1$ pseudofermion annihilation at $\bar{q}(\pm k_{F\downarrow})$ exactly cancels the momentum $\pm k_{F\downarrow}$ stemming from the overall $s1$ band momentum shift $q_j \rightarrow q_j \pm \pi/L$ associated with $\Phi_{s1}^0 = \pm 1/2$.

Within a k extended zone scheme, the $\omega < 0$ spectrum generated by application of the \uparrow one-electron removal leading-order generator, Eq. (73), onto the ground state reads $-\omega = -\varepsilon_c(q) + \varepsilon_{s1}(k+q)$ and has the following two branches,

$$\begin{aligned} -\omega(k) &= -\varepsilon_c(q) + \varepsilon_{s1}(q'); & k &= -q + q', \\ k &\in [-k_{F\uparrow}, (2k_F + k_{F\uparrow})]; & q &\in [-2k_F, 2k_F]; & q' &\in [k_{F\downarrow}, k_{F\uparrow}], & \text{branch } A, \\ k &\in [-(2k_F + k_{F\uparrow}), k_{F\uparrow}]; & q &\in [-2k_F, 2k_F]; & q' &\in [-k_{F\uparrow}, -k_{F\downarrow}], & \text{branch } B. \end{aligned} \quad (74)$$

In the case of the \uparrow one-electron LHB addition processes (2) the leading-order operator is given by,

$$\begin{aligned} c_{k,\uparrow}^\dagger &\approx \hat{g}_\iota(k) \hat{c}_\odot, \\ \hat{c}_\odot &= \bar{f}_{\pm 2k_F, c}^\dagger; & \Phi_c^0 &= 0; & \Phi_{s1}^0 &= \iota/2, & \iota &= \pm 1, \\ \hat{g}_\iota(k) &= \bar{f}_{\bar{q}(\pm 2k_F), c} \bar{f}_{\bar{q}(-\iota k_{F\downarrow}), s1}^\dagger \left(\sum_{q=-\pi}^{-2k_F} + \sum_{q=2k_F}^{\pi} \right) \Theta(k_{F\downarrow} - |k - q|) \bar{f}_{\bar{q}(q), c}^\dagger \bar{f}_{\bar{q}(-k+q), s1}, \end{aligned} \quad (75)$$

where the momentum $\mp k_{F\downarrow}$ resulting from the $s1$ pseudofermion creation at $\bar{q}(\mp k_{F\downarrow})$ exactly cancels again the momentum $\pm k_{F\downarrow}$ stemming from an overall $s1$ band momentum shift $q_j \rightarrow q_j \pm \pi/L$ that occurs under the ground-state transition to the excited energy eigenstates.

The $\omega > 0$ spectrum generated by application of the \uparrow one-electron LHB addition leading-order generator, Eq. (75), onto the ground state reads $\omega = \varepsilon_c(q) - \varepsilon_{s1}(k - q)$ and has within a k extended zone scheme again two branches,

$$\begin{aligned} \omega(k) &= \varepsilon_c(q) - \varepsilon_{s1}(q'); & k &= q - q', \\ k &\in [k_{F\uparrow}, (\pi + k_{F\downarrow})]; & q &\in [2k_F, \pi]; & q' &\in [-k_{F\downarrow}, k_{F\downarrow}], & \text{branch } A, \\ k &\in [-(\pi + k_{F\downarrow}), -k_{F\uparrow}]; & q &\in [-\pi, -2k_F]; & q' &\in [-k_{F\downarrow}, k_{F\downarrow}], & \text{branch } B. \end{aligned} \quad (76)$$

In the case of the \uparrow one-electron UHB addition processes (3) the leading-order operator reads,

$$\begin{aligned} c_{k,\uparrow}^\dagger &\approx \hat{g}_\iota(k) \hat{c}_\odot, \\ \hat{c}_\odot &= \bar{f}_{\iota 2k_F, c} \bar{f}_{\pm k_{F\downarrow}, s1} \bar{f}_{-\iota(\pi - 2k_F), \eta 1}^\dagger; & \Phi_c^0 &= \Phi_{s1}^0 = 0, & \iota &= \pm 1, \\ \hat{g}_\iota(k) &= \bar{f}_{\bar{q}(\iota 2k_F), c}^\dagger \bar{f}_{\bar{q}(\pm k_{F\downarrow}), s1}^\dagger \sum_{q=-2k_F}^{2k_F} \Theta(k_{F\downarrow} - |k - \iota(\pi - 2k_F) + q|) \bar{f}_{\bar{q}(q), c} \bar{f}_{\bar{q}(-k + \iota(\pi - 2k_F) - q), s1}. \end{aligned} \quad (77)$$

In this case one has $N_{\eta 1}(q_j) = 1$ where $q_j = -\iota(\pi - 2k_F)$ and $M_{\eta, -1/2} = 1$ for the excited energy eigenstates in the general momentum expression, Eq. (24), so that the momentum $\pi M_{\eta, -1/2} = \pi$ combines with $(\pi - q_j) N_{\eta 1}(q_j) = \pi - q_j$ to give $2\pi - q_j = -q_j = \iota(\pi - 2k_F)$.

Within a k extended zone scheme, the $\omega > 0$ spectrum generated by application of the \uparrow one-electron UHB addition leading-order generator, Eq. (77), onto the ground state reads $\omega = 2\mu - \varepsilon_c(q) - \varepsilon_{s1}(k - \iota(\pi - 2k_F) + q)$ and has two branches corresponding to $\iota = \pm 1$,

$$\begin{aligned} \omega(k) &= 2\mu - \varepsilon_c(q) - \varepsilon_{s1}(q'); & k &= \iota(\pi - 2k_F) - q - q'; & q &\in [-2k_F, 2k_F]; & q' &\in [-k_{F\downarrow}, k_{F\downarrow}], \\ k &= (\pi - 2k_F) - q - q' \in [(\pi - 4k_F - k_{F\downarrow}), (\pi + k_{F\uparrow})], & & & & & \text{branch } A, \\ k &= -(\pi - 2k_F) - q - q' \in [-(\pi + k_{F\uparrow}), -(\pi - 4k_F - k_{F\downarrow})], & & & & & \text{branch } B. \end{aligned} \quad (78)$$

In the case of the \downarrow one-electron removal processes (4) the leading-order operator is given by,

$$\begin{aligned} c_{k,\downarrow} &\approx \hat{g}_\iota(k) \hat{c}_\odot, \\ \hat{c}_\odot &= \bar{f}_{\iota 2k_F, c} \bar{f}_{-\iota k_{F\downarrow}, s1}; & \Phi_c^0 &= \iota/2; & \Phi_{s1}^0 &= 0, & \iota &= \pm 1, \\ \hat{g}_\iota(k) &= \bar{f}_{\bar{q}(\iota 2k_F), c}^\dagger \bar{f}_{\bar{q}(-\iota k_{F\downarrow}), s1}^\dagger \sum_{q=-2k_F}^{2k_F} \Theta(k_{F\downarrow} - |k - \iota 2k_F + q|) \bar{f}_{\bar{q}(q), c} \bar{f}_{\bar{q}(-k + \iota 2k_F - q), s1}. \end{aligned} \quad (79)$$

The operator $\bar{f}_{\iota 2k_F, c}$ in \hat{c}_\odot leads to a momentum $-\iota 2k_F$ that exactly cancels the momentum $\iota 2k_F$ stemming from the overall c band momentum shift associated with $\Phi_c^0 = \iota/2$ whereas the operator $\bar{f}_{\bar{q}(\iota 2k_F), c}^\dagger$ in $\hat{g}_\iota(k)$ leads to a momentum contribution that restores such a momentum $\iota 2k_F$.

The $\omega < 0$ spectrum generated by application of the \downarrow one-electron removal leading-order generator, Eq. (79), onto the ground state reads $-\omega = -\varepsilon_c(q) - \varepsilon_{s1}(k - \iota 2k_F + q)$ and has two branches corresponding to $\iota = \pm 1$,

$$\begin{aligned} \omega(k) &= -\varepsilon_c(q) - \varepsilon_{s1}(q'); & k &= \iota 2k_F - q - q'; & q &\in [-2k_F, 2k_F]; & q' &\in [-k_{F\downarrow}, k_{F\downarrow}], \\ k &= 2k_F - q - q' \in [-k_{F\downarrow}, (4k_F + k_{F\uparrow})], & & & & & & \text{branch } A, \\ k &= -2k_F - q - q' \in [-(4k_F + k_{F\uparrow}), k_{F\downarrow}], & & & & & & \text{branch } B. \end{aligned} \quad (80)$$

In the case of the \downarrow one-electron LHB addition processes (5) the leading-order operator reads,

$$\begin{aligned} c_{k, \downarrow}^\dagger &\approx \hat{g}_\iota(k) \hat{c}_\odot, \\ \hat{c}_\odot &= \bar{f}_{-\iota 2k_F, c}^\dagger \bar{f}_{\iota k_{F\downarrow}, s1}^\dagger; & \Phi_c^0 &= \iota/2; & \Phi_{s1}^0 &= 0, & \iota &= \pm 1, \\ \hat{g}_\iota(k) &= \bar{f}_{\bar{q}(-\iota 2k_F), c} \bar{f}_{\bar{q}(\iota k_{F\downarrow}), s1} \\ &\times \left(\sum_{q=-\pi}^{-2k_F} + \sum_{q=2k_F}^{\pi} \right) \delta_{-\iota, \text{sgn}\{k - \iota 2k_F - q\}} \Theta(k_{F\uparrow} - |k - \iota 2k_F - q|) \Theta(|k - \iota 2k_F - q| - k_{F\downarrow}) \\ &\times \bar{f}_{\bar{q}(q), c}^\dagger \bar{f}_{\bar{q}(k - \iota 2k_F - q), s1}^\dagger. \end{aligned} \quad (81)$$

Here and throughout this paper one has that $\text{sgn}\{x\} = 1$ for $x > 0$, $\text{sgn}\{x\} = -1$ for $x < 0$, and $\text{sgn}\{x\} = 0$ for $x = 0$. The operator $\bar{f}_{-\iota 2k_F, c}^\dagger$ in the operator \hat{c}_\odot leads to a momentum $-\iota 2k_F$ that exactly cancels the momentum $\iota 2k_F$ stemming from the c band overall momentum shift whereas the operator $\bar{f}_{\bar{q}(-\iota 2k_F), c}$ in $\hat{g}_\iota(k)$ leads to a momentum contribution that restores such a momentum $\iota 2k_F$.

Within a k extended zone scheme the $\omega > 0$ spectrum generated by application of the \downarrow one-electron LHB addition leading-order generator, Eq. (81), onto the ground state reads $\omega = \varepsilon_c(q) + \varepsilon_{s1}(k - \iota 2k_F - q)$ and has four branches,

$$\begin{aligned} \omega(k) &= \varepsilon_c(q) + \varepsilon_{s1}(q'); & k &= \iota 2k_F + q + q'; & \text{sgn}\{q'\} &= -\iota \text{ for } q' \neq 0, \\ k &= 2k_F + q + q' \in [(4k_F + k_{F\uparrow}), (\pi + 2k_F + k_{F\uparrow})], & & & & & & \text{branch } A, \\ & & q &\in [2k_F, \pi]; & q' &\in [k_{F\downarrow}, k_{F\uparrow}], \\ k &= 2k_F + q + q' \in [-(\pi - 2k_F - k_{F\downarrow}), k_{F\uparrow}], & & & & & & \text{branch } B, \\ & & q &\in [-\pi, -2k_F]; & q' &\in [k_{F\downarrow}, k_{F\uparrow}], \\ k &= -2k_F + q + q' \in [-(\pi + 2k_F + k_{F\uparrow}), -(4k_F + k_{F\uparrow})], & & & & & & \text{branch } A', \\ & & q &\in [-\pi, -2k_F]; & q' &\in [-k_{F\uparrow}, -k_{F\downarrow}], \\ k &= -2k_F + q + q' \in [-k_{F\uparrow}, (\pi - 2k_F - k_{F\downarrow})], & & & & & & \text{branch } B', \\ & & q &\in [2k_F, \pi]; & q' &\in [-k_{F\uparrow}, -k_{F\downarrow}]. \end{aligned} \quad (82)$$

In the case of the UHB addition of one \downarrow electron processes (6) the leading-order operator is given by,

$$\begin{aligned} \hat{c}_{k, \downarrow}^\dagger &\approx \hat{g}(k) \hat{c}_\odot, \\ \hat{c}_\odot &= \bar{f}_{\iota 2k_F, c} \bar{f}_{-\iota(\pi - 2k_F), \eta 1}^\dagger; & \Phi_c^0 &= \iota/2; & \Phi_{s1}^0 &= \pm 1/2, & \iota &= \pm 1, \\ \hat{g}(k) &= \bar{f}_{\bar{q}(\iota 2k_F), c}^\dagger \bar{f}_{\bar{q}(\pm k_{F\downarrow}), s1} \sum_{q=-2k_F}^{2k_F} \Theta(k_{F\downarrow} - |k - \iota \pi + q|) \bar{f}_{\bar{q}(q), c} \bar{f}_{\bar{q}(k - \iota \pi + q), s1}^\dagger. \end{aligned} \quad (83)$$

The operator $\bar{f}_{\iota 2k_F, c}$ in \hat{c}_\odot leads to a momentum $-\iota 2k_F$ that exactly cancels the momentum $\iota 2k_F$ stemming from the c band overall momentum shift whereas the operator $\bar{f}_{\bar{q}(\iota 2k_F), c}^\dagger$ in $\hat{g}_\iota(k)$ leads to a momentum contribution that restores such a momentum $\iota 2k_F$. The latter momentum is finally cancelled by the momentum $-\iota 2k_F$ from the second term of the momentum $\iota(\pi - 2k_F)$ stemming from $\bar{f}_{-\iota(\pi - 2k_F), \eta 1}^\dagger$. Indeed, as in the case of the \uparrow one-electron UHB addition processes (3), Eq. (77), one has $N_{\eta 1}(q_j) = 1$ where $q_j = -\iota(\pi - 2k_F)$ and $M_{\eta, -1/2} = 1$ for the excited energy eigenstates in the general momentum expression, Eq. (24), so that the momentum $\pi M_{\eta, -1/2} = \pi$ combines with $(\pi - q_j) N_{\eta 1}(q_j) = \pi - q_j$ to give $2\pi - q_j = -q_j = \iota(\pi - 2k_F)$. Moreover, the momentum $\mp k_{F\downarrow}$ resulting from the

$s1$ pseudofermion annihilation at $\bar{q}(\pm k_{F\downarrow})$ exactly cancels the momentum $\pm k_{F\downarrow}$ stemming from the $s1$ band overall momentum shift.

The $\omega > 0$ spectrum generated by application of the \downarrow one-electron UHB addition leading-order generator, Eq. (83), onto the ground state reads $\omega = 2\mu - \varepsilon_c(q) + \varepsilon_{s1}(k - \iota\pi + q)$ and has within a k extended zone scheme the following two branches,

$$\begin{aligned} \omega(k) &= 2\mu - \varepsilon_c(q) + \varepsilon_{s1}(q'); & k &= \iota\pi - q + q' = \pi - q + q', \\ k &\in [(\pi - k_{F\uparrow}), (\pi + 2k_F + k_{F\uparrow})]; & q &\in [-2k_F, 2k_F]; & q' &\in [k_{F\downarrow}, k_{F\uparrow}], & \text{branch } A, \\ k &\in [(\pi - 2k_F - k_{F\uparrow}), (\pi + k_{F\uparrow})]; & q &\in [-2k_F, 2k_F]; & q' &\in [-k_{F\uparrow}, -k_{F\downarrow}], & \text{branch } B. \end{aligned} \quad (84)$$

In the above expressions, the c and/or $s1$ pseudofermion momentum values $\pm 2k_F$ and $\pm k_{F\downarrow}$, respectively, appearing in the operators \hat{c}_\circ belong to the initial ground state $\beta = c, s1$ band whereas the β pseudofermion momentum values $\bar{q}(q) = q + 2\pi\Phi_\beta(q)/L$ in the operators $\hat{g}(k)$ expressions belong to the excited energy eigenstates $\beta = c, s1$ bands.

C. The σ one-electron operators matrix elements between the ground state and the excited energy eigenstates and corresponding spectral functions in terms of $\beta = c, s1$ pseudofermion spectral functions

The σ one-electron spectral functions, Eq. (4), can be written in the pseudofermion representation as follows,

$$B(k, \omega) = \sum_{i'=0}^{\infty} \sum_{\nu} |\langle \nu | \hat{g}_{i'}(k) \hat{c}_\circ | GS \rangle|^2 \delta(\omega - \gamma(E_\nu - E_{GS})), \quad \gamma\omega > 0, \quad (85)$$

where for simplicity we have omitted from $B(k, \omega)$ the labels σ and $\gamma = \pm 1$ and denoted the excited-state indices ν^- and ν^+ generally by ν .

Following the above properties, one approximates the general spectral function, Eq. (85), by its pseudofermion leading-order term involving the operators given in Eqs. (73), (75), (77), (79), (81), and (83),

$$B(k, \omega) \approx B^\circ(k, \omega) = \sum_{\nu} |\langle \nu | \hat{g}(k) \hat{c}_\circ | GS \rangle|^2 \delta(\omega - \gamma(E_\nu - E_{GS})), \quad \gamma\omega > 0. \quad (86)$$

Both the generator onto the electron vacuum of the initial ground state in Eq. (60) and the operator \hat{c}_\circ in $\hat{c}_\circ | GS \rangle$ are written in terms of c and $s1$ pseudofermion creation and/or annihilation operators, Eqs. (57) and (59), whose discrete canonical momentum values equal the corresponding momentum values q_j , Eqs. (20) and (21), of that initial ground state. In the case of the σ one-electron UHB addition operators in Eqs. (77) and (83), the expression of the operator \hat{c}_\circ includes as well a $\eta 1$ pseudofermion creation operator of canonical momentum $\pm(\pi - 2k_F)$.

On the other hand, both the operator $\hat{g}(k)$ and the generators onto the electron vacuum of the excited energy eigenstates $|\nu\rangle$ are written in terms of c and $s1$ pseudofermion operators whose discrete canonical momentum values \bar{q}_j , Eq. (56), are those of these excited energy eigenstates. Interestingly, there is always an exact excited energy eigenstate $|f_G\rangle$ of the final $N_\sigma \pm 1$ ground state $|GS_f\rangle$ such that,

$$|f_G\rangle = \hat{g}(k)|GS_f\rangle. \quad (87)$$

In the case of the c and $s1$ bands, the two types of discrete canonical momentum values that correspond to the initial ground state and excited energy eigenstates, respectively, account for the Anderson orthogonality catastrophe [33, 66] occurring in these bands under the transitions to the excited energy eigenstates $|\nu\rangle$. Such an Anderson orthogonality catastrophe is behind the exotic character of the quantum overlaps that control the one-electron spectral functions. On the other hand, since the initial ground state is not populated by $\eta 1$ pseudofermions and in the case of σ one-electron UHB addition the $\eta 1$ band limiting canonical momentum values $\pm(\pi - 2k_F)$ of the created $\eta 1$ pseudofermion are unchanged relative to the corresponding $\eta 1$ pseudoparticle momentum values, the σ one-electron operators matrix elements overlaps involving such a $\eta 1$ pseudofermion are straightforwardly computed.

The excitation $\hat{g}(k) \hat{c}_\circ | GS \rangle$ in the matrix elements of the spectral function expression, Eq. (86), has finite overlap with the corresponding specific energy eigenstate, Eq. (87), which gives,

$$\begin{aligned} \langle f_G | \hat{g}(k) \hat{c}_\circ | GS \rangle &= \langle GS_f^{\text{ex}} | \hat{c}_\circ | GS \rangle \\ &= \langle 0 | \prod_{\beta=c, s1} \bar{f}_{\bar{q}_{N_\beta^\circ, \beta}} \bar{f}_{\bar{q}_{2, \beta}} \bar{f}_{\bar{q}_{1, \beta}} \bar{f}_{q'_{1, \beta}} \bar{f}_{q'_{2, \beta}} \cdots \bar{f}_{q'_{N_\beta^\circ, \beta}} | 0 \rangle \\ &= \langle 0 | \prod_{\beta=c, s1} \bar{f}_{q'_{N_\beta^\circ, \beta}} \bar{f}_{q'_{2, \beta}} \bar{f}_{q'_{1, \beta}} \bar{f}_{\bar{q}_{1, \beta}} \bar{f}_{\bar{q}_{2, \beta}} \cdots \bar{f}_{\bar{q}_{N_\beta^\circ, \beta}} | 0 \rangle^*, \end{aligned} \quad (88)$$

where $|GS_f^{\text{ex}}\rangle$ is a state with the same c and $s1$ pseudofermion occupancy as $|GS_f\rangle$ but whose $\beta = c, s1$ band discrete momentum values are those of its excited energy eigenstate $|f_G\rangle = \hat{g}(k)|GS_f\rangle$ and N_β^\ominus is the number of $\beta = c$ and $\beta = s1$ pseudofermions of the states $\hat{c}_\ominus|GS\rangle$ and $|GS_f\rangle$.

The $\beta = c, s1$ bands discrete canonical momentum values $q'_1, q'_2, \dots, q'_{N_\beta^\ominus}$ in Eq. (88) equal the corresponding initial ground state discrete momentum values whereas $\bar{q}_1, \bar{q}_2, \dots, \bar{q}_{N_\beta^\ominus}$ are the discrete canonical momentum values of the excited energy eigenstate $|f_G\rangle$, Eq. (87). Since these two sets of discrete momenta have different values, an Anderson orthogonality catastrophe occurs such that the excited energy eigenstates of general form,

$$\begin{aligned} |f_{Gc}\rangle &= \prod_{\beta=c,s1} \hat{g}_C(m_{\beta,+1}, m_{\beta,-1}) \hat{g}(k) |GS_f\rangle \\ &= \prod_{\beta=c,s1} \hat{g}_C(m_{\beta,+1}, m_{\beta,-1}) |f_G\rangle, \quad \beta = c, s1, \quad \iota = \pm 1, \end{aligned} \quad (89)$$

which result from application onto the state $|f_G\rangle$, Eq. (87), of the $\beta = c, s1$ generators $\hat{g}_C(m_{\beta,+1}, m_{\beta,-1})$ of the low-energy and small-momentum processes (C), also have overlap with the excitation $\hat{g}(k) \hat{c}_\ominus |GS\rangle$.

One then finds that,

$$\begin{aligned} \langle f_G | \prod_{\beta=c,s1} \hat{g}_C^\dagger(m_{\beta,+1}, m_{\beta,-1}) \hat{g}(k) \hat{c}_\ominus |GS\rangle &= \langle GS_f^{\text{ex}} | \prod_{\beta=c,s1} \hat{g}_C^\dagger(m_{\beta,+1}, m_{\beta,-1}) \hat{c}_\ominus |GS\rangle \\ &= \langle 0 | \prod_{\beta=c,s1} \bar{f}_{\bar{q}_{N_\beta^\ominus}, \beta} \dots \bar{f}_{\bar{q}_2, \beta} \bar{f}_{\bar{q}_1, \beta} \hat{g}_C^\dagger(m_{\beta,+1}, m_{\beta,-1}) \bar{f}_{q'_{1, \beta}}^\dagger \bar{f}_{q'_{2, \beta}}^\dagger \dots \bar{f}_{q'_{N_\beta^\ominus}, \beta}^\dagger |0\rangle \\ &= \langle 0 | \prod_{\beta=c,s1} \bar{f}_{q'_{N_\beta^\ominus}, \beta} \dots \bar{f}_{q'_{2, \beta}} \bar{f}_{q'_{1, \beta}} \hat{g}_C^\dagger(m_{\beta,+1}, m_{\beta,-1}) \bar{f}_{\bar{q}_1, \beta}^\dagger \bar{f}_{\bar{q}_2, \beta}^\dagger \dots \bar{f}_{\bar{q}_{N_\beta^\ominus}, \beta}^\dagger |0\rangle^* . \end{aligned} \quad (90)$$

The number of elementary $\beta = c, s1$ pseudofermion - pseudofermion-hole processes (C) of momentum $\pm 2\pi/L$ in the vicinity of the $\beta; \iota = \pm 1$ Fermi points of $|GS_f\rangle$ is denoted here and in the following by $m_{\beta, \iota} = 1, 2, 3, \dots$. Such processes conserve the number N_β^\ominus of $\beta = c, s1$ pseudofermions, so that the matrix elements, Eq. (90), have the same form as that in Eq. (88) but with the excited-state occupied discrete canonical momentum values $\bar{q}_1, \bar{q}_2, \dots, \bar{q}_{N_\beta^\ominus}$ in the vicinity of the $\beta = c, s1$ bands Fermi points being slightly different from those in that equation.

The function $B^\ominus(k, \omega)$, Eq. (86), is below expressed in terms of a sum of terms each of which is a convolution of c and $s1$ pseudofermion spectral functions. The expression of such pseudofermion spectral functions involves sums that run over the processes (C) numbers $m_{\beta, \iota} = 1, 2, 3, \dots$. It reads,

$$\begin{aligned} B_{Q_\beta}(k', \omega') &= \frac{L}{2\pi} \sum_{m_{\beta,+1}; m_{\beta,-1}} A_\beta^{(0,0)} a_\beta(m_{\beta,+1}, m_{\beta,-1}) \\ &\times \delta\left(\omega' - \frac{2\pi}{L} v_\beta \sum_{\iota=\pm 1} (m_{\beta, \iota} + \Delta_\beta^\iota)\right) \delta\left(k' - \frac{2\pi}{L} \sum_{\iota=\pm 1} \iota (m_{\beta, \iota} + \Delta_\beta^\iota)\right), \quad \beta = c, s1, \end{aligned} \quad (91)$$

where the $\beta = c, s1$ lowest peak weights $A_\beta^{(0,0)}$ are associated with a transition from the ground state to a PS excited energy eigenstate generated by processes (A) and (B), the relative weights $a_\beta = a_\beta(m_{\beta,+1}, m_{\beta,-1})$ are generated by additional processes (C) whose $\beta = c, s1$ generators $\hat{g}_C(m_{\beta,+1}, m_{\beta,-1})$ are those in Eq. (89), and Δ_β^ι refers to the functional $2\Delta_\beta^\iota = (\iota \delta N_{\beta, \iota}^F + \Phi_\beta(\iota q_{F\beta}))^2$ associated with the $\beta = c, s1$ pseudofermion number deviation $\delta N_{\beta, \iota}^F$ at the $\iota = \pm 1$ Fermi points and corresponding phase shift $2\pi \Phi_\beta(\iota q_{F\beta})$, Eq. (51), in units of 2π acquired by the $\beta = c, s1$ pseudofermions with momenta $\iota q_{F\beta} = \pm q_{F\beta}$ under the above transition. This functional plays a key role in the PDT and is found below to emerge naturally from the $\beta = c, s1$ pseudofermion spectral weights.

In the case of σ one-electron UHB addition, the $\beta = c, s1$ weights $A_\beta^{(0,0)} a_\beta(m_{\beta,+1}, m_{\beta,-1})$ in Eq. (91) are reached after the quantum overlap stemming from creation of the $\eta 1$ pseudofermion is trivially computed. For all the σ one-electron removal, LHB addition, and UHB addition processes that contribute to the spectral functions in the vicinity of their singular features the $\beta = c, s1$ weights $A_\beta^{(0,0)} a_\beta(m_{\beta,+1}, m_{\beta,-1})$ have the general form,

$$|\langle 0 | \bar{f}_{q'_{N_\beta^\ominus}, \beta} \dots \bar{f}_{q'_{2, \beta}} \bar{f}_{q'_{1, \beta}} \bar{f}_{\bar{q}_1, \beta}^\dagger \bar{f}_{\bar{q}_2, \beta}^\dagger \dots \bar{f}_{\bar{q}_{N_\beta^\ominus}, \beta}^\dagger |0\rangle|^2, \quad \beta = c, s1, \quad (92)$$

where N_β^\ominus stands for the number of $\beta = c, s1$ pseudofermions of the excited energy eigenstate generated by the processes (A) and (B). Such matrix element square can be expressed in terms of a Slater determinant of $\beta = c, s1$

pseudofermion operators, Eqs. (57) and (59), as follows,

$$\left\| \begin{array}{ccc} \{\bar{f}_{\bar{q}_1, \beta}^\dagger, \bar{f}_{q'_1, \beta}\} & \{\bar{f}_{\bar{q}_1, \beta}^\dagger, \bar{f}_{q'_2, \beta}\} & \cdots \{\bar{f}_{\bar{q}_1, \beta}^\dagger, \bar{f}_{q'_{N_\beta^\odot}, \beta}\} \\ \{\bar{f}_{\bar{q}_2, \beta}^\dagger, \bar{f}_{q'_1, \beta}\} & \{\bar{f}_{\bar{q}_2, \beta}^\dagger, \bar{f}_{q'_2, \beta}\} & \cdots \{\bar{f}_{\bar{q}_2, \beta}^\dagger, \bar{f}_{q'_{N_\beta^\odot}, \beta}\} \\ \dots\dots\dots \\ \{\bar{f}_{\bar{q}_{N_\beta^\odot}, \beta}^\dagger, \bar{f}_{q'_1, \beta}\} & \{\bar{f}_{\bar{q}_{N_\beta^\odot}, \beta}^\dagger, \bar{f}_{q'_2, \beta}\} & \cdots \{\bar{f}_{\bar{q}_{N_\beta^\odot}, \beta}^\dagger, \bar{f}_{q'_{N_{s1}}, \beta}\} \end{array} \right\|^2, \quad \beta = c, s1. \quad (93)$$

The $\beta = c, s1$ pseudofermion operators matrix elements $\langle 0 | \bar{f}_{q'_{N_\beta^\odot}, \beta} \cdots \bar{f}_{q'_2, \beta} \bar{f}_{q'_1, \beta} \bar{f}_{\bar{q}_1, \beta}^\dagger \bar{f}_{\bar{q}_2, \beta}^\dagger \cdots \bar{f}_{\bar{q}_{N_\beta^\odot}, \beta}^\dagger | 0 \rangle$ in Eq. (92) are associated with the two factors of the product $\prod_{\beta=c, s1}$ in the matrix elements, Eq. (88).

The function $B^\odot(k, \omega)$, Eq. (86), can be written as follows,

$$B^\odot(k, \omega) = \sum_{\nu} \Theta(\Omega - \delta\omega_{\nu}) \Theta(\delta\omega_{\nu}) \Theta(|v_{\nu}| - v_{\bar{\beta}}) \check{B}_{\nu}^{\odot}(\delta\omega_{\nu}, v_{\nu}). \quad (94)$$

The summation \sum_{ν} runs here over excited energy eigenstates generated by processes (A), (B), and (C) of the general form, Eq. (89), at fixed values of k and ω . Such states have excitation energy and momentum, Eq. (96), in the ranges $\delta E_{\nu}^{\odot} \in [\omega - \Omega, \omega]$ and $\delta P_{\nu}^{\odot} \in [k - \Omega/v_{\nu}, k]$ where,

$$\begin{aligned} \delta\omega_{\nu} &= (\omega - \gamma \delta E_{\nu}^{\odot}) = (\omega - \gamma E_{\nu}^{\odot} + \gamma E_{GS}); & \delta k_{\nu} &= k - \delta P_{\nu}^{\odot}, \\ \delta E_{\nu} &= \gamma \delta E_{\nu}^{\odot} + \delta\omega_{\nu} = \omega; & P_{\nu} &= \delta P_{\nu}^{\odot} + \delta k_{\nu} = k. \end{aligned} \quad (95)$$

Here the energy and momentum spectra,

$$\delta E_{\nu}^{\odot} = E_{\nu}^{\odot} - E_{GS}; \quad \delta P_{\nu}^{\odot} = P_{\nu}^{\odot} - P_{GS}, \quad (96)$$

are those of the excited energy eigenstates $|f_G\rangle$, Eq. (87), generated by the processes (A) and (B), which have finite quantum overlap with the excitation $\hat{g}(k) \hat{c}_{\odot} |GS\rangle$. The velocities in Eq. (94) read,

$$v_{\nu} = \delta\omega_{\nu} / \delta k_{\nu}; \quad v_{\bar{\beta}} = \min\{v_c, v_{s1}\}; \quad v_{\beta} = \max\{v_c, v_{s1}\}, \quad (97)$$

where v_c and v_{s1} are the $\beta = c, s1$ Fermi velocities, Eq. (50). The energy deviation $\delta E_{\nu} = \omega$ and momentum deviation $\delta P_{\nu} = k$ in Eq. (95) denote the excitation energy and momentum of the excited energy eigenstates, respectively. Ω is the processes (C) energy range. It is self-consistently determined as that for which the velocity v_{ν} , Eq. (95), remains nearly unchanged.

The lack of c and $s1$ pseudofermion interaction terms in the PS finite- u energy spectrum, Eq. (67), enables the function $\check{B}_{\nu}^{\odot}(\delta\omega_{\nu}, v_{\nu})$ in Eq. (94) being expressed as the following convolution of c and $s1$ pseudofermion spectral functions, Eq. (91),

$$\check{B}_{\nu}^{\odot}(\delta\omega_{\nu}, v_{\nu}) = \frac{\text{sgn}(v_{\nu})}{2\pi} \int_0^{\delta\omega_{\nu}} d\omega' \int_{-\text{sgn}(v_{\nu})\delta\omega_{\nu}/v_{\beta}}^{+\text{sgn}(v_{\nu})\delta\omega_{\nu}/v_{\beta}} dk' B_{Q_{\bar{\beta}}}(\delta\omega_{\nu}/v_{\nu} - k', \delta\omega_{\nu} - \omega') B_{Q_{\beta}}(k', \omega'). \quad (98)$$

Here $\bar{\beta} = c, s1$ and $\beta = s1, c$, respectively, are chosen according to the criterion, Eq. (97), concerning the relative magnitudes of the two c and $s1$ Fermi velocities, Eq. (50).

In addition to leading to a non-interacting like spectral-function matrix-element overlap, the σ one-electron UHB addition processes involving the creation of one $\eta 1$ pseudofermion of momentum $\pm(\pi - 2k_F)$ are accounted for by their contributions 2μ and $\mp(\pi - 2k_F)$ to the excitation energy and momentum spectra δE^{\odot} and δP^{\odot} , Eq. (96), respectively. On the other hand and as mentioned above, under transitions from the present $n_e \in [0, 1[$ and $m \in [0, n_e]$ initial ground states, the zero-momentum $q_{\eta, +1/2} = 0$ and $q_{s, +1/2} = 0$, Eq. (25), and zero-energy $\varepsilon_{\eta, +1/2} = 0$ and $\varepsilon_{s, +1/2} = 0$, Eq. (45), unpaired $+1/2$ rotated η -spin and unpaired $+1/2$ rotated spin processes are accounted for by the c and $s1$ pseudofermion holes, respectively. This follows from they playing the role of unoccupied sites of the c and $s1$ effective lattices, respectively.

The Slater determinant of $\beta = c, s1$ pseudofermion operators, Eq. (93), involves the pseudofermion anti-commutators. The apparent simplicity of such a Slater determinant masks the complexity of the main technical problem of the PDT, which lays in performing the state summations in the spectral functions Lehmann representation, Eq. (4). As reported in the following, it results from the involved form of such anti-commutators and thus of the corresponding Slater determinants of $\beta = c, s1$ pseudofermion operators.

The unitarity of the pseudoparticle - pseudofermion transformation implies that the local $\beta = c, s1$ pseudofermion operators $f_{j',\beta}^\dagger$ and $\bar{f}_{j',\beta}$ in Eq. (59) obey the following fermionic algebra similar to that in Eqs. (36) and (39) for the corresponding local $\beta = c, s1$ pseudoparticle operators,

$$\{f_{j,\beta}^\dagger, \bar{f}_{j',\beta}\} = \delta_{j,j'}, \quad \beta = c, s1. \quad (99)$$

Consider two $\beta = c, s1$ pseudofermions of canonical momentum \bar{q}_j and $\bar{q}_{j'}$, respectively. Here \bar{q}_j and $\bar{q}_{j'} = q_{j'}$ correspond to the $\beta = c, s1$ bands of a PS excited energy eigenstate and the corresponding ground state, respectively. Due to the $\beta = c, s1$ pseudofermion phase-shift functional $2\pi \Phi_\beta(q_j)$, Eq. (51), being incorporated in the canonical momentum, Eq. (56), one straightforwardly finds from the use of Eqs. (59) and (99) that the anti-commutator of $f_{j',\beta}^\dagger$ and $\bar{f}_{j',\beta}$ reads,

$$\{f_{\bar{q}_j,\beta}^\dagger, \bar{f}_{\bar{q}_{j'},\beta}\} = \frac{1}{L_\beta} e^{-i(\bar{q}_j - \bar{q}_{j'})/2} e^{i2\pi \Phi_\beta^T(q_j)/2} \frac{\sin(2\pi \Phi_\beta^T(q_j)/2)}{\sin([\bar{q}_j - \bar{q}_{j'}]/2)}; \quad \Phi_\beta^T(q_j) = \Phi_\beta^0 + \Phi_\beta(q_j), \quad \beta = c, s1, \quad (100)$$

whereas $\{f_{\bar{q}_j,\beta}^\dagger, \bar{f}_{\bar{q}_{j'},\beta}^\dagger\} = \{\bar{f}_{\bar{q}_j,\beta}, \bar{f}_{\bar{q}_{j'},\beta}\} = 0$. Here $2\pi \Phi_\beta^T(q_j)$ is the overall phase shift acquired by a $\beta = c, s1$ pseudofermion of momentum q_j under the transition from the ground state to the PS excited energy eigenstate, $2\pi \Phi_\beta^0$, Eq. (43), is the corresponding non-scattering part of that phase shift, and $2\pi \Phi_\beta(q_j)$, Eq. (51), is its scattering part.

For $2\pi \Phi_\beta^T(q_j) \rightarrow 0$ the anti-commutator relation, Eq. (100), would be the usual one, $\{f_{\bar{q}_j,\beta}^\dagger, \bar{f}_{\bar{q}_{j'},\beta}\} = \delta_{\bar{q}_j,\bar{q}_{j'}}$. That such an anti-commutator relation has not that simple form is the price to pay to render the $\beta = c, s1$ pseudofermions without interaction terms in their energy spectrum, which is of the form, Eq. (67). Indeed this is achieved by incorporating the β pseudofermion scattering phase shift $2\pi \Phi_\beta(q_j)$, Eq. (51), in the $\beta = c, s1$ band canonical momentum, Eq. (56). The unusual form, Eq. (100), of that anti-commutator relation is behind such a scattering phase shift controlling the spectral weight distributions of the σ one-electron spectral functions, Eq. (4), as confirmed below.

The unitarity of the pseudoparticle - pseudofermion transformation would preserve the pseudoparticle operator algebra provided that the sets of $\beta = c, s1$ band $j = 1, \dots, L_\beta$ and $j' = 1, \dots, L_\beta$ canonical momentum values $\{\bar{q}_j\}$ and $\{\bar{q}_{j'}\}$, respectively, were the same. The exotic form of the anti-commutator, Eq. (100), follows from \bar{q}_j and $\bar{q}_{j'}$ corresponding to different sets of slightly shifted canonical momentum values. This is due to the shakeup effects introduced by the state-dependent $\beta = c, s1$ pseudofermion scattering phase-shift functional $2\pi \Phi_\beta(q_j)$.

The derivation of the spectral weights in the $\beta = c, s1$ pseudofermion spectral functions, Eq. (91), which include the $\beta = c, s1$ lowest peak weights $A_\beta^{(0,0)}$ generated by processes (A) and (B) and the relative weights $a_\beta = a_\beta(m_{\beta,+1}, m_{\beta,-1})$ generated by processes (C) resulting from the application of the $\beta = c, s1$ operators $\hat{g}_C(m_{\beta,+1}, m_{\beta,-1})$, Eq. (89), onto the energy eigenstates generated by the processes (A) and (B), proceeds much as for the corresponding $u \rightarrow \infty$ spinless fermion spectral function in Ref. [33]. Following the procedures of such a reference, after some algebra that involves the use of the pseudofermion anti-commutators, Eq. (100), in Eq. (93) one arrives to the expressions given in Eqs. (A25) of Appendix A for the lowest peak weights $A_\beta^{(0,0)}$ and in Eqs. (A26) and (A27) of that Appendix for the relative weights $a_\beta = a_\beta(m_{\beta,+1}, m_{\beta,-1})$.

Also the corresponding computation of the one-electron spectral-weight (k, ω) -plane distributions follows steps similar to those used in Ref. [33]. The PDT is indeed an extension to finite u of the method used in that reference for $u \rightarrow \infty$ [38]. Note though that the mapping to a Heisenberg chain used in that reference to deal with the spin part of the problem is valid only at $m = 0$ and $u \gg 1$. In our case for which u is finite and $m \in [0, n_e]$ the alternative use of the $s1$ pseudofermion representation renders the treatment of the corresponding rotated spins $1/2$ formally similar to that of the related c pseudofermion representation.

For $m_{\beta,\iota} = 1$ the relative weights given in Eq. (A27) of Appendix A read,

$$2\Delta_\beta^\iota \equiv a_{\beta,\iota}(1) = \left(\frac{\delta \bar{q}_{F\beta}^\iota}{(2\pi/L)} \right)^2 = (\iota \delta N_{\beta,\iota}^F + \Phi_\beta(\iota q_{F\beta}))^2, \quad \beta = c, s1, \quad \iota = \pm 1. \quad (101)$$

These four $\beta = c, s1$ and $\iota = \pm 1$ relative weights $2\Delta_\beta^\iota \equiv a_{\beta,\iota}(1)$, which appear in the c and $s1$ pseudofermion spectral function expression, Eq. (91), are controlled by the $\beta = c, s1$ and $\iota = \pm 1$ Fermi-points pseudofermion scattering phase shifts $2\pi \Phi_\beta(\iota q_{F\beta})$, Eq. (51), and corresponding excited energy eigenstate canonical momentum deviations $\delta \bar{q}_{F\beta}^\iota = (\iota 2\pi \delta N_{\beta,\iota}^F + 2\pi \Phi_\beta(\iota q_{F\beta}))/L$. Here $\delta N_{\beta,\iota}^F = \delta N_{\beta,\iota}^{0,F} + \iota \Phi_\beta^0$ so that $\delta \bar{q}_{F\beta}^\iota = (\iota 2\pi \delta N_{\beta,\iota}^{0,F} + 2\pi \Phi_\beta^T(\iota q_{F\beta}))/L$. The bare deviation $\delta N_{\beta,\iota}^{0,F}$ accounts for the number of $\beta = c, s1$ pseudofermions created or annihilated at the right ($\iota = +1$)

and left ($\iota = +1$) $\beta = c, s1$ Fermi points. The overall deviation $\delta N_{\beta, \iota}^F$ accounts in addition to the non-scattering phase shifts Φ_{β}^0 .

For general PS excited energy eigenstates populated by c pseudofermions and composite αn pseudofermions with arbitrary numbers $n \geq 1$ of pairs such that $(\delta N_c + \delta N_{\text{ps}}^{SU(2)})/L \rightarrow 0$ as $L \rightarrow \infty$ where the deviations from the initial ground state refer to the number N_c of c pseudofermions and $N_{\text{ps}}^{SU(2)}$ of αn pseudofermions of the different αn branches, Eq. (22), the four $\beta = c, s1$ and $\iota = \pm 1$ functionals, Eq. (101), can be written as,

$$2\Delta_{\beta}^{\iota} = \left(\sum_{\beta'=c, s1} \left(\iota \xi_{\beta\beta'}^0 \frac{\delta N_{\beta'}^F}{2} + \xi_{\beta\beta'}^1 \delta J_{\beta'}^F \right) + \sum_{\beta''=c, \alpha n} \sum_{j'=1}^{L_{\beta''}} \Phi_{\beta, \beta''}(\iota q_{F\beta}, q_{j'}) \delta N_{\beta''}^{NF}(q_{j'}) \right)^2. \quad (102)$$

In this expression $\xi_{\beta\beta'}^0$ and $\xi_{\beta\beta'}^1$ are the $\beta = c, s1$ pseudofermion phase-shift parameters, Eq. (63), $\delta N_{\beta'}^F = \sum_{\iota=\pm 1} \delta N_{\beta', \iota}$, and $\delta J_{\beta'}^F = \frac{1}{2} \sum_{\iota=\pm 1} (\iota) \delta N_{\beta', \iota}$. The deviations $\delta N_{\beta''}^{NF}(q_{j'})$ refer to $\beta'' = c, \alpha n$ band momentum values $q_{j'}$, which for the $\beta'' = c, s1$ branches are away from the $\beta'' = c, s1$ Fermi points. (The c and $s1$ pseudofermion creation or annihilation at and in the vicinity of such points is rather accounted for by the deviations $\delta N_{\beta'}^F$ and $\delta J_{\beta'}^F$ in Eq. (102).)

A property that in the present TL plays a key role in our derivation of the σ one-electron spectral weights is that the δ -functions in the $\beta = c, s1$ pseudofermion spectral function expression, Eq. (91), impose that,

$$\frac{L}{4\pi v_{\beta}} (\omega' + \iota v_{\beta} k') - \Delta_{\beta}^{\iota} = m_{\beta, \iota}, \quad \beta = c, s1, \quad \iota = \pm 1. \quad (103)$$

That the quantity $((L/4\pi v_{\beta})(\omega' + \iota v_{\beta} k') - \Delta_{\beta}^{\iota})$ on the left-hand side of this equation is proportional to L implies that for any arbitrarily small k' and ω' values for which $0 < (\omega' + \iota v_{\beta} k')/(4\pi v) \ll 1$ the corresponding values of the $\iota = \pm 1$ integer numbers $m_{\beta, \iota} = ((L/4\pi v_{\beta})(\omega' + \iota v_{\beta} k') - \Delta_{\beta}^{\iota})$ are in the TL such that $m_{\beta, \iota} \gg 1$. Hence the following asymptotic behavior of the β, ι relative weight, Eq. (A27) of Appendix A, is *exact* within the TL and is thus used in the derivation of the spectral-function expressions given below,

$$a_{\beta, \iota}(m_{\beta, \iota}) \approx \frac{1}{\Gamma(2\Delta_{\beta}^{\iota})} \left(m_{\beta, \iota} + \Delta_{\beta}^{\iota} \right)^{2\Delta_{\beta}^{\iota} - 1}; \quad 2\Delta_{\beta}^{\iota} \neq 0, \quad \beta = c, s1, \quad \iota = \pm 1. \quad (104)$$

A relation also useful for such a derivation involves the $\beta = c, s1$ lowest peak weight $A_{\beta}^{(0,0)}$, Eq. (A25) of Appendix A, in the $\beta = c, s1$ pseudofermion spectral function $B_{Q_{\beta}}(k', \omega')$, Eq. (91). It reads,

$$A_{\beta}^{(0,0)} = \frac{F_{\beta}^{(0,0)}}{(L S_{\beta})^{-1+2\Delta_{\beta}^{+1}+2\Delta_{\beta}^{-1}}}, \quad \beta = c, s1. \quad (105)$$

Here $F_{\beta}^{(0,0)}$ and S_{β} are in the $L \rightarrow \infty$ limit independent of L and $2\Delta_c^{+1}$, $2\Delta_c^{-1}$, $2\Delta_{s1}^{+1}$, and $2\Delta_{s1}^{-1}$ are the four functionals, Eq. (102). (The product $S_c \times S_{s1} \approx 1$ is given by 1 both in the $u \rightarrow 0$ and $u \rightarrow \infty$ limits.)

In the general case in which the four $\beta = c, s1$ and $\iota = \pm 1$ parameters $2\Delta_{\beta}^{\iota}$ are finite, one finds that the $\beta = c, s1$ pseudofermion spectral function $B_{Q_{\beta}}(k', \omega')$, Eq. (91), reads in the TL,

$$\begin{aligned} B_{Q_{\beta}}(k', \omega') &= \frac{L}{4\pi v_{\beta}} A_{\beta}^{(0,0)} \prod_{\iota=\pm 1} a_{\beta, \iota} \left(\frac{\omega' + \iota v_{\beta} k'}{4\pi v_{\beta} L} \right) \\ &\approx \frac{F_{\beta}^{(0,0)}}{4\pi v_{\beta} S_{\beta}} \prod_{\iota=\pm 1} \frac{\Theta(\omega' + \iota v_{\beta} k')}{\Gamma(2\Delta_{\beta}^{\iota})} \left(\frac{\omega' + \iota v_{\beta} k'}{4\pi v_{\beta} S_{\beta}} \right)^{-1+2\Delta_{\beta}^{\iota}}, \quad \beta = c, s1. \end{aligned} \quad (106)$$

To reach the second expression, which in the TL is exact, Eqs. (104) and (105) were used. The $\beta = c, s1$ pseudofermion spectral functions, Eq. (91), have a different form when $2\Delta_{\beta}^{\iota} > 0$ and $2\Delta_{\beta}^{-\iota} = 0$, as given in Eq. (A28) of Appendix A. When $2\Delta_{\beta}^{\iota} = 2\Delta_{\beta}^{-\iota} = 0$ it is δ -function like, Eq. (A29) of that Appendix.

D. The small higher-order pseudofermion contributions to the σ one-electron spectral weight

The pseudofermion representation spectral functions expression, Eq. (85), includes all higher-order processes that generate little σ one-electron spectral weight and do not contribute to the line shape near singular spectral features

studied in this paper. The PDT also accounts for the corresponding contributions of ground-state transitions to excited energy eigenstates of general form,

$$|f_G(i')\rangle = \hat{g}_{i'}(k)|GS_f\rangle, \quad i' = 0, 1, \dots, \infty. \quad (107)$$

Those may be populated by αn pseudofermions of branches with $n > 1$ pairs. For finite values of the spin density, the small weight contribution from such transitions higher-order pseudofermion processes appear at high excitation energy scales, which for each created $n > 1$ αn pseudofermion is around $n 2\mu_\alpha$, Eq. (46).

The contribution to the σ electron operators matrix elements of the creation of such composite αn pseudofermions is simpler to compute than that of the c and $s1$ pseudofermions. As above for the $i' = 0$ operator $\hat{g}(k)$, the αn pseudofermion operators in the expression of any $i' \geq 0$ operator $\hat{g}_{i'}(k)$ in the spectral function expression, Eq. (85), and energy eigenstate, Eq. (107), have discrete canonical momentum values that belong to the excited energy eigenstate αn band. One then finds that,

$$\langle f_G|\hat{g}_{i'}(k)\hat{c}_\ominus|GS\rangle = \langle GS_f|\hat{g}_{i'}^\dagger(k)\hat{g}_{i'}(k)\hat{c}_\ominus|GS\rangle = \langle GS_f^{\text{ex}(i')}|\hat{c}_\ominus|GS\rangle, \quad (108)$$

where $|GS_f^{\text{ex}(i')}\rangle$ is a state with the same c and $s1$ pseudofermion occupancy as $|GS_f\rangle$ but whose c and $s1$ band discrete momentum values are those of its excited energy eigenstate $|f_G(i')\rangle = \hat{g}_{i'}(k)|GS_f\rangle$.

That the σ one-electron matrix elements quantum overlaps resulting from the creation of $n > 1$ αn pseudofermions by the operators $\hat{g}_{i'}^\dagger(k)\hat{g}_{i'}(k)$ in Eq. (108) are Fermi-liquid like is due to the lack of such occupancies in the ground states $|GS_f\rangle$ and $|GS\rangle$. Their creation is thus not associated with Anderson orthogonality catastrophes. This is why after computing such trivial quantum overlaps, one is left with matrix elements $\langle GS_f^{\text{ex}(i')}|\hat{c}_\ominus|GS\rangle$, Eq. (108), that only involve c and $s1$ pseudofermion operators and have the same general form as that in Eq. (88). The same applies to higher-order additional $\beta = c, s1$ pseudofermion particle-hole processes of type (A) also generated by the operators $\hat{g}_{i'}^\dagger(k)\hat{g}_{i'}(k)$.

However, $|\langle GS_f^{\text{ex}(i')}|\hat{c}_\ominus|GS\rangle|$ strongly decreases upon increasing the index $i' = 0, 1, \dots, \infty$, most of the spectral weight being associated with the $i' = 0$ matrix element $\langle GS_f^{\text{ex}(0)}|\hat{c}_\ominus|GS\rangle = \langle GS_f^{\text{ex}}|\hat{c}_\ominus|GS\rangle$, Eq. (88). As a result, the corresponding higher-order pseudofermion processes lead to very small σ one-electron spectral weight contributions. Moreover, the transitions to the excited energy eigenstates, Eq. (107), generated from the ground state by such higher-order pseudofermion processes do not contribute to the σ one-electron spectral weight in the vicinity of the singular features, which is the issue studied in this paper.

E. The involved state summations problem and analytical expressions obtainable near singular spectral features

The numerical computation of the momentum and state summations in Eqs. (85) and (86) needed to access the corresponding finite- u spectral-weight distributions over the whole (k, ω) plane is a very involved technical problem. This is a procedure that enormously simplifies in the $u \rightarrow \infty$ limit. The reason is that within it the c pseudofermion phase-shift functional $2\pi\Phi_c^T(q_j)$ defined by Eqs. (51) and (100) becomes independent of q_j , being the quantity called $Q' - Q$ in Ref. [33]. This enables, in the case of the $u \rightarrow \infty$ and $m = 0$ one-electron removal and LHB addition spectral functions, the numerical computation of all state summations. The authors of Refs. [32, 33] have performed that exercise. They obtained the beautiful one-electron spectral-weight distributions plotted in Fig. 1 of Ref. [32] for the whole (k, ω) plane, $u \gg 1$, $n_e = 0.5$, and $m = 0$.

On the other hand, for finite u values the $\beta = c, s1$ pseudofermion phase-shift functionals $\Phi_\beta^T(q_j)$ are both momentum q_j and densities n_e and m dependent and have different values for each excited energy eigenstate. Hence the numerical computation of the momentum and state summations needed to access the corresponding finite- u spectral-weight distributions over the whole (k, ω) plane becomes an extremely difficult technical task.

Fortunately, though, the use of Eq. (106) and Eqs. (A28) and (A29) of Appendix A for the β pseudofermion spectral function $B_{Q_\beta}(k', \omega')$, Eq. (91), in the function $\check{B}_\nu^\ominus(\delta\omega_\nu, \nu_\nu)$, Eq. (98), that appears in the expression of the spectral function leading-order term $B^\ominus(k, \omega)$, Eq. (94), enables partially performing the summations in the latter equation for the (k, ω) -plane vicinity of most σ one-electron singular spectral features.

An important such a feature is a *branch line*. In the present case of the σ one-electron spectral functions, Eq. (4), the one-parametric branch lines that at least for some momentum interval correspond to a singular feature are all contained in the two-parametric spectra given in Eqs. (74), (76), (78), (80), (82), and (84). Those correspond to excited energy eigenstates generated by the leading-order pseudofermion processes.

Such a branch line results from transitions to a well-defined subclass of these excited energy eigenstates. Specifically, a particle and hole branch line is generated by creation of one $\beta = c$, $s1$ pseudofermion and one $\beta = c$, $s1$ pseudofermion hole, respectively, of canonical momentum $\bar{q} = \bar{q}(q)$ corresponding to a well-defined β band momentum value q as defined by Eq. (56). The set of such transitions scans the whole corresponding β band momentum range. Specifically, for a $\beta = c$ branch line the c band momentum q runs in the intervals $q \in [-\pi, -2k_F]$ and $q \in [2k_F, \pi]$ for a particle branch line and in the range $q \in [-2k_F, 2k_F]$ for a hole branch line. In the case of a $\beta = s1$ branch line, the $s1$ band momentum q runs in the ranges $q \in [-k_{F\uparrow}, -k_{F\downarrow}]$ and $q \in [k_{F\downarrow}, k_{F\uparrow}]$ for a particle branch line and in the interval $q \in [-k_{F\downarrow}, k_{F\downarrow}]$ for a hole branch line.

For a c and $s1$ branch line, the $s1$ and c , respectively, pseudofermion or pseudofermion hole created under the transitions to the excited energy eigenstates whose two-parametric spectra are given in Eqs. (74), (76), (78), (80), (82), and (84) is added to one of the $\iota = \pm 1$ corresponding Fermi points. As given in Eqs. (77) and (83), in the case of σ one-electron UHB addition the corresponding $\eta 1$ pseudofermion is created at one of the $\eta 1$ band limiting momentum values, $q = \pm(\pi - 2k_F)$.

The PS excited energy eigenstates generated from the ground state by the types of processes described above have a one-parametric (k, ω) -plane $\beta = c$, $s1$ branch line spectrum,

$$\omega_\beta^\sigma(k) = \omega_0 + \varepsilon_\beta(q) \delta N_\beta(q); \quad k = k_0 + q \delta N_\beta(q), \quad \beta = c, s1, \quad (109)$$

where $\sigma = \uparrow, \downarrow$ refers to the one-electron spectral function under consideration, $\varepsilon_\beta(q)$ is the $\beta = c$, $s1$ band energy dispersion, Eq. (47), $\delta N_\beta(q) = +1$ and $\delta N_\beta(q) = -1$ for a particle and hole branch line, respectively, and the energy scale ω_0 and momentum k_0 are given by,

$$\begin{aligned} \omega_0 &= 2\mu \delta N_{\eta 1}, \quad \delta N_{\eta 1} = 0, 1, \\ k_0 &= 4k_F \delta J_c^F + 2k_{F\downarrow} \delta J_{s1}^F + 2(\pi - 2k_F) \delta J_{\eta 1}, \end{aligned} \quad (110)$$

respectively. Here the $\beta = c$, $s1$ current number deviations δJ_β^F are those in Eq. (102), $\delta N_{\eta 1} = \delta J_{\eta 1} = 0$ for both σ electron removal and σ electron LHB addition, $\delta N_{\eta 1} = 1$ and $\delta J_{\eta 1} = -\frac{1}{2} \sum_{\iota = \pm 1} (\iota) \delta N_{\eta 1, \iota} = \mp 1/2$ for σ electron UHB addition, and $\delta N_{\eta 1, \iota} = 1$ for creation of the $\eta 1$ pseudofermion at the $\iota = \pm 1$ limiting $\eta 1$ band momentum $\iota(\pi - 2k_F)$.

In the case of the (k, ω) -plane region in the vicinity of a $\beta = c$, $s1$ branch line, the summation \sum_ν in Eq. (94) runs over excited energy eigenstates with the specific k and ω values that appear in the argument of the corresponding function $B^\circ(k, \omega)$. At such fixed values, the two corresponding $\beta = c$, $s1$ lowest peak weights $A_\beta^{(0,0)}$, Eq. (A25) of Appendix A, have nearly the same magnitude for all such states. The state summations can then be partially performed. The technical details of such summations are provided in Appendix B of Ref. [38]. They lead to the following general behavior in the vicinity of a σ one-electron $\beta = c$, $s1$ branch line,

$$\begin{aligned} B_{\sigma, \gamma}(k, \omega) &= C_{\sigma, \gamma, \beta} \left(\gamma \omega - \omega_\beta^\sigma(k) \right)^{\xi_\beta^\sigma(k)}; \quad (\gamma \omega - \omega_\beta^\sigma(k)) \geq 0, \quad \gamma = \pm 1, \\ \xi_\beta^\sigma(k) &= -1 + \sum_{\beta' = c, s1} \sum_{\iota = \pm 1} 2\Delta_{\beta'}^\iota(q)|_{q=(k-k_0)\delta N_\beta(q)}. \end{aligned} \quad (111)$$

Here $C_{\sigma, \gamma, \beta}$ is a n_e , m , and u dependent constant that is independent of k and ω , $\omega \geq 0$ and $\omega \leq 0$ for $\gamma = 1$ and $\gamma = -1$, respectively, and $2\Delta_{\beta'}^\iota(q)$ refers to the following specific form that the functionals, Eq. (102), have for the excited energy eigenstates that control the σ one-electron spectral weight distribution near the $\beta = c$, $s1$ branch line,

$$\begin{aligned} 2\Delta_c^\iota(q) &= \left(\sum_{\beta' = c, s1} \left(\iota \xi_{c\beta'}^0 \frac{\delta N_{\beta'}^F}{2} + \xi_{c\beta'}^1 \delta J_{\beta'}^F \right) + \xi_{cc}^1 \delta J_{\eta 1} + \Phi_{c\beta}(\iota 2k_F, q) \delta N_\beta^{NF}(q) \right)^2, \\ 2\Delta_{s1}^\iota(q) &= \left(\sum_{\beta' = c, s1} \left(\iota \xi_{s1\beta'}^0 \frac{\delta N_{\beta'}^F}{2} + \xi_{s1\beta'}^1 \delta J_{\beta'}^F \right) + \xi_{s1c}^1 \delta J_{\eta 1} + \Phi_{s1\beta}(\iota k_{F\downarrow}, q) \delta N_\beta^{NF}(q) \right)^2. \end{aligned} \quad (112)$$

In these expressions one has that $\delta N_\beta^{NF}(q) = +1$ and $\delta N_\beta^{NF}(q) = -1$ for a particle and hole $\beta = c$, $s1$ branch line, respectively, and q is not at the $\beta = c$, $s1$ Fermi points. For the σ one-electron UHB addition energy eigenstates for which $\delta J_{\eta 1} = \mp 1/2$ the relation $\Phi_{\beta'', \eta 1}(\iota q_{F\beta''}, \pm(\pi - 2k_F)) = \pm \xi_{\beta''c}^1/2$, Eq. (65), was used to express the phase shift acquired by the $\beta'' = c$, $s1$ pseudofermions of $\iota = \pm 1$ Fermi momenta $\iota q_{F\beta''}$ due to the creation of the $\eta 1$ pseudofermion of $\eta 1$ band momentum $\pm(\pi - 2k_F)$.

In addition to the parameter,

$$\begin{aligned} \gamma &= -1 \quad \text{for electron removal,} \\ &= +1 \quad \text{for electron addition,} \end{aligned} \quad (113)$$

the one σ one-electron spectra associated with the singular spectral features considered in Sec. IV involve a second parameter γ_σ and the use of the symbol $\bar{\sigma}$ that are given by,

$$\begin{aligned}\gamma_\uparrow &= +1; & \bar{\uparrow} &= \downarrow, \\ \gamma_\downarrow &= -1; & \bar{\downarrow} &= \uparrow.\end{aligned}\quad (114)$$

That in Eq. (111) the $\beta = c, s1$ branch line spectrum $\omega_\beta^\sigma(k)$ is not multiplied by γ is justified by it being according to Eq. (109) always such that $\omega_\beta^\sigma(k) \geq 0$.

The σ one-electron spectral function line shapes near the branch lines, Eq. (111), are beyond the reach of the techniques associated with the low-energy Tomonaga-Luttinger-liquid. In the limit of low-energy, the PDT describes the well-known behaviors predicted by such techniques. This refers specifically to the vicinity of (k, ω) -plane points $(k_0, 0)$ of which (k_0, ω_0) is a generalization for $\omega_0 > 0$. Near them, the $\sigma = \uparrow, \downarrow$ one-electron spectral function $B_{\sigma, \gamma}(k, \omega)$, Eq. (4), behavior rather is [39],

$$\begin{aligned}B_{\sigma, \gamma}(k, \omega) &\propto (\gamma\omega - \omega_0)^{\zeta^\sigma}, & (\gamma\omega - \omega_0) &\geq 0, \\ \zeta^\sigma &= -2 + \sum_{\beta'=c, s1} \sum_{\iota=\pm 1} 2\Delta_{\beta'}^\iota, & (\gamma\omega - \omega_0) &\neq \pm v_\beta(k - k_0), \quad \beta = c, s1, \\ B_{\sigma, \gamma}(k, \omega) &\propto (\gamma\omega - \omega_0 \mp v_\beta(k - k_0))^{\zeta_\pm^\sigma}, & (\gamma\omega - \omega_0 \mp v_\beta(k - k_0)) &\geq 0, \\ \zeta_\pm^\sigma &= -1 - 2\Delta_\beta^{\mp 1} + \sum_{\beta'=c, s1} \sum_{\iota=\pm 1} 2\Delta_{\beta'}^\iota, & (\gamma\omega - \omega_0) &\approx \pm v_\beta(k - k_0), \quad \beta = c, s1,\end{aligned}\quad (115)$$

where the form of the $\beta' = c, s1$ functionals $2\Delta_{\beta'}^\iota$, Eq. (102), simplifies to,

$$\begin{aligned}2\Delta_c^\iota &= \left(\sum_{\beta'=c, s1} \left(\iota \xi_{c\beta'}^0 \frac{\delta N_{\beta'}^F}{2} + \xi_{c\beta'}^1 \delta J_{\beta'}^F \right) + \xi_{c c}^1 \delta J_{\eta 1} \right)^2, \\ 2\Delta_{s1}^\iota(q) &= \left(\sum_{\beta'=c, s1} \left(\iota \xi_{s1\beta'}^0 \frac{\delta N_{\beta'}^F}{2} + \xi_{s1\beta'}^1 \delta J_{\beta'}^F \right) + \xi_{s1 c}^1 \delta J_{\eta 1} \right)^2.\end{aligned}\quad (116)$$

The σ spectral function expressions, Eq. (115), apply to the small finite-weight region very near and above ($\gamma = 1$) or below ($\gamma = -1$) the (k, ω) -plane point (k_0, ω_0) .

There is a third type of σ one-electron spectral feature in the vicinity of which the PDT provides an analytical expression. It is generated by processes where one c pseudofermion or c pseudofermion hole is created at a momentum value q and one $s1$ pseudofermion or one $s1$ pseudofermion hole is created at a momentum value q' , such that their group velocities, Eq. (50), obey the equality $v_c(q) = v_{s1}(q')$. It corresponds to a $c - s1$ border line whose (k, ω) -plane spectrum is,

$$\omega_{c-s1}^\sigma(k) = (\omega_0 + |\epsilon_c(q)| + |\epsilon_{s1}(q')|) \delta_{v_c(q), v_{s1}(q')}; \quad k = k_0 + q \delta N_c(q) + q' \delta N_{s1}(q') \quad (117)$$

Whether each of the deviations $\delta N_c(q)$ and $\delta N_{s1}(q')$ reads $+1$ or -1 is unrelated and is specific to border line under consideration.

The following σ one-electron spectral function behavior in the vicinity of such a $c - s1$ border line,

$$B_{\sigma, \gamma}(k, \omega) \propto (\gamma\omega - \omega_{c-s1}^\sigma(k))^{-1/2}, \quad (\gamma\omega - \omega_{c-s1}^\sigma(k)) \geq 0, \quad (118)$$

is determined by the density of the two-parametric states generated upon varying q and q' within the corresponding c and $s1$ band values, respectively. A σ one-electron border line is part of the boundary line of the two-parametric spectra, Eqs. (74), (76), (78), (80), (82), and (84), (k, ω) -plane regions.

F. Validity of the expressions for the line shape near the singular spectral features

The general behavior $B_{\sigma, \gamma}(k, \omega) = C_{\sigma, \gamma, \beta} (\gamma\omega - \omega_\beta^\sigma(k))^{\xi_\beta^\sigma(k)}$ for small $(\gamma\omega - \omega_\beta^\sigma(k)) > 0$ in the vicinity of $\beta = c, s1$ branch lines, Eq. (111), also occurs in the case of two-particle dynamical correlation functions $B(k, \omega)$ for which the

convention is $\gamma = 1$ and $\omega \geq 0$. However, such a $B(k, \omega)$ expression near a $\beta = c, s1$ branch line is in that case exact provided that the branch line coincides with a lower threshold of the (k, ω) -plane finite spectral-weight region [40], *i.e.* for which $B(k, \omega) = 0$ for $(\omega - \omega_\beta(k)) < 0$.

The (k, ω) -plane spectral weight distribution of two-particle dynamical correlation functions is in general plateau-like. It then follows that for k ranges of a branch line for which $B(k, \omega) > 0$ for $(\omega - \omega_\beta(k)) < 0$ there is a sufficient amount of two-particle spectral weight just below the line for the coupling to that generated by the processes that contribute to the weight distribution as given in Eq. (111) changing the type of k and ω dependence for $(\omega - \omega_\beta(k)) > 0$. The microscopic processes behind such a coupling are accounted for by the PDT yet performing the corresponding state summations needed to reach a simple analytical expression for $B(k, \omega)$ at small $(\omega - \omega_\beta(k)) > 0$ turns out to be a complex technical problem.

In the present case of the σ one-electron spectral functions $B_{\sigma, \gamma}(k, \omega)$, Eq. (4), the behavior, Eq. (111), in the vicinity of a $\beta = c, s1$ branch line is exact for k ranges for which such a line coincides with a lower threshold ($\gamma = 1$) or an upper threshold ($\gamma = -1$) of the (k, ω) -plane finite spectral-weight regions associated with the corresponding two-parametric spectra. This requires that $B_{\sigma, \gamma}(k, \omega) = 0$ for $\gamma\omega < \omega_\beta^\sigma(k)$.

The physically more important $\beta = c, s1$ branch line k ranges are those for which the exponent $\xi_\beta^\sigma(k)$, Eq. (111), is negative and that line corresponds to a singular feature. Fortunately and in contrast to two-particle dynamical correlation functions, along the line k ranges for which $\xi_\beta^\sigma(k) < 0$ in Eq. (111) and $B_{\sigma, \gamma}(k, \omega) > 0$ for small $(\gamma\omega - \omega_\beta^\sigma(k)) < 0$ the corresponding spectral weight at $\gamma\omega < \omega_\beta^\sigma(k)$ is much smaller than that at $\gamma\omega > \omega_\beta^\sigma(k)$. As a result, the coupling of the small weight at $\gamma\omega < \omega_\beta^\sigma(k)$ to that at $\gamma\omega > \omega_\beta^\sigma(k)$ changes the distribution near the singular feature, Eq. (111), very little. The processes behind the small weight at $\gamma\omega < \omega_\beta^\sigma(k)$ are generated as well by the pseudofermion leading-order operator term that depending on the σ one-electron spectral function is one of the operators given in Eqs. (73), (75), (77), (79), (81), and (83). Indeed, the subclass of one-parametric processes that generate the line shape, Eq. (111), just above ($\gamma = +1$) or below ($\gamma = -1$) the branch line refers to a particular case of such more general two-parametric processes.

For the k ranges for which $B_{\sigma, \gamma}(k, \omega) > 0$ at $\gamma\omega < \omega_\beta^\sigma(k)$, the spectral function $B_{\sigma, \gamma}(k, \omega)$ remains having the power-law like behavior, Eq. (111), in the vicinity of the line for $\gamma\omega > \omega_\beta^\sigma(k)$. Specifically, the line spectrum $\omega_\beta^\sigma(k)$, Eq. (109), remains insensitive to the coupling, which only slightly affects the value of the exponent $\xi_\beta^\sigma(k)$. Such an effect is small and very small when $0 < \xi_\beta^\sigma(k) < 1$ and $\xi_\beta^\sigma(k) < 0$, respectively, in Eq. (111). The theory includes actually a small k dependent parameter,

$$\gamma_{\sigma, \gamma}(k) = \left(\frac{\int_{\omega_\beta^\sigma(k) - \Omega}^{\omega_\beta^\sigma(k)} B_{\sigma, \gamma}(k, \omega) d\omega}{\int_{\omega_\beta^\sigma(k)}^{\omega_\beta^\sigma(k) + \Omega} B_{\sigma, \gamma}(k, \omega) d\omega} \right)^\gamma, \quad \gamma = \pm 1. \quad (119)$$

Here Ω stands for the processes (C) energy range for $\omega > \gamma\omega_\beta^\sigma(k)$. It is self-consistently determined as that for which the velocity v_ν , Eq. (95), remains nearly unchanged. One can then expand the exponent expression in that small parameter, the zeroth order leading term being $\xi_\beta^\sigma(k)$, as given in Eq. (111).

In the vicinity of the line k ranges for which $\xi_\beta^\sigma(k)$, Eq. (111), is negative there is a much larger amount of spectral weight for $\omega > \gamma\omega_\beta^\sigma(k)$ than for $\omega < \gamma\omega_\beta^\sigma(k)$. The k dependent parameter, Eq. (119), is thus extremely small for such k intervals, *i.e.* $\gamma_{\sigma, \gamma}(k) \ll 1$. Since the corresponding exponent corrections are also extremely small and do not change the physics, for simplicity in the studies of Sec. IV we use the leading-order exponent expression $\xi_\beta^\sigma(k)$, Eq. (111). The otherwise very small exponent corrections vanish in a $\beta = c, s1$ branch line k ranges for which it coincides with the a lower threshold ($\gamma = 1$) or upper threshold ($\gamma = -1$) of the (k, ω) -plane finite spectral-weight region.

Moreover, the σ one-electron spectral function expression near a $\beta = c, s1$ branch line, Eq. (111), is valid provided that the exponent in it obeys the inequality $\xi_\beta^\sigma(k) > -1$. When for a given $\beta = c, s1$ branch line k range one finds that $\xi_\beta^\sigma(k) = -1$, the exact expression of the spectral function is not that given in Eq. (111). For these k ranges one has that the four functionals $2\Delta_\beta^\iota$, Eq. (116) for $\beta = c, s1$ and $\iota = \pm 1$, vanish. This corresponds to the $\beta = c, s1$ pseudofermion spectral function form, Eq. (A29) of Appendix A. One then finds that the corresponding σ one-electron spectral function behavior is also δ -function-like and given by,

$$B_{\sigma, \gamma}(k, \omega) = \delta(\gamma\omega - \omega_\beta^\sigma(k)). \quad (120)$$

As expected, it is confirmed in the ensuing section that only as $u \rightarrow 0$ some $\beta = c, s1$ branch line exponents read $\xi_\beta^\sigma(k) = -1$. For the corresponding k momentum ranges one recovers parts of the exact $u = 0$ σ one-electron spectrum, with $\omega_\beta^\sigma(k)$ on the right-hand side of Eq. (120) becoming the corresponding non-interacting electronic spectrum. This is confirmed by accounting for the $u \rightarrow 0$ limiting behaviors of the $\beta = c, s1$ energy dispersions $\varepsilon_\beta(q)$ appearing in the spectrum $\omega_\beta^\sigma(k)$, Eq. (109). Such limiting behaviors are reported in Eqs. (B1) and (B2) of Appendix B.

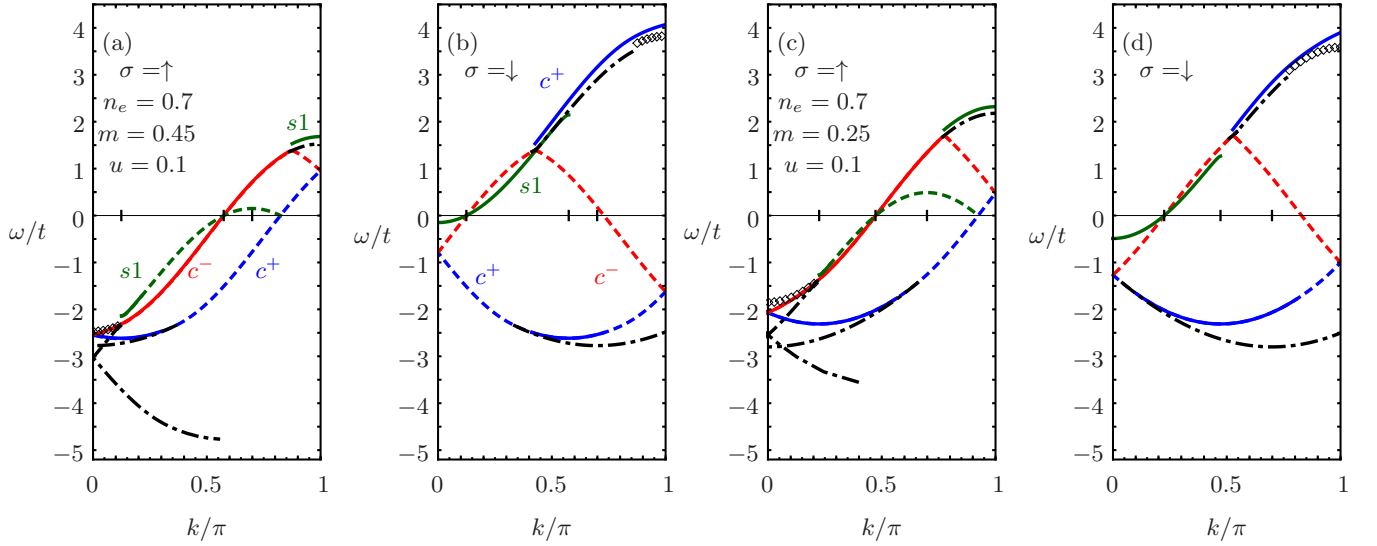


Figure 1: The (k, ω) -plane singular branch lines k ranges (solid lines) and other branch lines k ranges (dashed lines) for which the corresponding exponent $\xi_{\beta}^{\sigma}(k)$, Eq. (111), is negative and positive, respectively, and singular boundary lines (dashed-dotted lines) of the weight distribution associated with the \uparrow and \downarrow one-electron spectral function for $u = 0.1$, electronic density $n_e = 0.7$, and (a)-(b) spin densities $m = 0.45$ and (c)-(d) $m = 0.25$. The branch line spectra plotted here are defined in Section IV. The c^+ , c^- , and $s1$ branch-line labels appearing here in panels (a) for $\sigma = \uparrow$ and (b) for $\sigma = \downarrow$ apply to the branch lines with similar topology in the panels (c) and (d), respectively. (Online the c^+ , c^- , and $s1$ branch lines plotted here as defined in Section IV are blue, red, and green, respectively.) The lines represented by sets of diamond symbols contribute to the $u \rightarrow 0$ one-electron spectrum yet are not branch lines. For σ one-electron UHB addition only the branch lines that contribute to the $u \rightarrow 0$ spectral weight are represented.

Furthermore, the branch-line exponent expression, Eq. (111), is not valid in its limiting k points when they coincide with boundary points (k_0, ω_0) in the vicinity of which the line shape has rather the form given in Eqs. (115) and (116). The PDT naturally accesses such an alternative behavior. For σ electron removal and LHB addition it corresponds to the known low-energy behavior of the spectral function in the vicinity of (k, ω) -plane points $(k_0, 0)$. Since for the densities ranges $n_e \in [0, 1[$ and $m \in [0, n_e]$ considered here the latter low-energy behavior is known and coincides with that reported in Eq. (5.7) of Ref. [30], we restrict our study of Section IV to the high-energy spectral features. The previous studies of the high-energy spectral features of the 1D Hubbard model by means of the PDT [44–47] and most of those relying on other methods [42, 43, 48, 49] have been limited to zero spin density. Hence the analysis of Sec. IV is mainly focused on finite spin densities $m \in]0, n_e]$.

Concerning the behavior of the spectral functions near the border lines, Eq. (118), in the related cases of charge-charge and spin-spin two-electron dynamical correlation functions the boundary line exponent $-1/2$ that results from the density of the two-parametric states is changed to $1/2$ by the two-electron matrix elements between the ground state and the excited energy eigenstate. This always occurs when the two values q and q' and corresponding group velocities $v_{\beta}(q)$ and $v_{\beta}(q')$ such that $v_{\beta}(q) = v_{\beta}(q')$ belong to the same $\beta = c, s1$ band.

In the present case of the σ one-electron spectral functions the border lines are generated by pairs of values q and q' belonging to the c and $s1$ bands, respectively, such that $v_c(q) = v_{s1}(q')$. The σ one-electron matrix elements between the ground state and the excited energy eigenstates do not change the exponent $-1/2$ resulting from the density of the two-parametric states, so that the border-line singularities, Eq. (118), prevail. The border lines of the σ one-electron removal and LHB addition spectral functions are plotted in Figs. 1-5 yet for simplicity their specific analytical form is not given in this paper.

In what the σ one-electron LHB and UHB addition spectral functions as defined in Eq. (9) for $u > 0$, $n_e \in [0, 1[$, and $m \in [0, n_e]$ is concerned, we have a few comments. At $n_e = 1$ there is no σ one-electron LHB. That electronic density refers to the Mott-Hubbard insulator phase at which there is a gap $2\mu_u$, Eq. (5), between the top of the σ one-electron removal band and the addition UHB. On the other hand, for the metallic phase electronic density range $n_e \in [0, 1[$ considered here, the spectral weight associated with the σ one-electron addition LHB has not an exact top, yet such a weight becomes very small above some $u > 0$, $n_e \in [0, 1[$, and $m \in [0, n_e]$ dependent finite energy scale. Hence for intermediate and large u values there emerges a pseudogap between that region of the σ one-electron addition LHB and the well-defined bottom of the UHB. Our study focuses on singular spectral features, such a pseudogap being clearly visible in Figs. 2-5 for intermediate and large u values, where as discussed below the

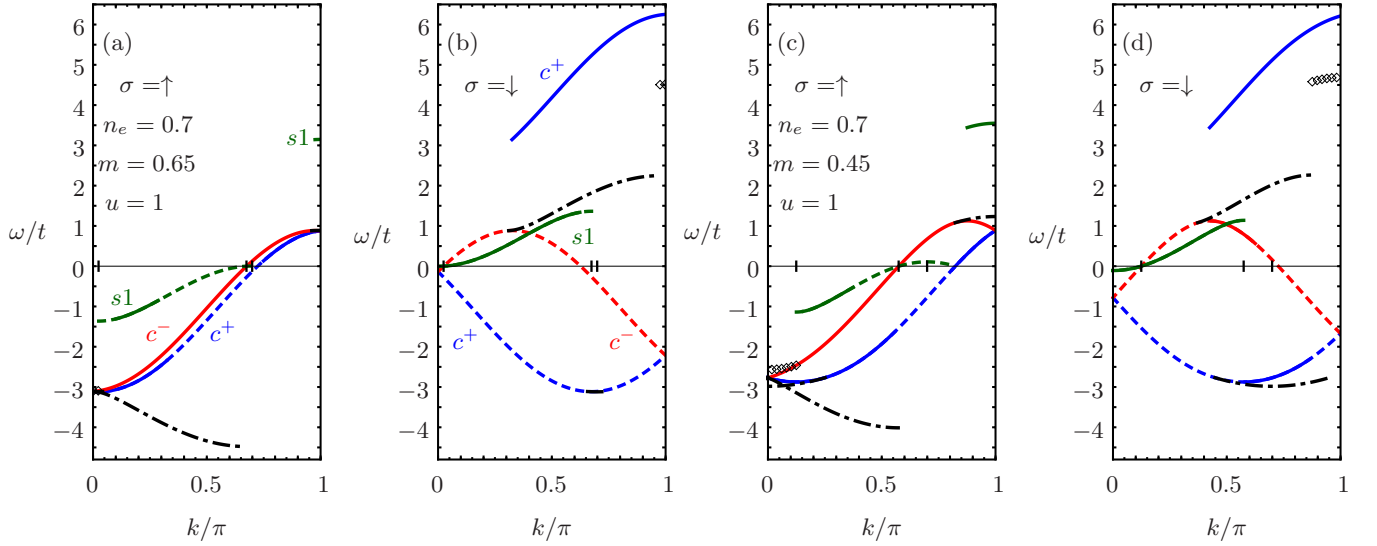


Figure 2: The same (k, ω) -plane lines as in Fig. 1 for $u = 1$, electronic density $n_e = 0.7$, and spin densities (a)-(b) $m = 0.65$ and (c)-(d) $m = 0.45$. (Online the c^+ , c^- , and $s1$ branch lines are blue, red, and green, respectively.)

(k, ω) -plane solid lines and dashed-dotted lines refer to negative-exponent singular branch lines k ranges and singular border lines, respectively.

An interesting property is that, when expressed as function of the $\beta = c, s1$ band momentum q , the $\sigma = \uparrow, \downarrow$ one-electron UHB addition $\beta = c, s1$ branch lines spectrum and exponent are exactly the same as for the $\beta = c, s1$ branch lines of the $\bar{\sigma} = \downarrow, \uparrow$ one-electron removal spectral function. That relation is also preserved in terms of the momentum k and energy ω provided that they are replaced by $\pi - k$ and $2\mu - \omega$, respectively.

Such a relation follows from model symmetries whose consequences are fully explicit at $n_e = 1$ for chemical potential $\mu = 0$ at the middle of the Mott-Hubbard gap. Then there is no σ one-electron LHB addition spectral function and the following exact relation holds,

$$B_{\sigma,+1}^{\text{UHB}}(k, \omega) = B_{\bar{\sigma},-1}(\pi - k, -\omega), \quad n_e = 1, \quad \mu = 0. \quad (121)$$

For $n_e \rightarrow 1$ and thus chemical potential $\mu \rightarrow \mu_u$ this relation is also valid yet reads $B_{\sigma,+1}^{\text{UHB}}(k, \omega) = B_{\bar{\sigma},-1}(\pi - k, 2\mu - \omega)$.

At $n_e = 1$ the rotated-electron doubly occupied site of the excited energy eigenstates associated with the σ one-electron UHB addition spectral function corresponds to a η -spin doublet configuration of a single unpaired rotated spin of projection $-1/2$. On the other hand, for electronic densities $n_e \in [0, 1[$ such states are rather populated by one $\eta1$ pseudofermion that corresponds to a η -spin singlet configuration of two paired rotated η -spins of opposite projection.

That the σ one-electron UHB addition $s1$ and c^\pm branch lines (k, ω) -plane spectrum and exponent momentum dependence studied below in Section IV are for electronic densities in the range $n_e \in [0, 1[$ and under the transformations $k \rightarrow \pi - k$ and $\omega \rightarrow 2\mu - \omega$ exactly the same as for the $\bar{\sigma}$ one-electron removal $s1$ and c^\pm branch lines, respectively, is a weaker consequence of the same symmetry. It follows from a $\eta1$ pseudofermion of momentum at the $\eta1$ band limiting values $\bar{q} = q = \pm(\pi - 2k_F)$, Eq. (41), being invariant under the pseudoparticle - pseudofermion unitary transformation. Indeed, for such σ one-electron UHB addition singular features the $\eta1$ pseudofermion is created at one of such two $\eta1$ band limiting values. Hence the corresponding $\eta1$ pseudofermion energy, Eq. (47) for $\beta = \eta1$, reads $\varepsilon_{\eta1}(\pm(\pi - 2k_F)) = 2\mu_\eta = 2\mu$. It thus equals that of two unpaired rotated η -spins of opposite projection, Eq. (52) with $2\mu_\alpha$ given by Eq. (46) for $\alpha = \eta$. The invariance under the pseudoparticle - pseudofermion unitary transformation of the $\eta1$ pseudofermion created at the momentum $\bar{q} = q = \pm(\pi - 2k_F)$ is behind this property by implying that the corresponding anti-bounding energy $\varepsilon_{\eta1}^0(q) \geq 0$ on the right-hand side of Eq. (53) vanishes, $\varepsilon_{\eta1}^0(\pm(\pi - 2k_F)) = 0$. This means that at these momentum values the two rotated η -spins within the composite $\eta1$ pseudofermion are in a η -spin singlet configuration yet are unpaired, similarly to the unpaired rotated η -spins in the multiplet configurations and specifically to the projection $-1/2$ unpaired and single rotated η -spin of the $n_e = 1$ η -spin doublet σ one-electron UHB addition spectral function $B_{\sigma,+1}^{\text{UHB}}(k, \omega)$, Eq. (121).

Although the σ one-electron UHB addition spectral weight generated by transitions to excited energy eigenstates for which the $\eta1$ pseudofermion emerges at a $\eta1$ band canonical momentum $\bar{q} = \bar{q}(q)$ corresponding to a bare momentum value $-(\pi - 2k_F) < q < (\pi - 2k_F)$ is small, such processes imply that the relation $B_{\sigma,+1}^{\text{UHB}}(k, \omega) = B_{\bar{\sigma},-1}(\pi - k, 2\mu - \omega)$

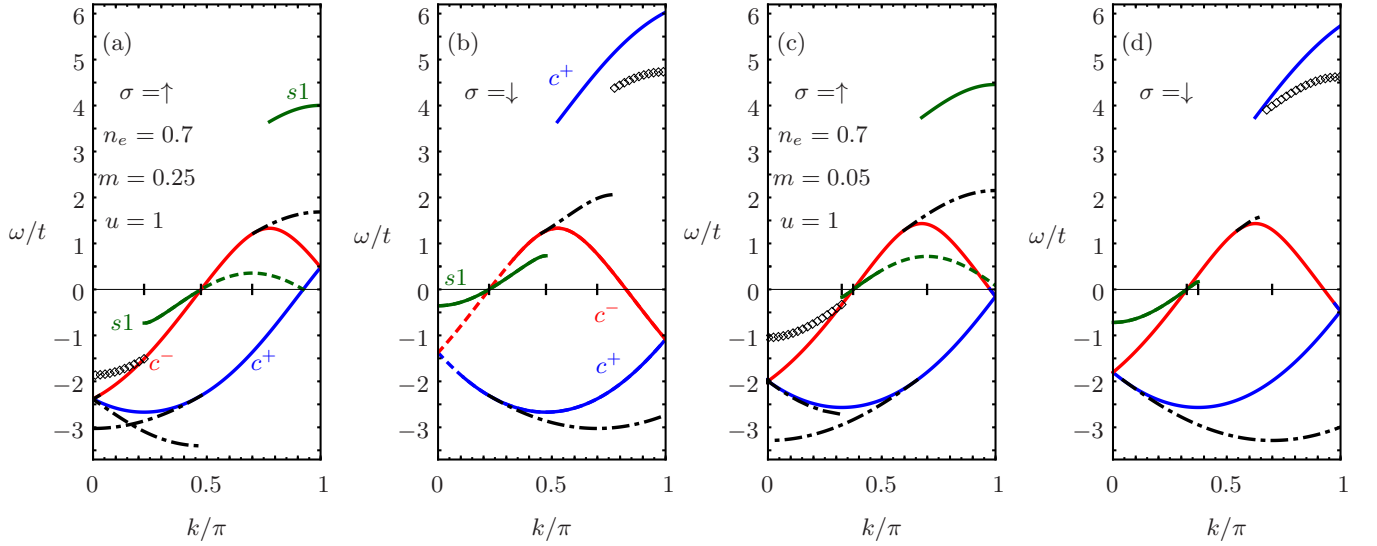


Figure 3: The same (k, ω) -plane lines as in Fig. 1 for $u = 1$, electronic density $n_e = 0.7$, and spin densities (a)-(b) $m = 0.25$ and (c)-(d) $m = 0.05$. (Online the c^+ , c^- , and $s1$ branch lines are blue, red, and green, respectively.)

is not exact for $n_e < 1$. It becomes exact only in the $n_e \rightarrow 1$ limit and thus for chemical potential $\mu \rightarrow \mu_u$ when $(\pi - 2k_F) \rightarrow 0$. In a weaker way it nevertheless survives for $n_e \in [0, 1[$ in what the σ one-electron UHB addition singular $\beta = c, s1$ branch lines (k, ω) -plane spectrum and exponent momentum dependence are concerned for the reasons reported above.

In Figs. 1-5 the \uparrow and \downarrow one-electron removal and LHB addition β branch lines whose exponent $\xi_\beta^\sigma(k)$, Eq. (111), is negative for at least some k interval and u , n_e , and m ranges and the boundary lines considered in the ensuing section are shown in the (k, ω) -plane for several values of u , electronic densities $n_e = 0.3$ and $n_e = 0.7$, and sets of spin density values $m < n_e$. For \uparrow and \downarrow one-electron UHB addition only the main branch lines that in the $u \rightarrow 0$ limit contribute to the $u = 0$ σ one-electron addition spectrum are shown. (Online the c^+ , c^- , and $s1$ branch lines defined in Section IV and plotted in these figures are blue, red, and green, respectively.)

Indeed, since the behavior of the \downarrow and \uparrow one-electron removal spectral functions near their $\beta = c, s1$ branch lines is studied in some detail, for simplicity in the following the study of the related \uparrow and \downarrow , respectively, one-electron UHB addition branch lines is limited to those that in the $u \rightarrow 0$ limit contribute to the $u = 0$ σ one-electron addition δ -function-like spectrum.

The σ one-electron β branch lines are in Figs. 1-5 represented by solid lines and dashed lines for the k ranges for which the corresponding exponent $\xi_\beta^\sigma(k)$, Eq. (111), is negative and positive, respectively. The σ one-electron removal and LHB addition boundary lines are represented by dashed-dotted lines. Most of the $u = 0$ δ -function like σ one-electron spectrum k ranges are obtained from branch lines in the $u \rightarrow 0$ limit. The two exceptions are the $u = 0$ \uparrow one-electron removal spectrum for the momentum range $k \in [-k_{F\downarrow}, k_{F\downarrow}]$ and the $u = 0$ \downarrow one-electron addition spectrum for the k interval $|k| \in [\pi - k_{F\downarrow}, \pi]$, which emerge in the $u \rightarrow 0$ limit from the non-branch lines that are represented in Figs. 1-5 by sets of diamond symbols.

IV. THE SINGULAR σ ONE-ELECTRON SPECTRAL FEATURES

In this section we study the line shape behavior of the σ one-electron spectral functions, Eq. (4), in the vicinity of the branch lines shown in Figs. 1-5. For the k ranges for which the exponents controlling the line shape near these lines are negative, there are singularity cusps in the corresponding σ one-electron spectral functions.

The σ one-electron removal and LHB addition c^\pm and $s1$ branch lines are the topics of Sections IV A and IV B, respectively. Section IV C addresses the issue of the σ one-electron UHB addition branch lines. Finally, the \uparrow one-electron removal and \downarrow one-electron UHB addition $s1'$ non-branch lines that for $m \neq 0$ contribute to the $u \rightarrow 0$ one-electron spectrum is the subject of Section IV D.

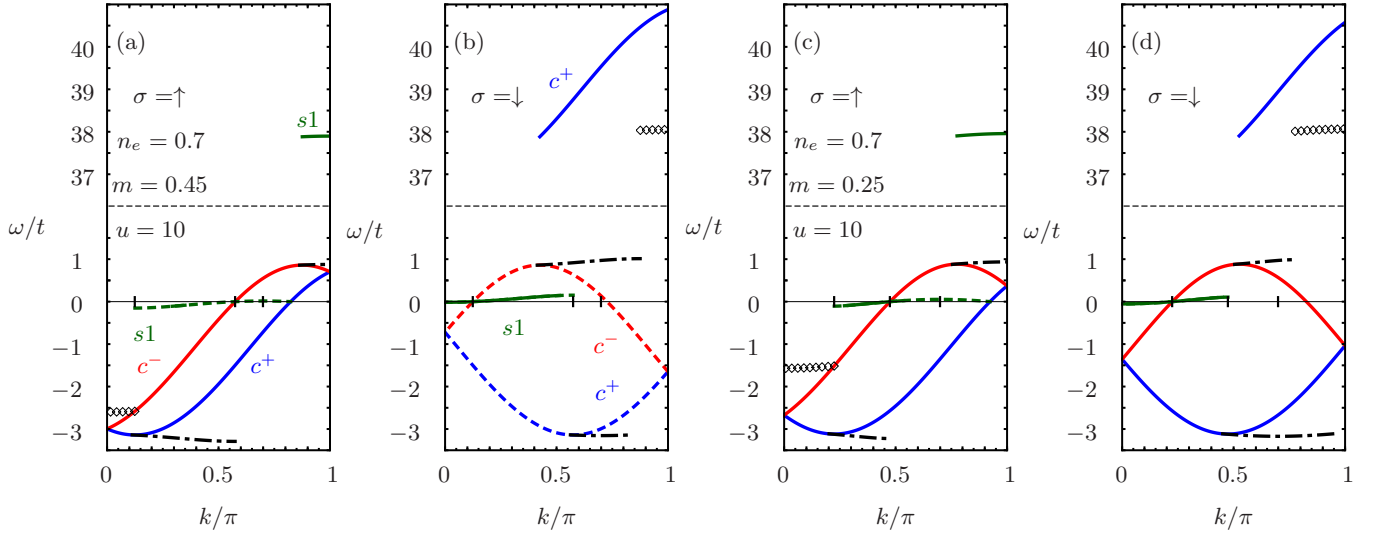


Figure 4: The same (k, ω) -plane lines as in Fig. 1 for $u = 10$, electronic density $n_e = 0.7$, and spin densities (a)-(b) $m = 0.45$ and (c)-(d) $m = 0.25$. Note the different ω intervals separated by a horizontal dashed line used for the removal and LHB addition spectral features and the UHB addition branch line, respectively. (Online the c^+ , c^- , and $s1$ branch lines are blue, red, and green, respectively.)

A. The σ one-electron removal and LHB addition c^\pm branch lines

The σ electron removal and LHB addition c^\pm branch lines are generated by processes that correspond to particular cases of those generated by the leading-order operators, Eqs. (73), (75), (79), and (81) that are behind the \uparrow one-electron removal spectrum, Eq. (74), \uparrow one-electron LHB addition spectrum, Eq. (76), \downarrow one-electron removal spectrum, Eq. (80), and \downarrow one-electron LHB addition spectrum, Eq. (82). Hence these lines one-parametric spectra plotted in Figs. 1-5 are contained within such two-parametric spectra that occupy well defined regions in the (k, ω) plane. (Online the c^+ and c^- branch lines are blue and red, respectively, in these figures.)

These one-parametric spectra $\omega_{c^\pm}^\sigma(k)$ and the exponents $\xi_{c^\pm}^\sigma(k)$ associated with these branch lines are such that,

$$\omega_{c^+}^\sigma(k) = \omega_{c^-}^\sigma(-k); \quad \xi_{c^+}^\sigma(k) = \xi_{c^-}^\sigma(-k), \quad \sigma = \uparrow, \downarrow. \quad (122)$$

Within a reduced first-Brillouin zone scheme, considering both the c^+ and c^- branch lines for $k \in [0, \pi]$ or only the c^+ branch line for $k \in [-\pi, \pi]$ contains exactly the same information. Here we chose the latter option.

The σ one-electron removal and LHB addition c^+ branch line refers to excited energy eigenstates with the following number deviations relative to those of the initial ground state,

$$\delta N_c^F = 0; \quad \delta J_c^F = \delta_{\sigma, \downarrow} / 2; \quad \delta N_c^{NF} = \gamma; \quad \delta N_{s1}^F = \delta_{\sigma, \downarrow} \gamma; \quad \delta J_{s1}^F = \gamma_\sigma / 2. \quad (123)$$

The spectrum of general form, Eq. (109), that defines the (k, ω) -plane shape of the σ one-electron removal and LHB addition c^+ branch line reads,

$$\begin{aligned} \omega_{c^+}^\sigma(k) &= \gamma \varepsilon_c(q), \quad \gamma = \pm 1, \\ q &\in [-2k_F, 2k_F] \quad \text{for } \sigma \text{ electron removal,} \\ q &\in [-\pi, -2k_F] \text{ and } q \in [2k_F, \pi] \quad \text{for } \sigma \text{ electron LHB addition,} \end{aligned} \quad (124)$$

where $\varepsilon_c(q)$ is the c band energy dispersion, Eq. (47) for $\beta = c$. The relation of the c band momentum q to the excitation momentum k is within an extended-zone scheme given by,

$$\begin{aligned} k &= \gamma q + k_{F\bar{\sigma}}, \\ k &\in [-k_{F\sigma}, (2k_F + k_{F\bar{\sigma}})] \quad \text{for } \gamma = -1 \\ k &\in [-(\pi - k_{F\bar{\sigma}}), -k_{F\sigma}] \text{ and } k \in [(2k_F + k_{F\bar{\sigma}}), (\pi + k_{F\bar{\sigma}})] \quad \text{for } \gamma = +1. \end{aligned} \quad (125)$$

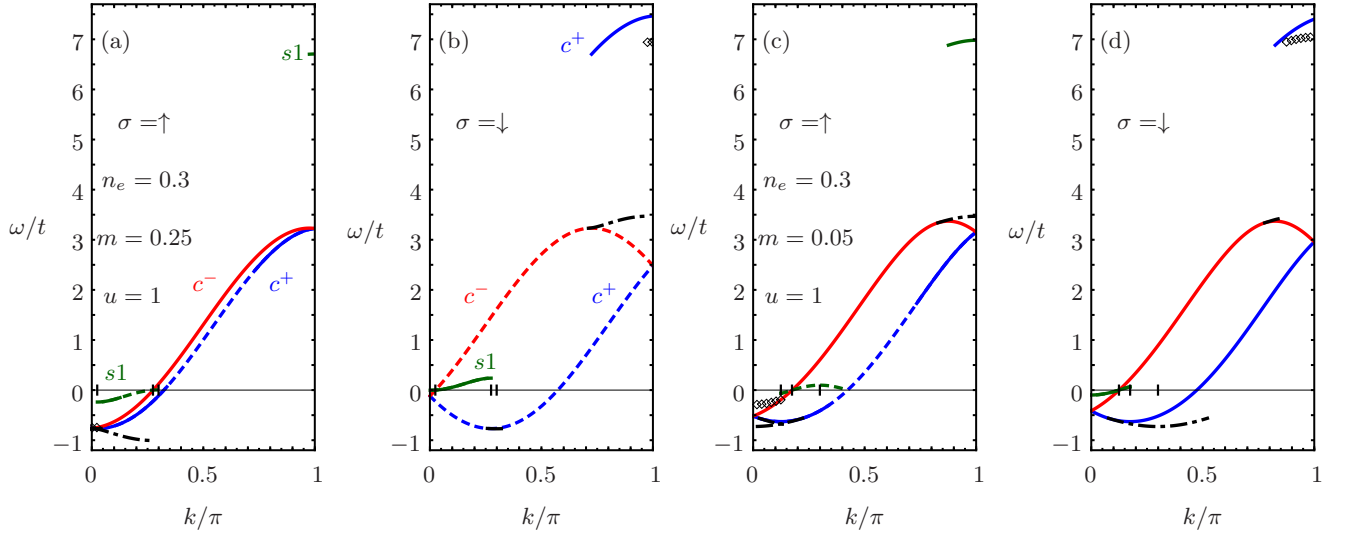


Figure 5: The same (k, ω) -plane lines as in Fig. 1 for $u = 1$, electronic density $n_e = 0.3$, and spin densities (a)-(b) $m = 0.25$ and (c)-(d) $m = 0.05$. (Online the c^+ , c^- , and $s1$ branch lines are blue, red, and green, respectively.)

As mentioned above, we consider a reduced first Brillouin-zone scheme for $k \in [-\pi, \pi]$ within which the c^+ branch line separates into several subbranches. One finds that these subbranches refer to the following momentum k intervals,

$$\begin{aligned}
 k &= \gamma q + k_{F\bar{\sigma}} \text{ subbranch,} \\
 k &\in [-k_{F\sigma}, (2k_F + k_{F\bar{\sigma}})] \quad \text{for } \gamma = -1 \\
 k &\in [-(\pi - k_{F\bar{\sigma}}), -k_{F\sigma}] \text{ and } k \in [(2k_F + k_{F\bar{\sigma}}), \pi] \quad \text{for } \gamma = +1, \\
 k &= q + k_{F\bar{\sigma}} - 2\pi \text{ subbranch,} \\
 k &\in [-\pi, -(\pi - k_{F\bar{\sigma}})] \quad \text{for } \gamma = +1,
 \end{aligned} \tag{126}$$

that are valid for the densities ranges,

$$\begin{aligned}
 \uparrow \text{ electron : } &(i) n_e \in [0, 2/3] \text{ and } m \in [0, n_e] \text{ and } (ii) n_e \in [2/3, 1] \text{ and } m \in [(3n_e - 2), n_e], \\
 \downarrow \text{ electron : } &(i) n_e \in [0, 1/2] \text{ and } m \in [0, n_e] \text{ and } (ii) n_e \in [1/2, 2/3] \text{ and } m \in [0, (2 - 3n_e)].
 \end{aligned}$$

On the other hand, the momentum k intervals,

$$\begin{aligned}
 k &= \gamma q + k_{F\bar{\sigma}} \text{ subbranch,} \\
 k &\in [-k_{F\sigma}, \pi] \quad \text{for } \gamma = -1 \\
 k &\in [-(\pi - k_{F\bar{\sigma}}), -k_{F\sigma}] \quad \text{for } \gamma = +1, \\
 k &= q + k_{F\bar{\sigma}} - 2\pi \text{ subbranch,} \\
 k &\in [-\pi, -(2\pi - 2k_F - k_{F\bar{\sigma}})] \quad \text{for } \gamma = -1 \\
 k &\in [-(2\pi - 2k_F - k_{F\bar{\sigma}}), -(\pi - k_{F\bar{\sigma}})] \quad \text{for } \gamma = +1,
 \end{aligned} \tag{127}$$

are valid for the densities ranges,

$$\begin{aligned}
 \uparrow \text{ electron : } &n_e \in [2/3, 1] \text{ and } m \in [0, (3n_e - 2)], \\
 \downarrow \text{ electron : } &(i) n_e \in [1/2, 2/3] \text{ and } m \in [(2 - 3n_e), n_e] \text{ and } (ii) n_e \in [2/3, 1] \text{ and } m \in [0, n_e].
 \end{aligned}$$

The corresponding k intervals of the c^- branch line subbranches are obtained from those provided here upon exchanging k by $-k$.

The one-parametric spectrum $\omega_{c^+}^\sigma(k)$ of each c^+ branch line subbranch is given by Eq. (124) with the relation between the excitation momentum k and the c band momentum q provided in the corresponding k interval, Eqs. (126) and (127). Combining the analysis of such momentum k intervals with the relation $\omega_{c^+}^\sigma(k) = \omega_{c^-}^\sigma(-k)$, Eq. (122), reveals that the σ one-electron LHB addition c^\pm branch lines are the natural continuation of the σ one-electron removal c^\pm branch lines.

From the use of the values of the functional, Eq. (112), specific to the excited energy eigenstates that determine spectral weight distribution near the c^\pm branch lines, one finds that the momentum dependent exponents of general form, Eq. (111), that control such a line shape read,

$$\xi_{c^+}^\uparrow(k) = \xi_{c^-}^\uparrow(-k) = -1 + \sum_{\iota=\pm 1} \left(\frac{\xi_{c s 1}^1}{2} + \gamma \Phi_{c,c}(\iota 2k_F, q) \right)^2 + \sum_{\iota=\pm 1} \left(\frac{\xi_{s 1 s 1}^1}{2} + \gamma \Phi_{s 1,c}(\iota k_{F\downarrow}, q) \right)^2, \quad (128)$$

for the $\sigma = \uparrow$ one-electron c^\pm branch lines and,

$$\begin{aligned} \xi_{c^+}^\downarrow(k) = \xi_{c^-}^\downarrow(-k) = -1 + \sum_{\iota=\pm 1} \left(\frac{\iota \gamma \xi_{c s 1}^0}{2} + \frac{(\xi_{c c}^1 - \xi_{c s 1}^1)}{2} + \gamma \Phi_{c,c}(\iota 2k_F, q) \right)^2 \\ + \sum_{\iota=\pm 1} \left(\frac{\iota \gamma \xi_{s 1 s 1}^0}{2} + \frac{(\xi_{s 1 c}^1 - \xi_{s 1 s 1}^1)}{2} + \gamma \Phi_{s 1,c}(\iota k_{F\downarrow}, q) \right)^2, \end{aligned} \quad (129)$$

for the $\sigma = \downarrow$ one-electron c^\pm branch lines. These \uparrow and \downarrow one-electron exponents are plotted in Figs. 6 and 7, respectively, as a function of the momentum $k/\pi \in]-1, 1[$ for several u values, electronic densities $n_e = 0.3$ and $n_e = 0.7$, and a set of spin density values $m < n_e$.

The specific form of the general expression, Eq. (111), of the σ one-electron spectral function $B_{\sigma,\gamma}(k, \omega)$, Eq. (4), in the vicinity of the present c^\pm branch lines is,

$$B_{\sigma,\gamma}(k, \omega) = C_{\sigma,\gamma,c^\pm} \left(\gamma \omega - \omega_{c^\pm}^\sigma(k) \right)^{\xi_{c^\pm}^\sigma(k)}; \quad (\gamma \omega - \omega_{c^\pm}^\sigma(k)) \geq 0, \quad \gamma = \pm 1, \quad (130)$$

where C_{σ,γ,c^\pm} are constants independent of k and ω , the spectra $\omega_{c^+}^\sigma(k) = \omega_{c^-}^\sigma(-k)$ of the several subbranches are given in Eqs. (124), (126), and (127), and the exponents $\xi_{c^+}^\sigma(k) = \xi_{c^-}^\sigma(-k)$ are defined in Eqs. (128) and (129) for $\sigma = \uparrow$ and $\sigma = \downarrow$, respectively.

The following exponents behaviors reached in the $u \rightarrow 0$ limit are derived from the use in Eqs. (128) and (129) of the values corresponding to that limit of the phase-shift parameters $\xi_{\beta\beta'}^j$ and $\beta = c, s1$ pseudofermion phase shifts in units of 2π , $\Phi_{\beta,\beta'}(\iota q_{F\beta}, q)$, given in Eqs. (B15) and (B10) of Appendix B, respectively. The found behaviors in the $u \rightarrow 0$ limit of the c^+ branch line subbranches exponents for $\sigma = \uparrow$ one-electron removal ($\gamma = -1$) are,

$$\begin{aligned} \lim_{u \rightarrow 0} \xi_{c^+}^\uparrow(k) = -1, \quad k \in [-k_{F\uparrow}, -k_{F\downarrow}] \text{ for } \gamma = -1 \\ \text{for } n_e \in [0, 1] \text{ and } m \in [0, n_e], \end{aligned} \quad (131)$$

$$\begin{aligned} \lim_{u \rightarrow 0} \xi_{c^+}^\uparrow(k) = 0, \\ k \in [-k_{F\downarrow}, 3k_{F\downarrow}] \text{ for } \gamma = -1 \\ \text{for } n_e \in [0, 2/3] \text{ and } m \in [0, n_e] \\ \text{for } n_e \in [2/3, 1] \text{ and } m \in [(n_e - 2/3), n_e] \\ k \in [-k_{F\downarrow}, \pi] \text{ and } k \in [-\pi, -(2\pi - 3k_{F\downarrow})] \text{ for } \gamma = -1 \\ \text{for } n_e \in [2/3, 1] \text{ and } m \in [0, (n_e - 2/3)], \end{aligned} \quad (132)$$

$$\begin{aligned} \lim_{u \rightarrow 0} \xi_{c^+}^\uparrow(k) = 1, \\ k \in [3k_{F\downarrow}, (2k_F + k_{F\downarrow})] \text{ for } \gamma = -1 \\ \text{for } n_e \in [0, 2/3] \text{ and } m \in [0, n_e] \\ \text{for } n_e \in [2/3, 1] \text{ and } m \in [(3n_e - 2), n_e] \\ k \in [3k_{F\downarrow}, \pi] \text{ and } k \in [-\pi, -(2\pi - 2k_F - k_{F\downarrow})] \text{ for } \gamma = -1 \\ \text{for } n_e \in [2/3, 1] \text{ and } m \in [(n_e - 2/3), (3n_e - 2)] \\ k \in [-(2\pi - 3k_{F\downarrow}), -(2\pi - 2k_F - k_{F\downarrow})] \\ \text{for } n_e \in [2/3, 1] \text{ and } m \in [0, (n_e - 2/3)]. \end{aligned} \quad (133)$$

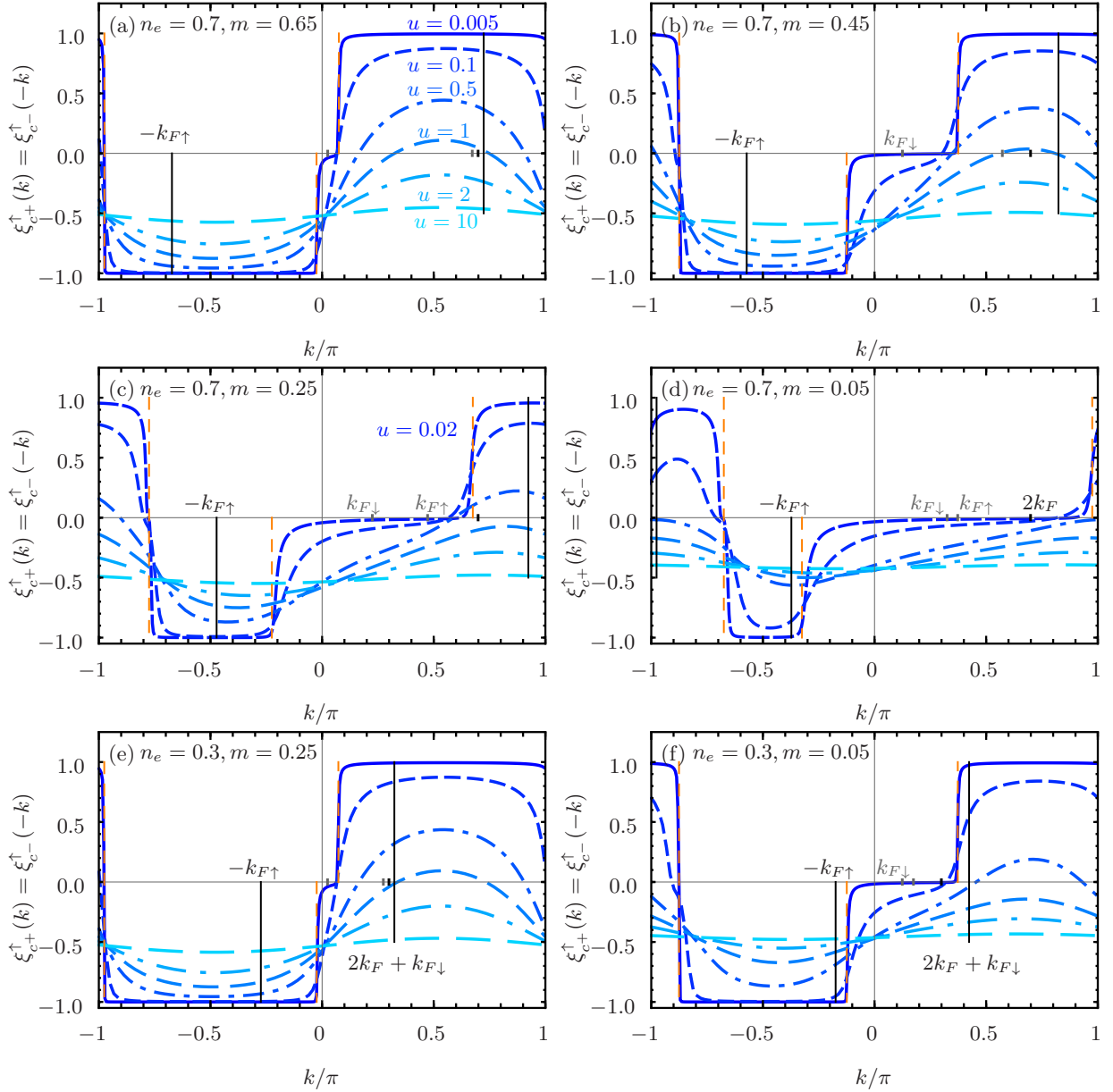


Figure 6: The exponent $\xi_{c^+}^\uparrow(k) = \xi_{c^-}^\uparrow(-k)$, Eq. (128), that controls the singularities in the vicinity of the c^+ branch line whose (k, ω) -plane one-parametric spectrum is defined by Eqs. (124), (126), and (127) for the $\sigma = \uparrow$ one-electron removal and LHB addition spectral function, Eq. (130), as a function of the momentum $k/\pi \in]-1, 1[$ for several u values, electronic density $n_e = 0.7$, and spin densities (a) $m = 0.65$, (b) $m = 0.45$, (c) $m = 0.25$, and (d) $m = 0.05$, and for electronic density $n_e = 0.3$ and spin densities (e) $m = 0.25$ and (f) $m = 0.05$. The type of exponent line associated with each u value is for all figures the same. Full and dashed vertical lines denote specific momentum values between different subbranches and momenta where the $u \rightarrow 0$ limiting value of the exponent changes, respectively.

For LHB addition ($\gamma = +1$), one finds,

$$\begin{aligned}
 \lim_{u \rightarrow 0} \xi_{c^+}^\uparrow(k) &= -1, & k \in [-(\pi - k_{F\downarrow}), -k_{F\uparrow}] \text{ for } \gamma = +1 \\
 &\text{for } n_e \in [0, 1] \text{ and } m \in [0, n_e], \\
 \lim_{u \rightarrow 0} \xi_{c^+}^\uparrow(k) &= 1 \text{ for } \gamma = +1 \\
 &\text{for the other } k \text{ ranges in Eqs. (126) and (127) with } \sigma = \uparrow \text{ and } \bar{\sigma} = \downarrow.
 \end{aligned} \tag{134}$$

Similar values for the exponent $\xi_{c^-}^\downarrow(k)$ are obtained upon exchanging k by $-k$. Important c^- branch line subbranches

are those for which $\lim_{u \rightarrow 0} \xi_{c-}^{\uparrow}(k) = -1$. They refer to the k ranges,

$$\begin{aligned} \lim_{u \rightarrow 0} \xi_{c-}^{\uparrow}(k) &= -1, \\ k &\in [k_{F\downarrow}, k_{F\uparrow}] \text{ for } \gamma = -1 \text{ and } k \in [k_{F\uparrow}, (\pi - k_{F\downarrow})] \text{ for } \gamma = +1, \end{aligned} \quad (135)$$

that are valid for $n_e \in [0, 1[$ and $m \in [0, n_e]$.

For the k ranges for which $\lim_{u \rightarrow 0} \xi_{c\pm}^{\uparrow}(k) = -1$ the line shape has not the form given in Eq. (130) and rather becomes δ -function like, Eq. (120). In the present case this gives,

$$\begin{aligned} \lim_{u \rightarrow 0} B_{\uparrow, -1}(k, \omega) &= \delta(\omega + \omega_{c+}^{\uparrow}(k)) = \delta(\omega - 2t(\cos k - \cos k_{F\uparrow})), \quad k \in [-k_{F\uparrow}, -k_{F\downarrow}], \\ \lim_{u \rightarrow 0} B_{\uparrow, +1}(k, \omega) &= \delta(\omega - \omega_{c+}^{\uparrow}(k)) = \delta(\omega + 2t(\cos k - \cos k_{F\uparrow})), \quad k \in [-(\pi - k_{F\downarrow}), -k_{F\uparrow}], \\ \lim_{u \rightarrow 0} B_{\uparrow, -1}(k, \omega) &= \delta(\omega + \omega_{c-}^{\uparrow}(k)) = \delta(\omega - 2t(\cos k - \cos k_{F\uparrow})), \quad k \in [k_{F\downarrow}, k_{F\uparrow}], \\ \lim_{u \rightarrow 0} B_{\uparrow, +1}(k, \omega) &= \delta(\omega - \omega_{c-}^{\uparrow}(k)) = \delta(\omega + 2t(\cos k - \cos k_{F\uparrow})), \quad k \in [k_{F\uparrow}, (\pi - k_{F\downarrow})]. \end{aligned} \quad (136)$$

The behaviors reported here thus recover parts of the exact $u = 0$ σ one-electron spectrum. That the spectra $\omega_{c\pm}^{\sigma}(k)$ become in the $u \rightarrow 0$ limit the corresponding non-interacting electronic spectra is confirmed by accounting for the limiting behavior of the c energy dispersion $\varepsilon_c(q)$ appearing in these $u > 0$ general spectra expression, Eq. (124). Such a limiting behavior is reported in Eq. (B1) of Appendix B.

On the other hand, for the k ranges for which the exponents are for $u \rightarrow 0$ given by 0 and/or 1 the \uparrow one-electron spectral weight at and near the corresponding branch lines vanishes in the $u \rightarrow 0$ limit.

One finds that in the $u \rightarrow 0$ limit the $\sigma = \downarrow$ one-electron removal exponent, Eq. (129), has the following behaviors,

$$\begin{aligned} \lim_{u \rightarrow 0} \xi_{c+}^{\downarrow}(k) &= 1, \\ k &\in [-k_{F\downarrow}, (k_{F\uparrow} - 2k_{F\downarrow})] \text{ for } \gamma = -1 \\ &\text{for } n_e \in [0, 1] \text{ and } m \in [0, n_e] \\ k &\in [(2k_F + k_{F\downarrow}), (2k_F + k_{F\uparrow})] \text{ for } \gamma = -1 \\ &\text{for } n_e \in [0, 1/2] \text{ and } m \in [0, n_e] \\ &\text{for } n_e \in [1/2, 2/3] \text{ and } m \in [0, (2 - 3n_e)] \\ k &\in [(2k_F + k_{F\downarrow}), \pi] \text{ and } k \in [-\pi, -(2\pi - 2k_F - k_{F\uparrow})] \text{ for } \gamma = -1 \\ &\text{for } n_e \in [1/2, 2/3] \text{ and } m \in [(2 - 3n_e), n_e] \\ &\text{for } n_e \in [2/3, 1] \text{ and } m \in [(3n_e - 2), n_e] \\ k &\in [-(2\pi - 2k_F - k_{F\downarrow}), -(2\pi - 2k_F - k_{F\uparrow})] \text{ for } \gamma = -1 \\ &\text{for } n_e \in [2/3, 1] \text{ and } m \in [0, (3n_e - 2)] \end{aligned} \quad (137)$$

and

$$\begin{aligned} \lim_{u \rightarrow 0} \xi_{c+}^{\downarrow}(k) &= 0, \\ k &\in [(k_{F\uparrow} - 2k_{F\downarrow}), (2k_F + k_{F\downarrow})] \text{ for } \gamma = -1 \\ &\text{for } n_e \in [0, 2/3] \text{ and } m \in [0, n_e] \\ &\text{for } n_e \in [2/3, 1] \text{ and } m \in [(3n_e - 2), n_e] \\ k &\in [(k_{F\uparrow} - 2k_{F\downarrow}), \pi] \text{ and } k \in [-\pi, -(2\pi - 2k_F - k_{F\downarrow})] \text{ for } \gamma = -1 \\ &\text{for } n_e \in [2/3, 1] \text{ and } m \in [0, (3n_e - 2)]. \end{aligned} \quad (138)$$

On the other hand, the $\sigma = \downarrow$ one-electron LHB exponent is found to behave as,

$$\lim_{u \rightarrow 0} \xi_{c+}^{\downarrow}(k) = 1 \text{ for } \gamma = +1 \text{ and the } k \text{ ranges in Eqs. (126) and (127) with } \sigma = \downarrow \text{ and } \bar{\sigma} = \uparrow. \quad (139)$$

Hence the \downarrow one-electron spectral weight at and near these branch lines vanishes in the $u \rightarrow 0$ limit both for electron removal and LHB addition. Similar values for the exponent $\xi_{c-}^{\downarrow}(k)$ are obtained upon exchanging k by $-k$.

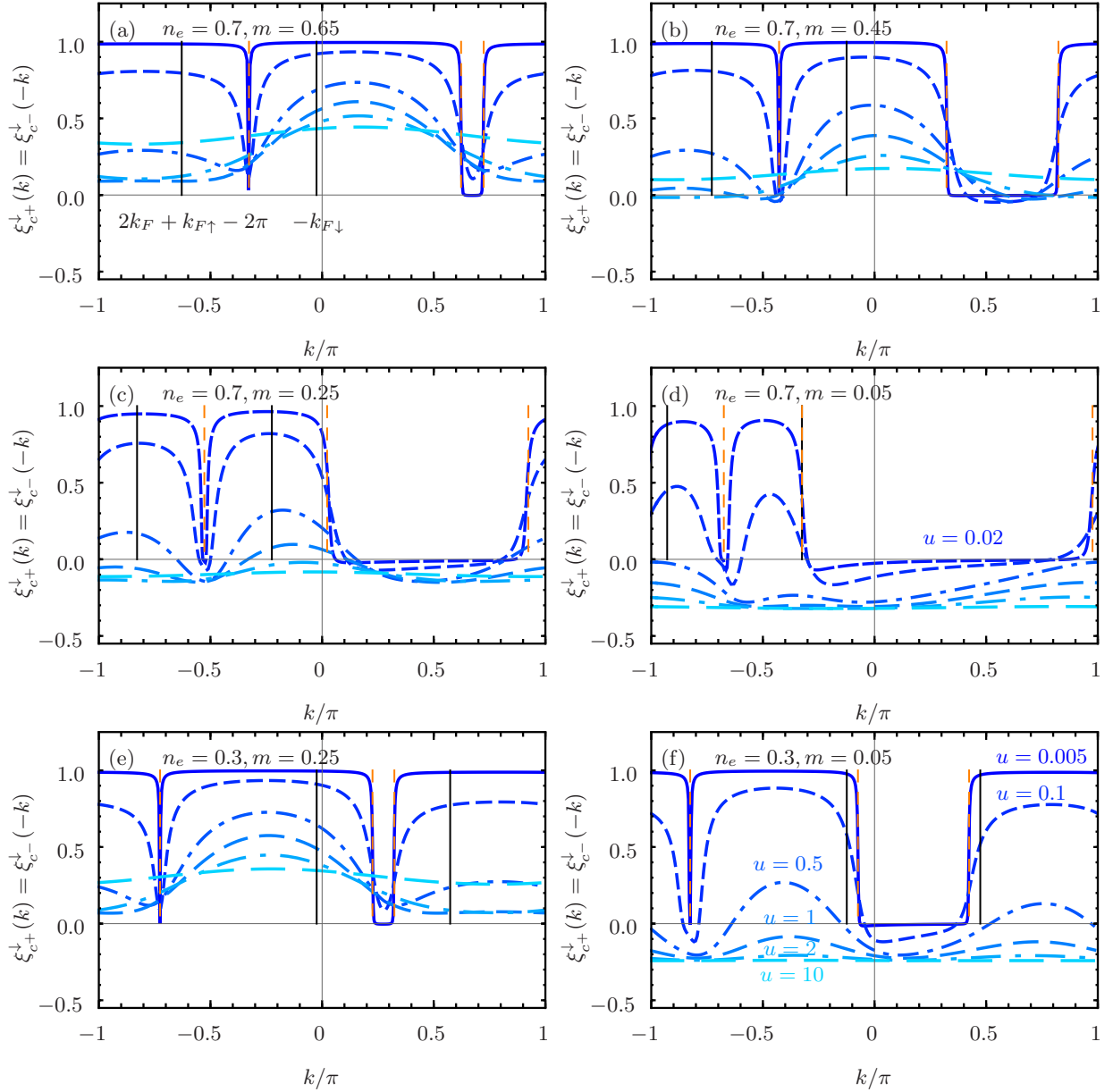


Figure 7: The exponent $\xi_{c^+}^\downarrow(k) = \xi_{c^-}^\downarrow(-k)$, Eq. (129), that controls the singularities in the vicinity of the c^+ branch line whose (k, ω) -plane shape is defined by Eqs. (124), (126), and (127) for the $\sigma = \downarrow$ one-electron removal and LHB addition spectral function, Eq. (130), as a function of the momentum $k/\pi \in]-1, 1[$ for the same values of u , electronic density n_e , and spin density m as in Fig. 6.

Analytical expressions for the above exponents can be derived for $u \gg 1$. These expressions are continuous functions of the spin density m whose limiting behaviors for $m \rightarrow 0$ and $m \rightarrow n_e$ we provide here. For $u \gg 1$ and spin density $m \rightarrow 0$ such expressions are derived from the use in Eqs. (128) and (129) of the parameters ξ_{β}^j , expressions obtained by combining Eqs. (B17) and (B18) of Appendix B for $u \gg 1$ and of those of the $\beta = c, s1$ pseudofermion phase shifts provided in Eq. (B12) of that Appendix. One then finds the following c^+ branch line exponent expression that applies to all its above subbranches k intervals whereas for the twin c^- branch line it refers to subbranches k intervals generated from those of the c^+ branch line upon exchanging k by $-k$,

$$\xi_{c^\pm}^\sigma(k) = -\frac{3}{8} + \frac{\ln 2}{4\pi u} \left(\sin(\pi n_e) \pm 2 \sin\left(k \mp \frac{\pi}{2} n_e\right) \right), \quad \sigma = \uparrow, \downarrow. \quad (140)$$

On the other hand, for $u \gg 1$ and spin density $m \rightarrow n_e$ one uses in Eqs. (128) and (129) the parameters ξ_{β}^j , expressions obtained by combining Eqs. (B19) and (B20) of Appendix B and those of the $\beta = c, s1$ pseudofermion

phase shifts provided in Eq. (B14) of that Appendix. One then finds that the c^\pm branch line exponents have different expressions for the \uparrow one-electron and \downarrow one-electron spectral functions that read,

$$\begin{aligned}\xi_{c^\pm}^\uparrow(k) &= -\frac{1}{2} \pm \frac{2}{\pi u} \sin k, \\ \xi_{c^\pm}^\downarrow(k) &= \frac{1}{2} - \frac{2}{\pi u} (\sin(\pi n_e) \pm \sin(k \mp \pi n_e)),\end{aligned}\quad (141)$$

respectively.

As shown in Fig. 6, the main effect on the k dependence of the \uparrow one-electron removal and LHB addition exponent $\xi_{c^\pm}^\uparrow(k) = \xi_{c^\pm}^\uparrow(-k)$, Eq. (128), of increasing the on-site repulsion u from $u \ll 1$ to $u \gg 1$ is to continuously changing its $u \rightarrow 0$ values -1 , 0 , and 1 for the k ranges given in Eqs. (131)-(134) to a k independent value for $k \in [-\pi, \pi]$ as $u \rightarrow \infty$, which smoothly changes from $-3/8$ for $m \rightarrow 0$ to $-1/2$ for $m \rightarrow n_e$. The general trend of such an exponent u dependence is thus that for the momentum k ranges for which it reads 0 and 1 in the $u \rightarrow 0$ limit it decreases upon increasing u whereas for the k intervals for which it is given by -1 in that limit it rather increases for increasing u values.

On other hand, the exponent $\xi_{c^\pm}^\downarrow(k) = \xi_{c^\pm}^\downarrow(k)$, Eq. (129), plotted in Fig. 7 becomes negative only for large u and small spin density values. For $u \rightarrow 0$ it reads 0 and 1 for the k intervals provided in Eqs. (137)-(139) whereas as $u \rightarrow \infty$ it continuously evolves to a k independent value for $k \in [-\pi, \pi]$ that smoothly changes from $-3/8$ for $m \rightarrow 0$ to $1/2$ for $m \rightarrow n_e$. The general trend of that exponent u dependence is different upon changing the densities. As shown in Fig. 7, for some densities it always decreases upon increasing u whereas for other densities it first decreases upon increasing u until reaching some minimum at a finite u value above which it increases upon further increasing u .

B. The σ one-electron removal and LHB addition $s1$ branch line

The σ electron removal and LHB addition $s1$ branch line is generated by processes that correspond again to a particular case of those generated by the leading-order operators, Eqs. (73), (75), (79), and (81). Hence for the \uparrow and \downarrow one-electron spectral functions its one-parametric spectrum plotted in Figs. 1-5 is contained within the (k, ω) -plane region occupied by the two-parametric spectra corresponding to such more general processes. (Online the $s1$ branch lines are green in these figures.)

The one-parametric spectrum of this branch line is such that $\omega_{s1}^\sigma(k) = \omega_{s1}^\sigma(-k)$ and the corresponding exponent given below is also such that $\xi_{s1}^\sigma(k) = \xi_{s1}^\sigma(-k)$. Hence for simplicity we restrict our following analysis to $k \geq 0$. For such a momentum range the σ electron removal and LHB addition parts of the $s1$ branch line refer to excited energy eigenstates with the following number deviations relative to those of the initial ground state,

$$\delta N_c^F = \gamma; \quad \delta J_c^F = \delta_{\sigma, \uparrow} / 2; \quad \delta N_{s1}^F = \delta_{\sigma, \uparrow} \gamma; \quad \delta J_{s1}^F = 0; \quad \delta N_{s1}^{NF} = -\gamma_\sigma \gamma. \quad (142)$$

The spectrum $\omega_{s1}^\sigma(k)$ of general form, Eq. (109), is for the present branch line given by,

$$\begin{aligned}\omega_{s1}^\sigma(k) &= -\gamma_\sigma \gamma \varepsilon_{s1}(q), \\ q &\in [-k_{F\uparrow}, -k_{F\downarrow}] \quad \text{for } \uparrow \text{ electron removal,} \\ q &\in [-k_{F\downarrow}, k_{F\downarrow}] \quad \text{for } \uparrow \text{ electron LHB addition,} \\ q &\in [-k_{F\downarrow}, 0] \quad \text{for } \downarrow \text{ electron removal,} \\ q &\in [k_{F\downarrow}, k_{F\uparrow}] \quad \text{for } \downarrow \text{ electron LHB addition,}\end{aligned}\quad (143)$$

where $\varepsilon_{s1}(q)$ is the $s1$ band energy dispersion, Eq. (47) for $\beta = s1$.

The relation of the $s1$ band momentum q to the excitation momentum k is,

$$k = \delta_{\sigma, \uparrow} 2k_F - \gamma_\sigma \gamma q \geq 0, \quad (144)$$

which gives,

$$\begin{aligned}k &\in [k_{F\downarrow}, k_{F\uparrow}] \quad \text{for } \uparrow \text{ electron removal,} \\ k &\in [k_{F\uparrow}, (2k_F + k_{F\downarrow})] \quad \text{for } \uparrow \text{ electron LHB addition,}\end{aligned}\quad (145)$$

and

$$\begin{aligned}k &\in [0, k_{F\downarrow}] \quad \text{for } \downarrow \text{ electron removal,} \\ k &\in [k_{F\downarrow}, k_{F\uparrow}] \quad \text{for } \downarrow \text{ electron LHB addition,}\end{aligned}\quad (146)$$

respectively.

Except for \uparrow one-electron LHB addition, the above $s1$ branch-line k ranges are within the first Brillouin-zone. In that specific case it refers for some densities to an extended-zone scheme. Here we consider a reduced first Brillouin-zone scheme for $k \in [0, \pi]$ within which the $s1$ branch line separates for \uparrow one-electron LHB addition into two subbranches. Actually, one of such subbranches stems for $k > 0$ from k momentum values that within an extended-zone scheme arise from second Brillouin-zone $k < 0$ momentum values. (For such processes one has in Eq. (142) that $\delta J_c^F = -1/2$ rather than $\delta J_c^F = 1/2$.) This gives,

$$\begin{aligned}
& k = 2k_F - q \text{ subbranch,} \\
& k \in [k_{F\uparrow}, (2k_F + k_{F\downarrow})] \quad \text{for } \gamma = 1, \\
& \quad \uparrow \text{ electron addition (i) } n_e \in [0, 2/3] \text{ and } m \in [0, n_e] \\
& \quad \text{and (ii) } n_e \in [2/3, 1] \text{ and } m \in [(3n_e - 2), n_e], \\
& k = 2k_F - q \text{ subbranch,} \\
& k \in [k_{F\uparrow}, \pi] \quad \text{for } \gamma = 1, \\
& k = -2k_F - q + 2\pi \text{ subbranch,} \\
& k \in [(2\pi - 2k_F - k_{F\downarrow}), \pi] \quad \text{for } \gamma = 1, \\
& \quad \uparrow \text{ electron addition } n_e \in [2/3, 1] \text{ and } m \in [0, (3n_e - 2)].
\end{aligned} \tag{147}$$

Analysis of the momentum k intervals in Eqs. (146) and (147) reveals that the σ one-electron LHB addition $s1$ branch line is the natural continuation of the σ one-electron removal $s1$ branch line. The momentum dependent exponent of general form, Eq. (111), that controls the line shape near the $\sigma = \uparrow$ one-electron removal and LHB addition $s1$ branch line is given by,

$$\begin{aligned}
\xi_{s1}^{\uparrow}(k) = & -1 + \sum_{\iota=\pm 1} \left(\frac{\iota\gamma(\xi_{cc}^0 + \xi_{c,s1}^0)}{2} + \frac{\xi_{cc}^1}{2} - \gamma \Phi_{c,s1}(\iota 2k_F, q) \right)^2 \\
& + \sum_{\iota=\pm 1} \left(\frac{\iota\gamma(\xi_{s1c}^0 + \xi_{s1,s1}^0)}{2} + \frac{\xi_{s1c}^1}{2} - \gamma \Phi_{s1,s1}(\iota k_{F\downarrow}, q) \right)^2,
\end{aligned} \tag{148}$$

whereas that that controls it in the vicinity of the $\sigma = \downarrow$ one-electron removal and LHB addition $s1$ branch line reads,

$$\xi_{s1}^{\downarrow}(k) = -1 + \sum_{\iota=\pm 1} \left(\frac{\iota\xi_{cc}^0}{2} + \Phi_{c,s1}(\iota 2k_F, q) \right)^2 + \sum_{\iota=\pm 1} \left(\frac{\iota\xi_{s1c}^0}{2} + \Phi_{s1,s1}(\iota k_{F\downarrow}, q) \right)^2. \tag{149}$$

This latter exponent has the same formal expression for $\gamma = -1$ and $\gamma = +1$ the corresponding q ranges being though different, as given in Eq. (143). These \uparrow and \downarrow one-electron exponents are plotted in Figs. 8 and 9, respectively, as a function of the momentum $k/\pi \in]0, 1[$ for several u values, electronic densities $n_e = 0.3$ and $n_e = 0.7$, and a set of spin density values $m < n_e$.

The general expression, Eq. (111), of the σ one-electron spectral function $B_{\sigma,\gamma}(k, \omega)$, Eq. (4), near the $s1$ branch lines is in the present case given by,

$$B_{\sigma,\gamma}(k, \omega) = C_{\sigma,\gamma,s1} \left(\gamma\omega - \omega_{s1}^{\sigma}(k) \right)^{\xi_{s1}^{\sigma}(k)}; \quad (\gamma\omega - \omega_{s1}^{\sigma}(k)) \geq 0, \quad \gamma = \pm 1, \tag{150}$$

where $C_{\sigma,\gamma,s1}$ is a constant independent of k and ω , the spectrum $\omega_{s1}^{\sigma}(k)$ is that in Eq. (143), and the exponent $\xi_{s1}^{\sigma}(k)$ is given in Eqs. (148) and (149).

The behaviors reached in the $u \rightarrow 0$ limit by the exponents, Eqs. (148) and (149), can be found by use in these equations of the parameters $\xi_{\beta\beta'}^j$ values given in Eq. (B15) of Appendix B and of the $\beta = c, s1$ pseudofermion phase shifts $\Phi_{\beta,\beta'}(\iota q_{F\beta}, q)$ expressions provided in Eq. (B10) of that Appendix. One then finds that the $\sigma = \uparrow$ one-electron removal exponent and the $\sigma = \downarrow$ one-electron LHB addition exponent have the following related behaviors,

$$\begin{aligned}
\lim_{u \rightarrow 0} \xi_{s1}^{\sigma}(k) &= \gamma_{\sigma}, \quad k \in [k_{F\downarrow}, k_{F\uparrow}] \\
& \quad \text{for } m \in [0, n_e] \quad \text{and} \quad n_e \in [0, 1/2] \quad \text{and} \quad \text{for } m \in [0, 1 - n_e] \quad \text{and} \quad n_e \in [1/2, 1] \\
\lim_{u \rightarrow 0} \xi_{s1}^{\sigma}(k) &= \gamma_{\sigma}, \quad k \in [k_{F\downarrow}, \pi - k_{F\uparrow}] \\
&= 0, \quad k \in [\pi - k_{F\uparrow}, k_{F\uparrow}] \\
& \quad \text{for } m \in [1 - n_e, n_e] \quad \text{and} \quad n_e \in [1/2, 1].
\end{aligned} \tag{151}$$

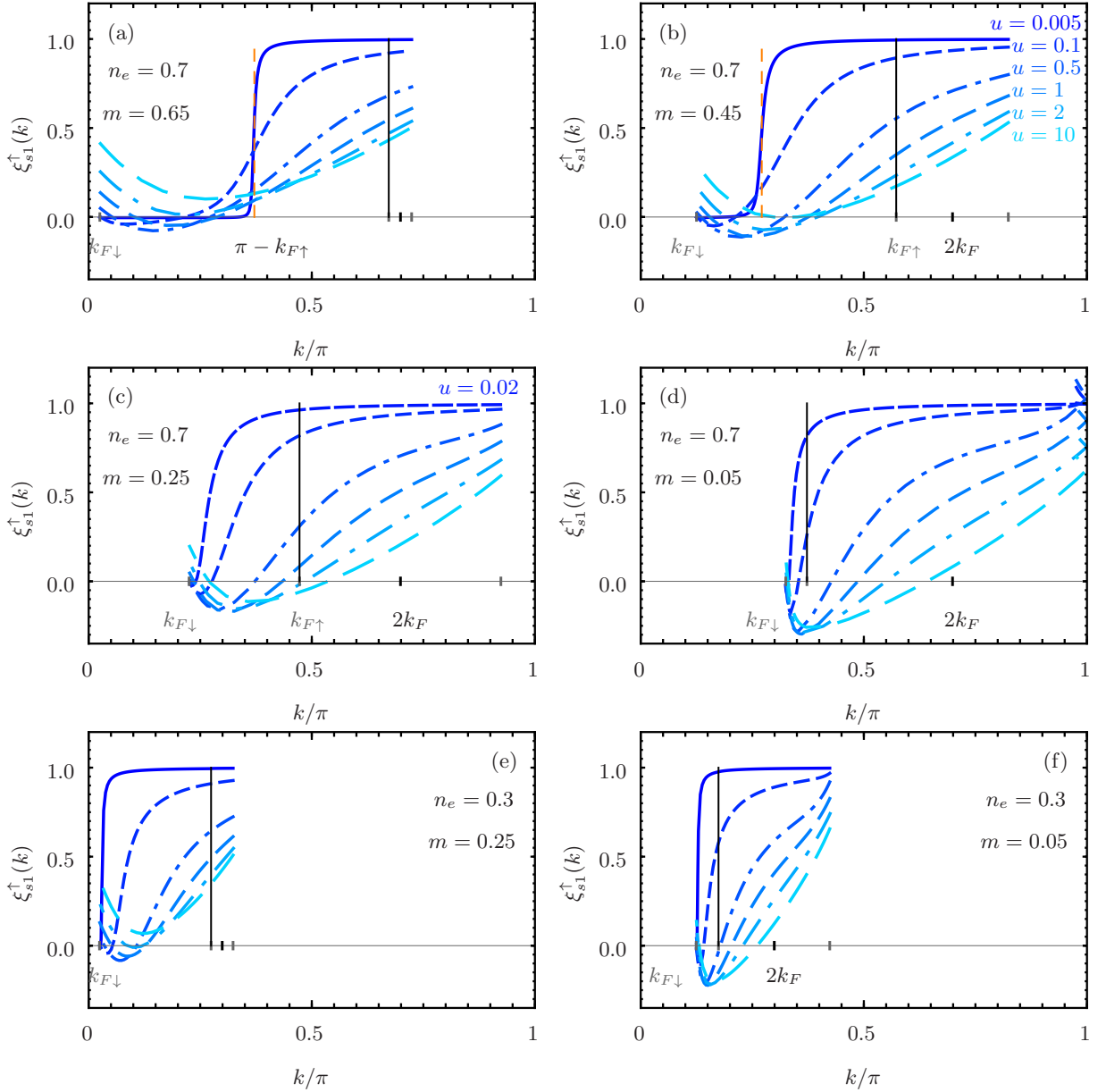


Figure 8: The exponent $\xi_{s1}^\uparrow(k)$, Eq. (148), that controls the singularities in the vicinity of the $s1$ branch line whose (k, ω) -plane shape is defined by Eqs. (143), (145), and (147) for the $\sigma = \uparrow$ one-electron removal and LHB addition spectral function, Eq. (150), as a function of the momentum $k/\pi \in]0, 1[$ for the same values of u , electronic density n_e , and spin density m as in Fig. 6. (For $k/\pi \in]-1, 0[$ the exponent $\xi_{s1}^\uparrow(k)$ is given by $\xi_{s1}^\uparrow(k) = \xi_{s1}^\uparrow(-k)$ with $-k/\pi \in]0, 1[$ as plotted here.)

Furthermore, one finds that the $\sigma = \uparrow$ electron LHB addition and $\sigma = \downarrow$ electron removal exponents have also related behaviors that read,

$$\lim_{u \rightarrow 0} \xi_{s1}^\sigma(k) = \gamma_\sigma \quad (\text{for the whole branch lines } k \text{ range}). \quad (152)$$

Hence the $\sigma = \uparrow$ one-electron spectral weight at and near these $s1$ branch lines vanishes in the $u \rightarrow 0$ limit both for $\sigma = \uparrow$ electron removal and LHB addition.

As given generally in Eq. (120), for the n_e , m , and k ranges for which $\lim_{u \rightarrow 0} \xi_{s1}^\downarrow(k) = -1$ the line shape near the branch line is not of the power-law form, Eq. (150). In that limit it rather corresponds to the following δ -function-like

$\sigma = \downarrow$ one-electron spectral weight distribution along it,

$$\begin{aligned} \lim_{u \rightarrow 0} B_{\downarrow,-1}(k, \omega) &= \delta\left(\omega + \omega_{s1}^\downarrow(k)\right) = \delta\left(\omega - 2t(\cos k - \cos k_{F\downarrow})\right), \quad k \in [-k_{F\downarrow}, k_{F\downarrow}], \\ \lim_{u \rightarrow 0} B_{\downarrow,+1}(k, \omega) &= \delta\left(\omega - \omega_{s1}^\downarrow(k)\right) = \delta\left(\omega + 2t(\cos k - \cos k_{F\downarrow})\right), \\ &k \in [k_{F\downarrow}, k_{F\uparrow}] \text{ for } m \in [0, n_e] \text{ and } n_e \in [0, 1/2] \text{ and for } m \in [0, 1 - n_e] \text{ and } n_e \in [1/2, 1] \\ &k \in [k_{F\downarrow}, \pi - k_{F\uparrow}] \text{ for } m \in [1 - n_e, n_e] \text{ and } n_e \in [1/2, 1]. \end{aligned} \quad (153)$$

The $u \rightarrow 0$ limiting behavior reported in Eq. (B2) of Appendix B for the $s1$ energy dispersion $\varepsilon_{s1}(q)$ appearing in the spectrum $\omega_{s1}^\downarrow(k)$, Eq. (143), confirms that the latter spectrum becomes in the $u \rightarrow 0$ limit the corresponding $u = 0$ non-interacting electronic spectrum, as given in Eq. (153).

On the other hand, for the k range for which $\lim_{u \rightarrow 0} \xi_{s1}^\downarrow(k) = 0$ the \downarrow one-electron addition spectral weight at and near the present $s1$ branch line vanishes in the $u \rightarrow 0$ limit.

For $u \gg 1$ the $s1$ branch line exponent expression is a continuous function of the spin density m . We have derived the corresponding exponent analytical expressions valid for $u \gg 1$ in the $m \rightarrow 0$ and $m \rightarrow n_e$ limits. The $s1$ branch line momentum width vanishes in the $m \rightarrow 0$ limit both for \downarrow one-electron LHB addition and \uparrow one-electron removal. On the other hand, in that limit the $s1$ branch line for \uparrow one-electron LHB addition and \downarrow one-electron removal becomes the $s1$ branch line for one-electron LHB addition and removal, respectively. By using in Eqs. (148) and (149) the values of the parameters $\xi_{\beta\beta'}^j$ obtained by combining Eqs. (B17) and Eq. (B18) of Appendix B for $u \gg 1$ and of the expressions of the $\beta = c, s1$ pseudofermion phase shifts provided in Eq. (B12) of that Appendix, which refer to $u \gg 1$ and spin density $m \rightarrow 0$, one finds that the exponent in the spectral function expression, Eq. (150), that controls the line shape near the \downarrow one-electron removal and \uparrow one-electron LHB addition $s1$ branch line reads in these limits,

$$\begin{aligned} \xi_{s1}^\sigma(k) &= -\frac{1}{2} \left(1 - \left(\frac{k}{\pi n_e}\right)^2\right) \left(1 + \frac{2 \ln 2}{\pi u} \sin(\pi n_e)\right) - \frac{1}{2u} \cos\left(\frac{k}{n_e}\right) \sin(\pi n_e), \\ &\sigma = \uparrow \text{ electron addition for } k \in [k_F, 3k_F] \text{ and } n_e \in [0, 2/3] \\ &\sigma = \uparrow \text{ electron addition for } k \in [k_F, \pi] \text{ and } n_e \in [2/3, 1] \\ &\sigma = \downarrow \text{ electron removal for } k \in [0, k_F] \text{ and } n_e \in [0, 1] \\ \xi_{s1}^\uparrow(k) &= -\frac{1}{2} \left(1 - \left(\frac{(k - 2\pi)}{\pi n_e}\right)^2\right) \left(1 + \frac{2 \ln 2}{\pi u} \sin(\pi n_e)\right) - \frac{1}{2u} \cos\left(\frac{k - 2\pi}{n_e}\right) \sin(\pi n_e), \\ &\uparrow \text{ electron addition for } k \in [(2\pi - 3k_F), \pi] \text{ and } n_e \in [2/3, 1], \end{aligned} \quad (154)$$

so that,

$$\begin{aligned} \lim_{k \rightarrow 0} \xi_{s1}^\downarrow(k) &= -\frac{1}{2} - \frac{1}{2u} \left(1 + \frac{2 \ln 2}{\pi}\right) \sin(\pi n_e), \\ \lim_{k \rightarrow k_F} \xi_{s1}^\sigma(k) &= -\frac{3}{8} - \frac{3 \ln 2}{4\pi u} \sin(\pi n_e); \quad \lim_{k \rightarrow 2k_F} \xi_{s1}^\sigma(k) = \frac{1}{2u} \sin(\pi n_e), \\ \lim_{k \rightarrow 3k_F} \xi_{s1}^\sigma(3k_F) &= \lim_{k \rightarrow 2\pi - 3k_F} \xi_{s1}^\uparrow(k) = \frac{5}{8} + \frac{5 \ln 2}{4\pi u} \sin(\pi n_e). \end{aligned} \quad (155)$$

To reach the second exponent expression given in Eq. (154) one can either (i) use a new general exponent expression obtained upon replacing $\delta J_c^F = 1/2$ by $\delta J_c^F = -1/2$, which changes the terms $\xi_{c,c}^1/2$ and $\xi_{s1,c}^1/2$ in Eq. (148) to $-\xi_{c,c}^1/2$ and $-\xi_{s1,c}^1/2$, respectively, or (ii) use the present exponent expression, Eq. (148), upon bringing a $k > 0$ second Brillouin zone contribution to $k \in [-\pi, -(2\pi - 3k_F)]$ and then relying on the $\xi_{s1}^\uparrow(k) = \xi_{s1}^\uparrow(-k)$ symmetry to reach the expression valid for $k \in [(2\pi - 3k_F), \pi]$. For $u \gg 1$ and $m \rightarrow 0$ the \uparrow one-electron LHB addition exponent $\xi_{s1}^\uparrow(k)$ continuously changes from $\xi_{s1}^\uparrow(k) = -3/8$ for $k \rightarrow k_F$ to $\xi_{s1}^\uparrow(k) = 0$ for $k \rightarrow 2k_F$. For its other k ranges it is positive. In these limits the \downarrow one-electron removal exponent $\xi_{s1}^\downarrow(k)$ continuously changes from $\xi_{s1}^\downarrow(k) = -1/2$ for $k \rightarrow 0$ to $\xi_{s1}^\sigma(k) = -3/8$ for $k \rightarrow k_F$.

On the other hand, in the $m \rightarrow n_e$ limit the situation is the opposite relative to that for $m \rightarrow 0$, as the $s1$ branch line momentum width vanishes in the former limit both for \uparrow one-electron LHB addition and \downarrow one-electron removal. The use in the exponent expressions, Eqs. (148) and (149), of the values for $u \gg 1$ and spin density $m \rightarrow n_e$ of the parameters $\xi_{\beta\beta'}^j$ obtained by combining Eq. (B19) and (B20) of Appendix B for $u \gg 1$ and of the expressions

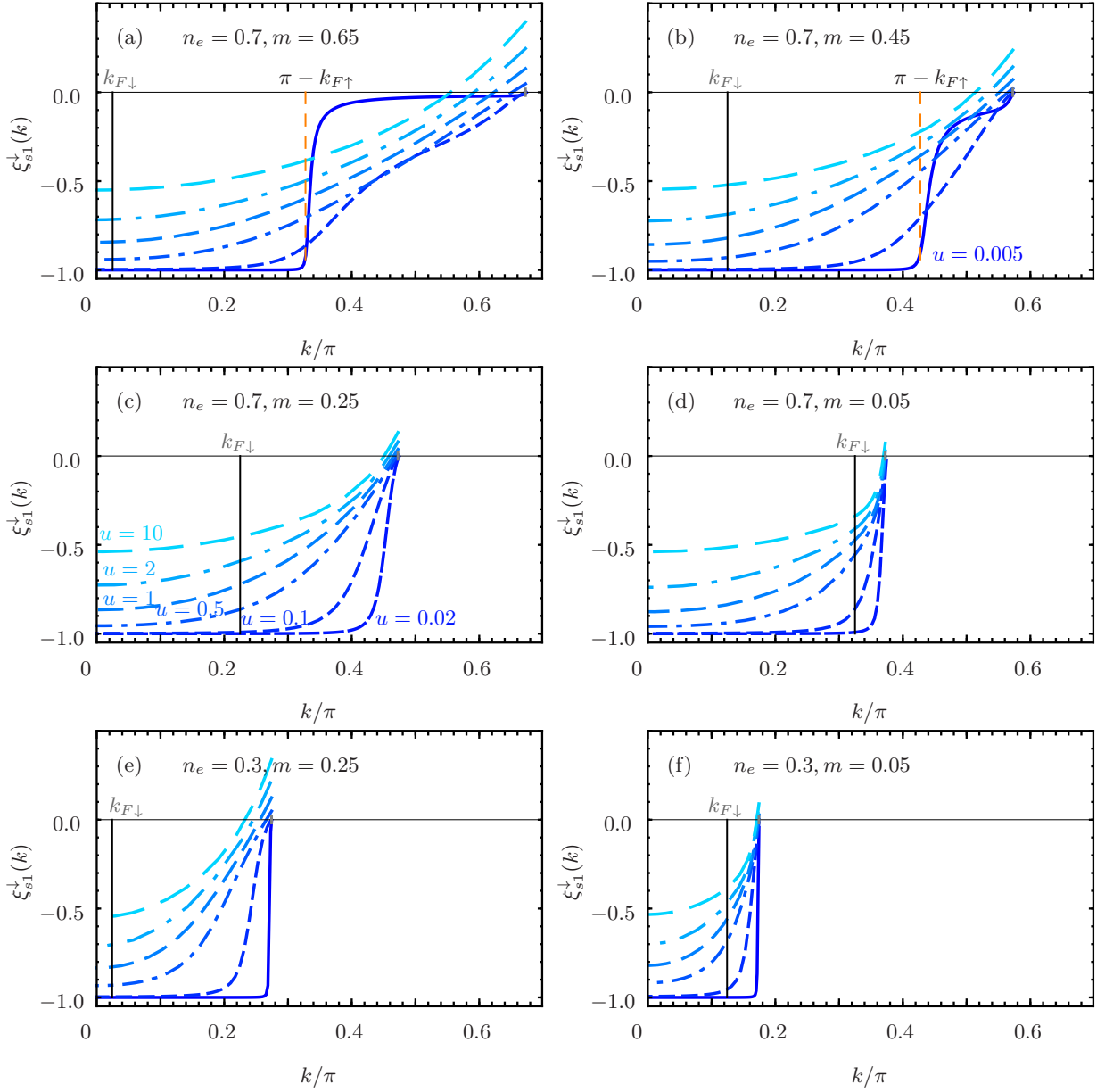


Figure 9: The exponent $\xi_{s1}^\downarrow(k)$, Eq. (149), that controls the singularities in the vicinity of the $s1$ branch line whose (k, ω) -plane one-parametric spectrum is defined by Eqs. (143) and (146) for the $\sigma = \downarrow$ one-electron removal and LHB addition spectral function, Eq. (150), as a function of the momentum $k/\pi \in]0, 1[$ for the same values of u , electronic density n_e , and spin density m as in Fig. 6. (For $k/\pi \in]-1, 0[$ the exponent $\xi_{s1}^\downarrow(k)$ is again given by $\xi_{s1}^\downarrow(k) = \xi_{s1}^\downarrow(-k)$ with $-k/\pi \in]0, 1[$ as plotted here.)

of the $\beta = c, s1$ pseudofermion phase shifts provided in Eq. (B14) of that Appendix we find the following exponent

expressions for the \uparrow one-electron removal and \downarrow one-electron LHB addition $s1$ branch line,

$$\begin{aligned}
\xi_{s1}^{\uparrow}(k) &= \frac{1}{2} \left(\frac{k}{\pi n_e} \right)^2 + \frac{2}{\pi^2} \left[\arctan \left(\frac{1}{2} \cot \left(\frac{k}{2n_e} \right) \right) \right]^2 \\
&\quad - \frac{2}{\pi u} \left[\cos^2 \left(\frac{k}{2n_e} \right) - \frac{k}{\pi n_e} \frac{2}{\pi} \arctan \left(\frac{1}{2} \cot \left(\frac{k}{2n_e} \right) \right) \right] \sin(\pi n_e), \\
&\quad \uparrow \text{electron removal for } k \in [0, 2k_F], \\
\xi_{s1}^{\downarrow}(k) &= -\frac{1}{2} \left(1 - \left(\frac{k}{\pi n_e} \right)^2 \right) + \frac{2}{\pi^2} \left[\arctan \left(\frac{1}{2} \tan \left(\frac{k}{2n_e} \right) \right) \right]^2 \\
&\quad - \frac{2}{\pi u} \left[\cos^2 \left(\frac{k}{2n_e} \right) + \frac{k}{\pi n_e} \frac{2}{\pi} \arctan \left(\frac{1}{2} \tan \left(\frac{k}{2n_e} \right) \right) \right] \sin(\pi n_e), \\
&\quad \downarrow \text{electron addition for } k \in [0, 2k_F],
\end{aligned} \tag{156}$$

so that,

$$\begin{aligned}
\lim_{k \rightarrow 0} \xi_{s1}^{\uparrow}(k) &= \frac{1}{2} - \frac{2}{\pi u} \sin(\pi n_e), \\
\lim_{k \rightarrow k_F} \xi_{s1}^{\uparrow}(k) &= \frac{1}{8} + 2 \left(\frac{1}{\pi} \arctan \left(\frac{1}{2} \right) \right)^2 - \frac{1}{\pi u} \left(1 - \frac{2}{\pi} \arctan \left(\frac{1}{2} \right) \right) \sin(\pi n_e), \\
&\approx 0.16856 - \frac{0.22436}{u} \sin(\pi n_e), \\
\lim_{k \rightarrow 2k_F} \xi_{s1}^{\uparrow}(k) &= \frac{1}{2}, \\
\lim_{k \rightarrow 0} \xi_{s1}^{\downarrow}(k) &= -\frac{1}{2} - \frac{2}{\pi u} \sin(\pi n_e), \\
\lim_{k \rightarrow k_F} \xi_{s1}^{\downarrow}(k) &= -\frac{3}{8} + 2 \left(\frac{1}{\pi} \arctan \left(\frac{1}{2} \right) \right)^2 - \frac{1}{\pi u} \left(1 + \frac{2}{\pi} \arctan \left(\frac{1}{2} \right) \right) \sin(\pi n_e), \\
&\approx -0.33144 - \frac{0.41226}{u} \sin(\pi n_e), \\
\lim_{k \rightarrow 2k_F} \xi_{s1}^{\downarrow}(k) &= \frac{1}{2} - \frac{2}{\pi u} \sin(\pi n_e).
\end{aligned} \tag{157}$$

Analysis of these expressions and values reveals that in the $u \gg 1$ limit and $m \rightarrow n_e$ the \uparrow one-electron removal exponent $\xi_{s1}^{\uparrow}(k)$ smoothly decreases from $\xi_{s1}^{\uparrow}(k) = 1/2$ for $k \rightarrow 0$ until it reaches a minimum value at $k = k_F$. For $k > k_F$ it continuously increases to $\xi_{s1}^{\uparrow}(k) = 1/2$ as $k \rightarrow 2k_F$. In the same limits the \downarrow one-electron LHB addition exponent $\xi_{s1}^{\downarrow}(k)$ smoothly varies from $\xi_{s1}^{\downarrow}(k) = -1/2$ for $k \rightarrow 0$ to $\xi_{s1}^{\downarrow}(k) = 1/2$ for $k \rightarrow 2k_F$.

Moreover, analysis of Fig. 8 shows that the exponent $\xi_{s1}^{\uparrow}(k)$ only becomes negative for a part of the $s1$ branch line k interval that starts at $k = k_{F\downarrow}$ and ends at a k momentum that for smaller and larger spin density values refers to one-electron LHB addition and removal, respectively. The u values for which it is negative are dependent of the densities. For the densities ranges $n_e \in [0, 1/2]$ and $m \in [0, 1 - n_e]$ and also for $n_e \in [1/2, 1]$ and $m \in [0, 1 - n_e]$ the exponent $\xi_{s1}^{\uparrow}(k)$ decreases upon increasing u from 1 for $u \rightarrow 0$ to its $u \gg 1$ values. In addition, according to Fig. 8 its u dependence is more involved for the densities intervals $n_e \in [1/2, 1]$ and $m \in [1 - n_e, n_e]$ for which it is given by 0 and 1 in the $u \rightarrow 0$ limit for different k ranges, respectively. For the k ranges for which it reads 1 for $u \rightarrow 0$ it remains being an increasing function of u for the whole u interval. For the k intervals for which it is given by 0 in the $u \rightarrow 0$ limit, upon increasing u it first decreases, goes through a minimum value, and then becomes an increasing function of u until reaching its $u \rightarrow \infty$ k dependent values.

On the other hand, for $u > 0$ the exponent $\xi_{s1}^{\downarrow}(k)$ whose k dependence is plotted in Fig. 9 is in general negative except for a small k region that corresponds to the larger k values of its range. Both for the densities ranges $n_e \in [0, 1/2]$ and $m \in [0, 1 - n_e]$ and for $n_e \in [1/2, 1]$ and $m \in [0, 1 - n_e]$ the exponent $\xi_{s1}^{\downarrow}(k)$ increases upon increasing u from -1 for $u \rightarrow 0$ to its $u \gg 1$ k dependent values. As also shown in that figure, its u dependence is more complex for the densities intervals $n_e \in [1/2, 1]$ and $m \in [1 - n_e, n_e]$ for which it is given by -1 and 0 in the $u \rightarrow 0$ limit for different k ranges, respectively. For the k ranges for which it reads -1 for $u \rightarrow 0$ it remains being an increasing function of u for the whole u interval. However, for the k domains for which it is given by 0 in the $u \rightarrow 0$ limit, upon increasing u it first decreases, goes through a minimum value, and then becomes an increasing function of u until reaching its $u \rightarrow \infty$ k dependent values.

C. The σ one-electron UHB addition branch lines

The σ one-electron UHB addition branch lines are generated by processes that correspond to particular cases of those generated by the leading-order operators, Eqs. (77) and (83), that are behind the \uparrow one-electron UHB addition spectrum, Eq. (78), and \downarrow one-electron UHB addition spectrum, Eq. (84). Hence they are contained within such two-parametric spectra that occupy well defined regions in the (k, ω) plane.

As discussed in Sec. III F, following the direct relation of the σ one-electron UHB addition branch lines spectra and exponents to those of the $\bar{\sigma}$ one-electron removal branch lines, for simplicity here we limit our study to the σ one-electron UHB addition branch lines that in the $u \rightarrow 0$ limit contribute to the $u = 0$ σ one-electron addition spectrum. In the case of the \uparrow and \downarrow one-electron UHB addition spectral functions those are the $s1$ branch line and one of the subbranches of the c^\pm branch lines, respectively.

As for the \downarrow one-electron removal $s1$ branch line, the spectrum that defines the (k, ω) -plane spectrum of the \uparrow one-electron UHB addition $s1$ branch line is such that $\omega_{s1}^\sigma(k) = \omega_{s1}^\sigma(-k)$ for $k \leq 0$ and the corresponding exponent given below is also such that $\xi_{s1}^\sigma(k) = \xi_{s1}^\sigma(-k)$ for $k \leq 0$. Hence for simplicity we restrict our following analysis to a reduced first Brillouin-zone scheme for positive momentum values $k \in [0, \pi]$.

This $s1$ branch line refers to excited energy eigenstates with the following number deviations relative to those of the initial ground state,

$$\delta N_c^F = -1; \quad \delta J_c^F = 1/2; \quad \delta N_{s1}^F = \delta J_{s1}^F = 0; \quad \delta N_{s1}^{NF} = -1; \quad \delta N_{\eta 1} = 1; \quad \delta J_{\eta 1} = -1/2. \quad (158)$$

Its (k, ω) -plane one-parametric spectrum reads,

$$\omega_{s1}^\uparrow(k) = 2\mu - \varepsilon_{s1}(q); \quad q \in [-k_{F\downarrow}, k_{F\downarrow}]. \quad (159)$$

Here $\varepsilon_{s1}(q)$ is the $s1$ band energy dispersion, Eq. (47) for $\beta = s1$, and 2μ stands for the energy scale defined in Eq. (55). Within an extended zone scheme the general relation of the $k > 0$ excitation momentum to the $s1$ band momentum q in Eq. (159) is,

$$k = \pi - q \in [(\pi - k_{F\downarrow}), (\pi + k_{F\downarrow})]. \quad (160)$$

Bringing this spectrum to the first Brillouin zone leads to two subbranches that refer to excitation momentum ranges $k \in [(\pi - k_{F\downarrow}), \pi]$ and $k \in [-\pi, -(\pi - k_{F\downarrow})]$, respectively. On the other hand, a contribution from $k < 0$ extended zone scheme second Brillouin zone interval also leads to the $k \in [(\pi - k_{F\downarrow}), \pi]$ range. We checked that the two corresponding spectral-function contributions to the momentum range $k \in [(\pi - k_{F\downarrow}), \pi]$ lead to the same power-law type of spectral-weight distributions in the vicinity of the $s1$ branch line. The corresponding reduced first-Brillouin-zone scheme used here for $k \in [0, \pi]$ excitation momentum relates to the $s1$ band momentum as,

$$k = \pi - q = [(\pi - k_{F\downarrow}), \pi], \quad (161)$$

for $q \in [0, k_{F\downarrow}]$. (Online the \uparrow one-electron UHB addition $s1$ branch line is green in Figs. 1-5; This branch line lays above the UHB pseudogap in Figs. 2-5, which refer to intermediate and large u values.)

The momentum dependent exponent of general form, Eq. (111), that controls the line shape near the branch line is given by,

$$\xi_{s1}^\uparrow(k) = -1 + \sum_{\iota=\pm 1} \left(-\frac{\iota \xi_{cc}^0}{2} - \Phi_{c,s1}(\iota 2k_F, q) \right)^2 + \sum_{\iota=\pm 1} \left(-\frac{\iota \xi_{s1c}^0}{2} - \Phi_{s1,s1}(\iota k_{F\downarrow}, q) \right)^2. \quad (162)$$

This exponent is plotted in Fig. 10 as a function of the momentum $k/\pi \in]0, 1[$ for several u values, electronic densities $n_e = 0.3$ and $n_e = 0.7$, and a set of spin density values $m < n_e$.

Near the present $s1$ branch line the $\sigma = \uparrow$ one-electron addition spectral function $B_{\uparrow,+1}(k, \omega)$, Eq. (4), corresponds to the UHB and has the following power-law behavior,

$$B_{\uparrow,+1}^{\text{UHB}}(k, \omega) = C_{\uparrow,s1}^{\text{UHB}} \left(\omega - \omega_{s1}^\uparrow(k) \right)^{\xi_{s1}^\uparrow(k)}; \quad (\omega - \omega_{s1}^\uparrow(k)) \geq 0, \quad (163)$$

where $C_{\uparrow,s1}^{\text{UHB}}$ is a constant independent of k and ω , the spectrum $\omega_{s1}^\uparrow(k)$ is that in Eq. (159), and the exponent $\xi_{s1}^\uparrow(k)$ is given in Eq. (162).

The direct relation of the exponent, Eq. (162), to that of the \downarrow one-electron removal $s1$ branch line enables deriving its behaviors for both $u \rightarrow 0$ and $u \gg 1$ from those of that other exponent. In the $u \rightarrow 0$ limit one finds the following value,

$$\lim_{u \rightarrow 0} \xi_{s1}^\uparrow(k) = -1 \quad (\text{for the whole above branch line } k \text{ range}). \quad (164)$$

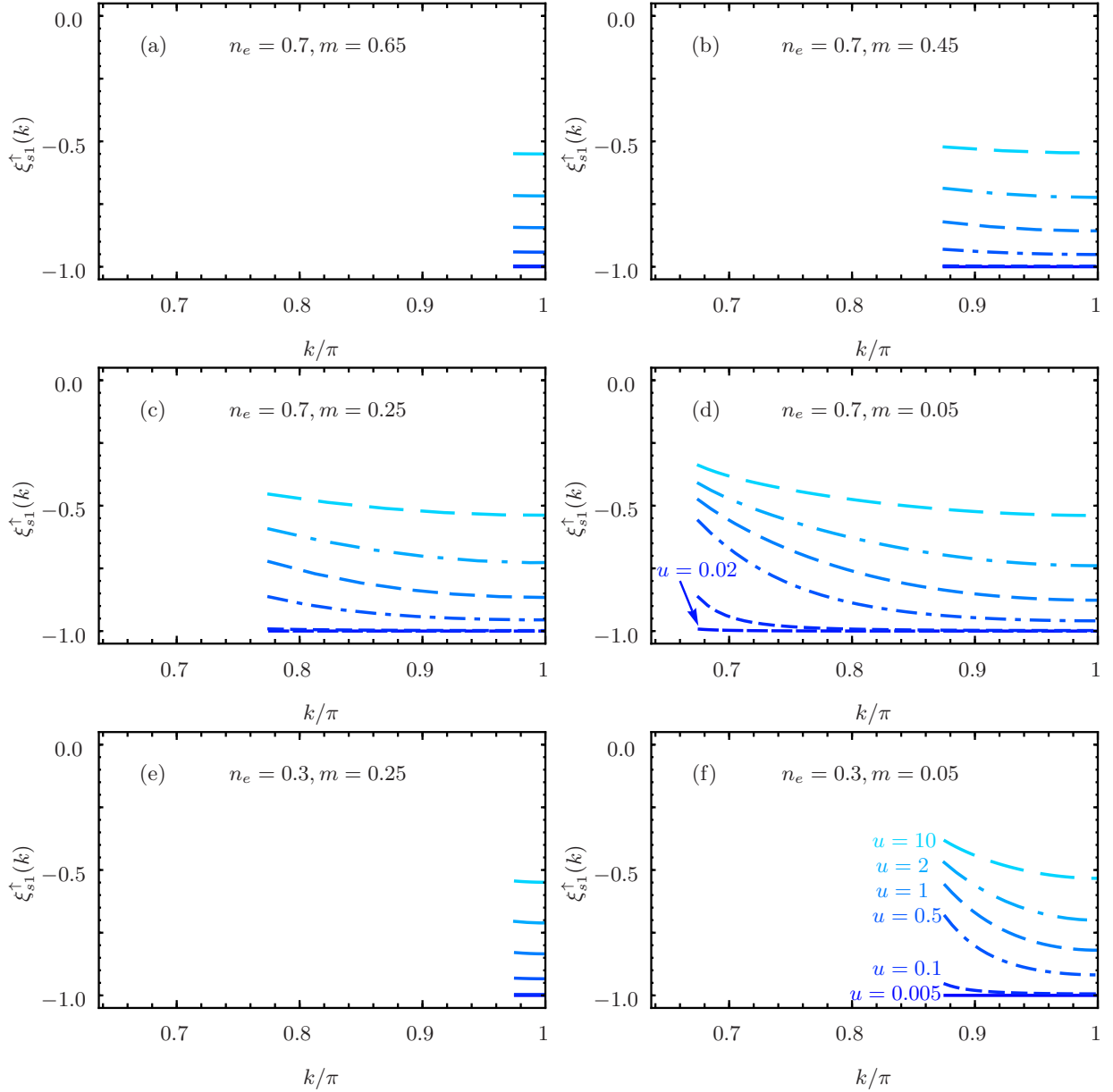


Figure 10: The exponent $\xi_{s1}^\uparrow(k)$, Eq. (162), that controls the singularities in the vicinity of the $s1$ branch line whose (k, ω) -plane one-parametric spectrum is defined by Eq. (159) for the $\sigma = \uparrow$ one-electron UHB addition spectral function, Eq. (163), as a function of the momentum $k/\pi \in]k_0/\pi, 1[$ where $]k_0/\pi, 1[$ with $0 < k_0 < \pi$ is a k interval that contains the branch line for the same values of u , electronic density n_e , and spin density m as in Fig. 6. (For $k/\pi \in]-1, -k_0/\pi[$ the exponent $\xi_{s1}^\uparrow(k)$ is given by $\xi_{s1}^\uparrow(k) = \xi_{s1}^\uparrow(-k)$ with $-k/\pi \in]k_0/\pi, 1[$ as plotted here.)

Hence, consistently with Eq. (120), for $u \rightarrow 0$ this branch line acquires the following δ -function-like one-electron spectral weight distribution along it,

$$\lim_{u \rightarrow 0} B_{\uparrow,+1}^{\text{UHB}}(k, \omega) = \delta(\omega - \omega_{s1}^\uparrow(k)) = \delta(\omega + 2t(\cos k - \cos k_{F\uparrow})), \quad |k| \in [(\pi - k_{F\downarrow}), \pi]. \quad (165)$$

The $u \rightarrow 0$ limiting behavior reported in Eq. (B2) of Appendix B for the $s1$ energy dispersion $\varepsilon_{s1}(q)$ appearing in the spectrum $\omega_{s1}^\uparrow(k)$, Eq. (159), confirms that the latter spectrum becomes in the $u \rightarrow 0$ limit the corresponding $u = 0$ non-interacting electronic spectrum, as given in Eq. (165).

The expression found for $u \gg 1$ and $m \rightarrow 0$ for the exponent, Eq. (162), is given by,

$$\xi_{s1}^\uparrow(k) = -\frac{1}{2} \left(1 - \left(\frac{\pi - k}{\pi n_e} \right)^2 \right) \left(1 + \frac{2 \ln 2}{\pi u} \sin(\pi n_e) \right) - \frac{1}{2u} \cos \left(\frac{\pi - k}{n_e} \right) \sin(\pi n_e), \quad (166)$$

so that,

$$\begin{aligned} \lim_{k \rightarrow \pi - k_F} \xi_{s1}^\sigma(k) &= -\frac{3}{8} - \frac{3 \ln 2}{4\pi u} \sin(\pi n_e), \\ \lim_{k \rightarrow \pi} \xi_{s1}^\downarrow(k) &= -\frac{1}{2} - \frac{1}{2u} \left(1 + \frac{2 \ln 2}{\pi} \right) \sin(\pi n_e). \end{aligned} \quad (167)$$

In the $m \rightarrow n_e$ limit the present $s1$ branch line momentum width vanishes so that it does not exist.

Analysis of Fig. 10 reveals that for $m < n_e$ the $s1$ branch-line exponent, Eq. (162), is a decreasing function of the momentum k . Moreover, it increases upon increasing u and remains negative for all momentum k and $m < n_e$ densities ranges.

Next, concerning the \downarrow one-electron UHB addition spectral function, the spectra $\omega_{c^\pm}^\sigma(k)$ that define the (k, ω) -plane shape of the c^+ branch line and its twin c^- branch line and the corresponding exponents $\xi_{c^\pm}^\sigma(k)$ are related as given in Eq. (122) for \uparrow electron removal. Considering the c^+ branch line in a reduced first Brillouin-zone scheme for which $k \in [-\pi, \pi]$ contains the same information as considering both the c^+ and c^- branch lines for the positive excitation momentum range $k \in [0, \pi]$. Below we only consider the k range associated with the subbranches for which the exponent $\xi_{c^+}^\downarrow(k) = \xi_{c^-}^\downarrow(-k)$ contributes to the \downarrow one-electron spectral weight as $u \rightarrow 0$. It turns out that for the exponent $\xi_{c^+}^\downarrow(k)$ such a subbranch is contained in the positive excitation momentum range $k \in [0, \pi]$.

The one σ one-electron UHB addition c^+ branch line is associated with excited energy eigenstates with the following number deviations relative to those of the initial ground state,

$$\delta N_c^F = 0; \quad \delta J_c^F = \mp 1/2; \quad \delta N_c^{NF} = -1; \quad \delta N_{s1}^F = 0; \quad \delta J_{s1}^F = 1/2; \quad \delta N_{\eta 1} = 1; \quad \delta J_{\eta 1} = \pm 1/2. \quad (168)$$

The one-parametric spectrum of general form, Eq. (109), that defines the (k, ω) -plane shape of this line reads,

$$\omega_{c^+}^\downarrow(k) = 2\mu - \varepsilon_c(q); \quad q \in [-2k_F, 2k_F], \quad (169)$$

where $\varepsilon_c(q)$ is the c band energy dispersion, Eq. (47) for $\beta = c$, and the corresponding c band momentum q is within an extended zone scheme related to the excitation momentum k as,

$$k = \pi + k_{F\downarrow} - q \in [(\pi - k_{F\uparrow}), (\pi + 2k_F + k_{F\downarrow})]. \quad (170)$$

Bringing this spectrum to the $k \in [-\pi, \pi]$ reduced first Brillouin-zone leads to two (k, ω) -plane c^+ branch line subbranches whose k intervals are given by $k = -\pi + k_{F\downarrow} - q \in [-\pi, -(\pi - 2k_F - k_{F\downarrow})]$ and $k = \pi + k_{F\downarrow} - q \in [(\pi - k_{F\uparrow}), \pi]$, respectively. As mentioned above, in the following we only consider the second of such momentum ranges,

$$k = \pi + k_{F\downarrow} - q \in [(\pi - k_{F\uparrow}), \pi]. \quad (171)$$

Indeed, it is that for which the exponent $\xi_{c^+}^\downarrow(k) = \xi_{c^-}^\downarrow(-k)$ reads -1 in the $u \rightarrow 0$ limit and thus the branch line contributes to the δ -function-like \downarrow one-electron spectrum in that limit. (Online the \downarrow one-electron UHB addition c^+ branch line is blue in Figs. 1-5; This branch line lays above the UHB pseudogap in Figs. 2-5, which refer to intermediate and large u values.)

The momentum dependent exponent of general form, Eq. (111), that controls the line shape near the branch line is in the present case given by,

$$\xi_{c^+}^\downarrow(k) = \xi_{c^-}^\downarrow(-k) = -1 + \sum_{\iota=\pm 1} \left(\frac{\xi_{c s1}^\iota}{2} - \Phi_{c,c}(\iota 2k_F, q) \right)^2 + \sum_{\iota=\pm 1} \left(\frac{\xi_{s1 s1}^\iota}{2} - \Phi_{s1,c}(\iota k_{F\downarrow}, q) \right)^2. \quad (172)$$

It is plotted in Fig. 11 as a function of the momentum $k/\pi \in]0, 1[$ for several u values, electronic densities $n_e = 0.3$ and $n_e = 0.7$, and a set of spin density values $m < n_e$.

In the vicinity of the present c^\pm branch lines the $\sigma = \downarrow$ one-electron addition spectral function $B_{\downarrow,+1}(k, \omega)$, Eq. (4), refers to the UHB and has the following power-law behavior,

$$B_{\downarrow,+1}^{\text{UHB}}(k, \omega) = C_{\downarrow,c^\pm}^{\text{UHB}} \left(\omega - \omega_{c^\pm}^\downarrow(k) \right)^{\xi_{c^\pm}^\downarrow(k)}; \quad (\omega - \omega_{c^\pm}^\downarrow(k)) \geq 0, \quad (173)$$

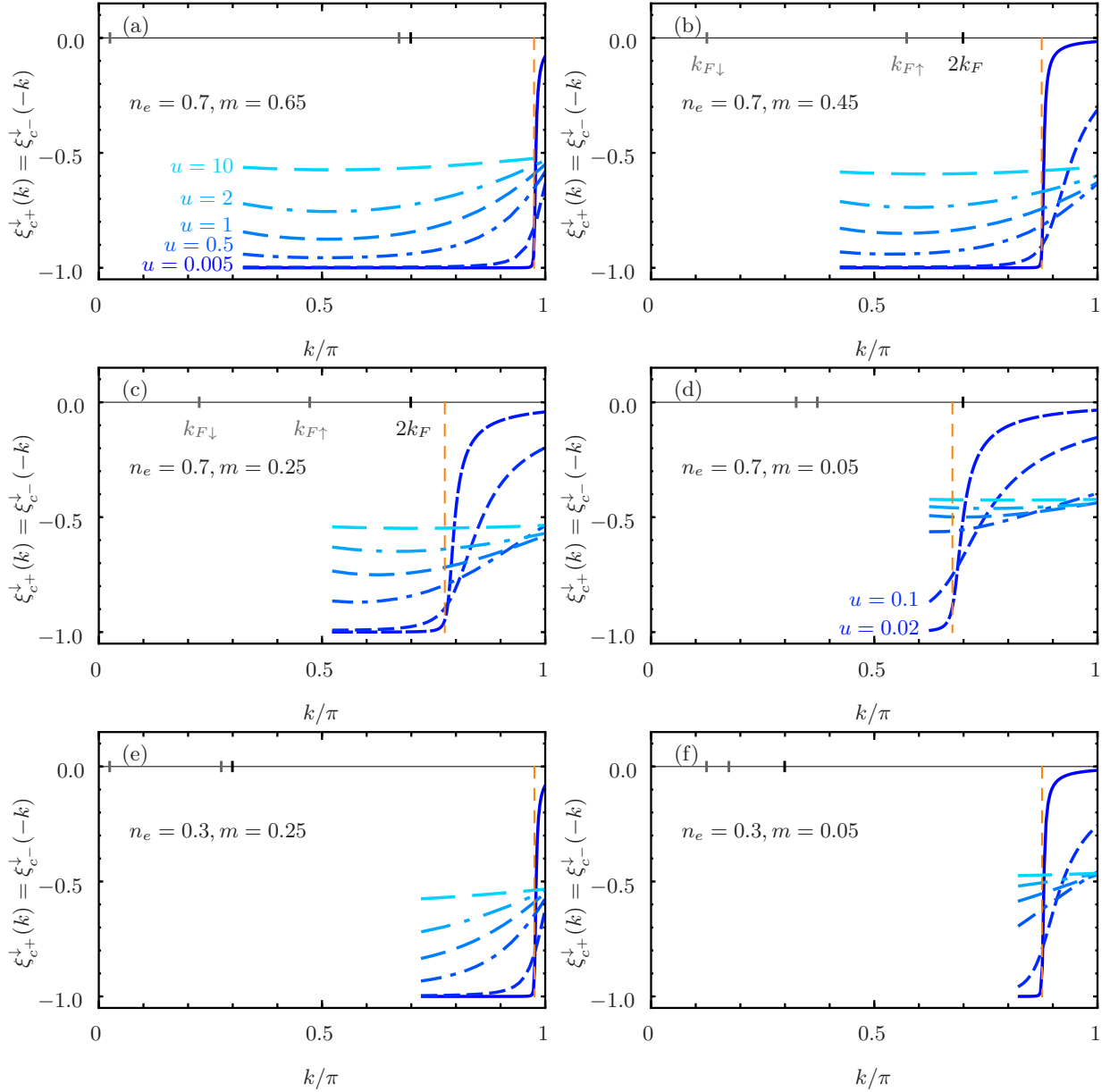


Figure 11: The exponent $\xi_{c+}^{\downarrow}(k) = \xi_{c-}^{\downarrow}(-k)$, Eq. (172), that controls the singularities in the vicinity of the c^+ branch line whose (k, ω) -plane one-parametric spectrum is defined by Eq. (169) for the $\sigma = \downarrow$ one-electron UHB addition spectral function, Eq. (173), as a function of the momentum $k/\pi \in]0, 1[$ for the same values of u , electronic density n_e , and spin density m as in Fig. 6.

where $C_{\downarrow, c^{\pm}}^{UHB}$ is a constant independent of k and ω , the spectrum $\omega_{c+}^{\downarrow}(k)$ is that in Eqs. (169) and (171), and the exponent $\xi_{c+}^{\downarrow}(k)$ is given in Eq. (172). Furthermore, $\omega_{c-}^{\downarrow}(k) = \omega_{c+}^{\downarrow}(-k)$ and $\xi_{c-}^{\downarrow}(k) = \xi_{c+}^{\downarrow}(-k)$.

The direct relation of the exponent, Eq. (172), to that of the corresponding \uparrow one-electron removal c^{\pm} branch lines subbranches enables deriving its behaviors for both $u \rightarrow 0$ and $u \gg 1$ from those of these other exponents. In the $u \rightarrow 0$ limit one finds the following values in the k range, Eq. (171),

$$\begin{aligned}
 \lim_{u \rightarrow 0} \xi_{c+}^{\downarrow}(k) &= 0, & k \in [(\pi - k_{F\downarrow}), \pi], \\
 &= -1, & k \in [(\pi - k_{F\uparrow}), (\pi - k_{F\downarrow})] \\
 \lim_{u \rightarrow 0} \xi_{c-}^{\downarrow}(k) &= -1, & k \in [-\pi, -(\pi - k_{F\downarrow})] \\
 &= 0, & k \in [-\pi, -(\pi - k_{F\downarrow})].
 \end{aligned} \tag{174}$$

For the k ranges for which such exponents read -1 the line shape becomes δ -function-like for $u \rightarrow 0$, as given in Eq. (120). In the present cases we find,

$$\begin{aligned} \lim_{u \rightarrow 0} B_{\downarrow,+1}^{\text{UHB}}(k, \omega) &= \delta\left(\omega - \omega_{c-}^{\downarrow}(k)\right) = \delta\left(\omega + 2t(\cos k - \cos k_{F\downarrow})\right), \quad k \in [-(\pi - k_{F\downarrow}), -(\pi - k_{F\uparrow})], \\ &= \delta\left(\omega - \omega_{c+}^{\downarrow}(k)\right) = \delta\left(\omega + 2t(\cos k - \cos k_{F\downarrow})\right), \quad k \in [(\pi - k_{F\uparrow}), (\pi - k_{F\downarrow})]. \end{aligned} \quad (175)$$

That the spectrum $\omega_{c+}^{\downarrow}(k) = \omega_{c-}^{\downarrow}(-k)$, Eq. (169), becomes in the $u \rightarrow 0$ limit the corresponding $u = 0$ non-interacting electronic spectrum is confirmed by the $u \rightarrow 0$ limiting behavior reported in Eq. (B1) of Appendix B for the c band energy dispersion $\varepsilon_c(q)$ appearing in the $u > 0$ spectrum general expression, Eq. (169). On the other hand, for the k ranges for which the exponent is given by 0 for $u \rightarrow 0$ the one-electron spectral weight at and near the corresponding branch lines vanishes in the $u \rightarrow 0$ limit.

For $u \gg 1$ and $m \rightarrow 0$ one finds the following expressions,

$$\xi_{c\pm}^{\downarrow}(k) = -\frac{3}{8} + \frac{\ln 2}{4\pi u} \left(\sin(\pi n_e) \mp 2 \sin\left(k \mp \frac{\pi}{2} n_e\right) \right). \quad (176)$$

In the $m \rightarrow n_e$ limit the exponents expressions are found to read,

$$\xi_{c\pm}^{\downarrow}(k) = -\frac{1}{2} \mp \frac{2}{\pi u} \sin k. \quad (177)$$

As it follows from analysis of Fig. 11, the main effect on the k dependence of the \downarrow one-electron UHB addition exponent $\xi_{c+}^{\downarrow}(k) = \xi_{c-}^{\downarrow}(-k)$, Eq. (172), of increasing the on-site repulsion u from $u \ll 1$ to $u \gg 1$ is to continuously changing its $u \rightarrow 0$ values -1 and 0 for the k ranges given in Eq. (174) to a k independent value for $k \in [0, \pi]$ as $u \rightarrow \infty$, which smoothly changes from $-3/8$ for $m \rightarrow 0$ to $-1/2$ for $m \rightarrow n_e$.

D. The \uparrow one-electron removal and \downarrow one-electron UHB addition $s1'$ non-branch lines for $0 < m < n_e$

The importance of the branch lines is confirmed by in the $u \rightarrow 0$ limit they recovering most of the $u = 0$ δ -function-like σ one-electron spectrum k ranges, as confirmed by combining Eqs. (136), (153), (165), (175). Interestingly, part of that spectral weight stems from the $u > 0$ UHB.

The k subrange of the $u = 0$ σ one-electron spectrum that does not stem from branch lines refers for $0 < m < n_e$ to the momentum interval $k \in [-k_{F\downarrow}, k_{F\downarrow}]$ for \uparrow one-electron removal and $|k| \in [\pi - k_{F\downarrow}, \pi]$ for \downarrow one-electron addition. That spectral weight stems from well-defined $u > 0$ spectral features whose line-shape expressions involve state summations difficult to compute.

Specifically, the $u = 0$ \uparrow one-electron removal spectral weight missing for $k \in [-k_{F\downarrow}, k_{F\downarrow}]$ and $0 < m < n_e$ stems from a $u > 0$ $s1'$ non-branch line that is generated by transitions to excited energy eigenstates with the following number deviations relative to those of the initial ground state,

$$\delta N_c^F = \delta J_c^F = 0; \quad \delta N_c^{NF} = -1; \quad \delta N_{s1}^F = 1; \quad \delta J_{s1}^F = \pm 1; \quad \delta N_{s1}^{NF} = -1. \quad (178)$$

The one-parametric spectrum of this line is given by,

$$\begin{aligned} \omega_{s1'}^{\uparrow}(k) &= -\varepsilon_{s1}(-k) - \varepsilon_c(\pm 2k_{F\downarrow}) = -\varepsilon_{s1}(q) - \varepsilon_c(\pm 2k_{F\downarrow}), \quad q \in [-k_{F\downarrow}, k_{F\downarrow}], \\ k &= -q \in [-k_{F\downarrow}, k_{F\downarrow}], \end{aligned} \quad (179)$$

where $\varepsilon_{s1}(q)$ is the $s1$ band energy dispersion, Eq. (47) for $\beta = s1$.

While the line shape analytical expression near this $s1'$ non-branch line remains an unsolved problem for $u > 0$, in the $u \rightarrow 0$ limit it becomes δ -function-like,

$$\lim_{u \rightarrow 0} B_{\uparrow,-1}(k, \omega) = \delta\left(\omega + \omega_{s1'}^{\uparrow}(k)\right) = \delta\left(\omega - 2t(\cos k - \cos k_{F\uparrow})\right), \quad k \in [-k_{F\downarrow}, k_{F\downarrow}]. \quad (180)$$

On the other hand, the $u = 0$ \downarrow one-electron addition spectral weight missing for $|k| \in [\pi - k_{F\downarrow}, \pi]$ and $0 < m < n_e$ stems from a $u > 0$ UHB $s1'$ non-branch line that is generated by transitions to excited energy eigenstates with the following number deviations relative to those of the initial ground state,

$$\delta N_c^F = -1; \quad \delta J_c^F = 0; \quad \delta N_{s1}^F = 0; \quad \delta J_{s1}^F = 1/2; \quad \delta N_{\eta 1} = 1; \quad \delta J_{\eta 1} = -1/2. \quad (181)$$

There is another such a $s1'$ non-branch line for $k < 0$.

The one-parametric spectrum that defines the (k, ω) -plane form of this line reads,

$$\begin{aligned}\omega_{s1'}^\downarrow(k) &= 2\mu - \varepsilon_{s1}(\pi - k) + \varepsilon_{s1}(k_{F\uparrow}) = 2\mu - \varepsilon_{s1}(q) + \varepsilon_{s1}(k_{F\uparrow}), \quad q \in [0, k_{F\downarrow}]. \\ k &= \pi - q \in [\pi - k_{F\downarrow}, \pi].\end{aligned}\tag{182}$$

The line shape analytical expression near this $s1'$ non-branch line remains again an open problem for $u > 0$ except in the $u \rightarrow 0$ limit in which it is δ -function-like,

$$\lim_{u \rightarrow 0} B_{\downarrow,+1}^{\text{UHB}}(k, \omega) = \delta\left(\omega - \omega_{s1'}^\downarrow(k)\right) = \delta\left(\omega + 2t(\cos k - \cos k_{F\downarrow})\right), \quad |k| \in [\pi - k_{F\downarrow}, \pi].\tag{183}$$

The \uparrow one-electron removal and \downarrow one-electron UHB addition $s1'$ non-branch lines are represented in Figs. 1-5 by sets of diamond symbols.

V. CONCLUDING REMARKS

In this paper we have studied the momentum and energy dependence of the σ one-electron spectral functions, Eq. (4), of the 1D Hubbard model at finite magnetic field in the vicinity of two types of singular features: The branch lines and border lines whose (k, ω) -plane spectra general form is given in Eqs. (109) and (117), respectively. The branch lines are represented in Figs. 1-5 by solid lines and dashed lines for the k ranges for which the corresponding exponent $\xi_\beta^\sigma(k)$, Eq. (111), is negative and positive, respectively. The one-electron removal and LWS addition boundary lines are in these figures represented by dashed-dotted lines.

To access the line shapes near these singular features we have used the PDT introduced in Refs. [38, 39] whose applications to the study of the 1D Hubbard model one-electron spectral functions have been limited to zero magnetic field [44-47]. The momentum dependence of the exponents that in the TL control the line shapes in the vicinity of the σ one-electron spectral functions branch lines was derived. For the k ranges for which such exponents $\xi_\beta^\sigma(k)$ (which are plotted in Figs. (6)-(11)) are negative, there are singularity cusps in the corresponding σ one-electron spectral functions, Eq. (4). The same occurs in the (k, ω) -plane vicinity of the border lines.

The important role played by the branch lines singularity cusps is confirmed by in the $u \rightarrow 0$ limit they recovering the $u = 0$ δ -function-like σ one-electron spectrum for most of its momentum k range, as confirmed by combining Eqs. (136), (153), (165), (175). The low-energy behavior of the correlation functions of the 1D Hubbard model at finite magnetic field has been the subject of several previous studies [14, 29-31]. To our knowledge, no previous investigations accessed for finite magnetic fields the repulsion u , electronic density n_e , spin density m , and momentum dependence of the exponents that in the TL control at high-energy the σ one-electron spectral functions in the vicinity of such branch lines singularity cusps.

The momentum subrange for which the $u = 0$ δ -function-like σ one-electron spectrum does not stem from branch lines is $k \in [0, k_{F\downarrow}]$ for \uparrow one-electron removal and $k \in [\pi - k_{F\downarrow}, \pi]$ for \downarrow one-electron addition. The PDT also accounts for the non-branch-line processes that give rise in the $u \rightarrow 0$ limit to the $u = 0$ one-electron spectrum at such a k interval yet the line shape of the corresponding spectral features remains for $u > 0$ an involved unsolved technical problem. (These $u > 0$ non-branch lines are represented in Figs. 1-5 by sets of diamond symbols.)

Complementarily, we have clarified beyond the results of Refs. [38, 39] how the σ one-electron creation and annihilation operators matrix elements between the ground state and excited energy eigenstates are accounted for by the PDT. Specifically, we have shown that the corresponding microscopic processes involve the rotated electrons as a needed link of the non-perturbative relation between the electrons and the pseudofermions. Moreover, in this paper the σ one-electron addition LHB and UHB were defined in terms of the occupancy configurations of such rotated electrons for the whole $u > 0$ range and all electronic densities and spin densities.

Concerning the relation of our theoretical results to actual condensed-matter systems, angle-resolved photoemission spectroscopy at finite magnetic field is not possible, since the field would severely deflect the photoelectrons. However, it is possible to measure the local spectral function on quasi-1D metals by (scanning) tunneling spectroscopy at finite magnetic field. Such experiments would provide some partial information on the spectral features theoretically studied in this paper by means of the 1D Hubbard model at finite magnetic field.

On the other hand, such a model has been implemented with ultra-cold atoms on optical lattices [67, 68] and the related antiferromagnetic Heisenberg spin chain has been prepared to characterize its spin configurations [69]. An interesting program would be the observation of the one-atom spectral weight distributions over the (k, ω) plane associated with the spectral functions studied in this paper in systems of spin 1/2 ultra-cold atoms on optical lattices.

Acknowledgments

We thank Ralph Claessen, Henrik Johannesson, Alexander Moreno, and Pedro D. Sacramento for illuminating discussions and the support by the Beijing CSRC and the FEDER through the COMPETE Program and the Portuguese FCT in the framework of the Strategic Projects PEST-C/FIS/UI0607/2013 and UID/CTM/04540/2013. J. M. P. C. acknowledges the hospitality of the Department of Physics at the University of Gothenburg, where the final part of this work was conducted.

Appendix A: The Bethe-ansatz equations within the β pseudoparticle representation and related quantities needed for the studies of this paper

Here we provide the pseudoparticle momentum distribution functional notation used in this paper for the 1D Hubbard model BA equations introduced in Ref. [5] for the TL, express the energy eigenvalues in terms of the rapidities that are the solutions of such equations, and provide useful information on the specific solutions of these equations for the excited energy eigenstates belonging to a PS as defined in Section II D.

Moreover, the integral equations that define the rapidity dressed phase shifts $2\pi\Phi_{\beta,\beta'}(r, r')$ in the expression, Eq. (49), of the related β pseudofermion phase shifts $2\pi\Phi_{\beta,\beta'}(q_j, q_{j'})$ are introduced, the f functions in the second-order terms of the energy functional, Eq. (44), are expressed in terms of such β pseudofermion phase shifts, and the $\beta = c, s1$ lowest peak weights $A_\beta^{(0,0)}$ and relative weights $a_\beta = a_\beta(m_{\beta,+1}, m_{\beta,-1})$ in the β pseudofermion spectral functions, Eq. (91), are written in terms of the related β pseudofermion phase-shift functional $\Phi_\beta^T(q_j)$, Eq. (100), which is a well-defined superposition of β pseudofermion phase shifts $2\pi\Phi_{\beta,\beta'}(q_j, q_{j'})$. Two different forms that the $\beta = c, s1$ pseudofermion spectral function $B_{Q_\beta}(k', \omega')$ whose general expression, Eq. (91), involves these lowest peak weights and relative weights acquires in the TL as a result of the specific values of four functionals controlled by $\Phi_\beta^T(q_j)$ are also provided.

Within the pseudoparticle momentum distribution functional notation used in this paper the BA equations considered in Ref. [5] read,

$$q_j = k^c(q_j) + \frac{2}{L} \sum_{n=1}^{\infty} \sum_{j'=1}^{L_{sn}} N_{sn}(q_{j'}) \arctan\left(\frac{\sin k^c(q_j) - \Lambda^{sn}(q_{j'})}{nu}\right) + \frac{2}{L} \sum_{n=1}^{\infty} \sum_{j'=1}^{L_{\eta n}} N_{\eta n}(q_{j'}) \arctan\left(\frac{\sin k^c(q_j) - \Lambda^{\eta n}(q_{j'})}{nu}\right), \quad j = 1, \dots, L, \quad (\text{A1})$$

and

$$q_j = \delta_{\alpha,\eta} \sum_{\iota=\pm 1} \arcsin(\Lambda^{\alpha n}(q_j) - i\iota u) + \frac{2(-1)^{\delta_{\alpha,\eta}}}{L} \sum_{j'=1}^L N_c(q_{j'}) \arctan\left(\frac{\Lambda^{\alpha n}(q_j) - \sin k^c(q_{j'})}{nu}\right) - \frac{1}{L} \sum_{n'=1}^{\infty} \sum_{j'=1}^{L_{\alpha n'}} N_{\alpha n'}(q_{j'}) \Theta_{n n'}\left(\frac{\Lambda^{\alpha n}(q_j) - \Lambda^{\alpha n'}(q_{j'})}{u}\right), \quad j = 1, \dots, L_{\alpha n}, \quad \alpha = \eta, s, \quad n = 1, \dots, \infty. \quad (\text{A2})$$

The sets of $j = 1, \dots, L$ and $j = 1, \dots, L_{\alpha n}$ quantum numbers q_j in Eqs. (A1) and (A2), respectively, which are defined in Eqs. (20) and (21), play the role of microscopic momentum values of different BA excitation branches. The corresponding β -band momentum distribution functions $N_\beta(q_j)$ read $N_\beta(q_j) = 1$ and $N_\beta(q_j) = 0$ for occupied and unoccupied discrete momentum values, respectively, the rapidity function $\Lambda^{\alpha n}(q_j)$ is the real part of the complex rapidity, Eq. (18), and $\Theta_{n n'}(x)$ is the function,

$$\Theta_{n n'}(x) = \delta_{n,n'} \left\{ 2 \arctan\left(\frac{x}{2n}\right) + \sum_{l=1}^{n-1} 4 \arctan\left(\frac{x}{2l}\right) \right\} + (1 - \delta_{n,n'}) \left\{ 2 \arctan\left(\frac{x}{|n-n'|}\right) + 2 \arctan\left(\frac{x}{n+n'}\right) + \sum_{l=1}^{\frac{n+n'-|n-n'|}{2}-1} 4 \arctan\left(\frac{x}{|n-n'|+2l}\right) \right\}, \quad (\text{A3})$$

where $n, n' = 1, \dots, \infty$. The indices $\alpha = \eta, s$ and numbers $n = 1, \dots, \infty$ refer to different BA excitation branches that are associated with the composite αn pseudoparticles as defined in this paper.

The corresponding energy eigenvalues have for densities ranges $n_e \in [0, 1[$ and $m \in [0, n_e]$ the following form,

$$E = \sum_{j=1}^L (N_c(q_j) E_c(q_j) + U/4 - \mu_\eta) + \sum_{\alpha=\eta, s} \sum_{n=1}^{\infty} \sum_{j=1}^{L_{\alpha n}} N_{\alpha n}(q_j) E_{\alpha n}(q_j) + \sum_{\alpha=\eta, s} 2\mu_\alpha (S_\alpha + S_\alpha^z), \quad (\text{A4})$$

where the $\alpha = \eta, s$ energy scales $2\mu_\alpha$ are given in Eq. (46) and the spectra $E_c(q_j)$ and $E_{\alpha n}(q_j)$ read,

$$\begin{aligned} E_c(q_j) &= -2t \cos k^c(q_j) - U/2 + \mu_\eta - \mu_s, \\ E_{\alpha n}(q_j) &= n 2\mu_\alpha + \delta_{\alpha, \eta} \left(4t \operatorname{Re} \left\{ \sqrt{1 - (\Lambda^{\eta n}(q_j) - i nu)^2} \right\} - nU \right), \quad \alpha = \eta, s, \quad n = 1, \dots, \infty, \end{aligned} \quad (\text{A5})$$

respectively. (The corresponding momentum eigenvalues of general $u > 0$ energy and momentum eigenstates are provided in Eq. (24).)

Useful solutions for our studies of the BA equations, Eqs. (A1) and (A2), are those for a ground state and its excited energy eigenstates that span a PS, as defined in Section IID. We denote the c and $s1$ band PS ground-state rapidity functions by $\Lambda_0^c(q_j) = \sin k_0^c(q_j)$ and $\Lambda_0^{s1}(q_j)$, respectively. They are the solutions of the BA equations, Eq. (A1) and Eq. (A2) for $\alpha n = s1$, respectively, with the $\beta = c, \alpha n$ band momentum distribution functions as given in Eq. (28). Hence they read,

$$\begin{aligned} q_j &= k_0^c(q_j) + \frac{2}{L} \sum_{q'=-k_{F\downarrow}}^{k_{F\downarrow}} \arctan \left(\frac{\sin k_0^c(q_j) - \Lambda_0^{s1}(q')}{u} \right), \quad j = 1, \dots, L, \\ q_j &= \frac{2}{L} \sum_{q'=-2k_F}^{2k_F} \arctan \left(\frac{\Lambda_0^{s1}(q_j) - \sin k_0^c(q')}{u} \right) \\ &\quad - \frac{2}{L} \sum_{q'=-k_{F\downarrow}}^{k_{F\downarrow}} \arctan \left(\frac{\Lambda_0^{s1}(q_j) - \Lambda_0^{s1}(q')}{2u} \right), \quad j = 1, \dots, N_\uparrow. \end{aligned} \quad (\text{A6})$$

In the TL the ground state momentum rapidity function $k_0^c(q)$ and rapidity function $\Lambda_0^{s1}(q)$ have well-defined inverse functions $q^c = q^c(k)$ where $k \in [-\pi, \pi]$ and $q^{s1} = q^{s1}(\Lambda)$ where $\Lambda \in [-\infty, \infty]$, respectively. One can then derive coupled integral equations from the coupled algebraic equations, Eq. (A6), whose solutions are the distributions $2\pi\rho(k) = \partial q^c(k)/\partial k$ and $2\pi\sigma(\Lambda) = \partial q^{s1}(\Lambda)/\partial \Lambda$. From such solutions one can then access the TL ground-state momentum rapidity function $k_0^c(q)$ and rapidity function $\Lambda_0^{s1}(q)$, respectively.

A result that plays a key role in the pseudoparticle - pseudofermion unitary transformation studied in Section III A is that the c and $s1$ band rapidity functions $\Lambda^c(q_j) = \sin k^c(q_j)$ and $\Lambda^{s1}(q_j)$ of a PS excited energy eigenstates can be expressed in terms of those of the corresponding initial ground state. From straightforward yet lengthly manipulations of the BA equations, Eqs. (A1) and (A2), that involve expansions up to arbitrary order in the deviations $\delta N_\beta(q_j)$, Eq. (42), one finds that,

$$\begin{aligned} \Lambda^c(q_j) &= \Lambda_0^c(\bar{q}(q_j)) = \sin k_0^c(\bar{q}(q_j)), \quad j = 1, \dots, L_c, \\ \Lambda^{s1}(q_j) &= \Lambda_0^{s1}(\bar{q}(q_j)), \quad j = 1, \dots, L_{s1}, \end{aligned} \quad (\text{A7})$$

where $\bar{q}_j = \bar{q}(q_j)$ with $j = 1, \dots, L_\beta$ are the discrete $\beta = c, s1$ band canonical momentum values given in Eq. (56).

The integral equations that define the rapidity dressed phase shifts $2\pi \bar{\Phi}_{\beta, \beta'}(r, r')$ in Eq. (49) are for densities in the ranges $n_e \in [0, 1]$ and $m \in [0, n_e]$ derived by solving such BA equations up to first order in the deviations $\delta N_\beta(q_j)$. In the following we write the rapidity dressed phase shifts in units of 2π . A first set of rapidity dressed phase shifts obey integral equations by their own. These equations read,

$$\bar{\Phi}_{s1, c}(r, r') = -\frac{1}{\pi} \arctan(r - r') + \int_{-r_s^0}^{r_s^0} dr'' G(r, r'') \bar{\Phi}_{s1, c}(r'', r'), \quad (\text{A8})$$

$$\bar{\Phi}_{s1, \eta n}(r, r') = -\frac{1}{\pi^2} \int_{-r_c^0}^{r_c^0} dr'' \frac{\arctan\left(\frac{r'' - r'}{n}\right)}{1 + (r - r'')^2} + \int_{-r_s^0}^{r_s^0} dr'' G(r, r'') \bar{\Phi}_{s1, \eta n}(r'', r'), \quad (\text{A9})$$

and

$$\begin{aligned} \bar{\Phi}_{s1,sn}(r, r') &= \delta_{1,n} \frac{1}{\pi} \arctan\left(\frac{r-r'}{2}\right) + (1-\delta_{1,n}) \frac{1}{\pi} \left\{ \arctan\left(\frac{r-r'}{n-1}\right) + \arctan\left(\frac{r-r'}{n+1}\right) \right\} \\ &\quad - \frac{1}{\pi^2} \int_{-r_c^0}^{r_s^0} dr'' \frac{\arctan\left(\frac{r''-r'}{n}\right)}{1+(r-r'')^2} + \int_{-r_s^0}^{r_s^0} dr'' G(r, r'') \bar{\Phi}_{s1,s1}(r'', r'). \end{aligned} \quad (\text{A10})$$

The parameters r_c^0 and r_s^0 appearing in these equations are defined in Eq. (48) and the kernel $G(r, r')$ is given by,

$$G(r, r') = -\frac{1}{2\pi} \left[\frac{1}{1+((r-r')/2)^2} \right] \left[1 - \frac{1}{2} \left(t(r) + t(r') + \frac{l(r)-l(r')}{r-r'} \right) \right]. \quad (\text{A11})$$

Here

$$t(r) = \frac{1}{\pi} [\arctan(r+r_c^0) - \arctan(r-r_c^0)], \quad (\text{A12})$$

and

$$l(r) = \frac{1}{\pi} [\ln(1+(r+r_c^0)^2) - \ln(1+(r-r_c^0)^2)]. \quad (\text{A13})$$

A second set of rapidity dressed phase shifts are expressed in terms of those in Eqs. (A8)-(A10) as follows,

$$\bar{\Phi}_{c,c}(r, r') = \frac{1}{\pi} \int_{-r_s^0}^{r_s^0} dr'' \frac{\bar{\Phi}_{s1,c}(r'', r')}{1+(r-r'')^2}, \quad (\text{A14})$$

$$\bar{\Phi}_{c,\eta n}(r, r') = -\frac{1}{\pi} \arctan\left(\frac{r-r'}{n}\right) + \frac{1}{\pi} \int_{-r_s^0}^{r_s^0} dr'' \frac{\bar{\Phi}_{s1,\eta n}(r'', r')}{1+(r-r'')^2}, \quad (\text{A15})$$

and

$$\bar{\Phi}_{c,sn}(r, r') = -\frac{1}{\pi} \arctan\left(\frac{r-r'}{n}\right) + \frac{1}{\pi} \int_{-r_s^0}^{r_s^0} dr'' \frac{\bar{\Phi}_{s1,sn}(r'', r')}{1+(r-r'')^2}. \quad (\text{A16})$$

Finally, the remaining rapidity dressed phase shifts can be expressed either in terms of those in Eqs. (A14)-(A16) only,

$$\bar{\Phi}_{\eta n,c}(r, r') = \frac{1}{\pi} \arctan\left(\frac{r-r'}{n}\right) - \frac{1}{\pi} \int_{-r_c^0}^{+r_c^0} dr'' \frac{\bar{\Phi}_{c,c}(r'', r')}{n[1+(\frac{r-r''}{n})^2]}, \quad (\text{A17})$$

$$\bar{\Phi}_{\eta n,\eta n'}(r, r') = \frac{\Theta_{n,n'}(r-r')}{2\pi} - \frac{1}{\pi} \int_{-r_c^0}^{+r_c^0} dr'' \frac{\bar{\Phi}_{c,\eta n'}(r'', r')}{n[1+(\frac{r-r''}{n})^2]}, \quad (\text{A18})$$

$$\bar{\Phi}_{\eta n,sn'}(r, r') = -\frac{1}{\pi} \int_{-r_c^0}^{+r_c^0} dr'' \frac{\bar{\Phi}_{c,sn'}(r'', r')}{n[1+(\frac{r-r''}{n})^2]}, \quad (\text{A19})$$

or in terms of both those in Eqs. (A8)-(A10) and in Eqs. (A14)-(A16),

$$\bar{\Phi}_{sn,c}(r, r') = -\frac{1}{\pi} \arctan\left(\frac{r-r'}{n}\right) + \frac{1}{\pi} \int_{-r_c^0}^{r_c^0} dr'' \frac{\bar{\Phi}_{c,c}(r'', r')}{n[1+(\frac{r-r''}{n})^2]} - \int_{-r_s^0}^{r_s^0} dr'' \bar{\Phi}_{s1,c}(r'', r') \frac{\Theta_{n,1}^{[1]}(r-r'')}{2\pi}; \quad n > 1, \quad (\text{A20})$$

$$\bar{\Phi}_{sn,\eta n'}(r, r') = \frac{1}{\pi} \int_{-r_c^0}^{r_c^0} dr'' \frac{\bar{\Phi}_{c,\eta n'}(r'', r')}{n[1+(\frac{r-r''}{n})^2]} - \int_{-r_s^0}^{r_s^0} dr'' \bar{\Phi}_{s1,\eta n'}(r'', r') \frac{\Theta_{n,1}^{[1]}(r-r'')}{2\pi}; \quad n > 1, \quad (\text{A21})$$

$$\bar{\Phi}_{sn,sn'}(r, r') = \frac{\Theta_{n,n'}(r-r')}{2\pi} + \frac{1}{\pi} \int_{-r_c^0}^{r_c^0} dr'' \frac{\bar{\Phi}_{c,sn'}(r'', r')}{n[1 + (\frac{r-r''}{n})^2]} - \int_{-r_s^0}^{r_s^0} dr'' \bar{\Phi}_{s1,sn'}(r'', r') \frac{\Theta_{n,1}^{[1]}(r-r'')}{2\pi}. \quad (\text{A22})$$

In the above equations, $\Theta_{n,n'}(x)$ is the function given in Eq. (A3) and $\Theta_{n,n'}^{[1]}(x)$ is its derivative,

$$\begin{aligned} \Theta_{n,n'}^{[1]}(x) &= \frac{\partial \Theta_{n,n'}(x)}{\partial x} = \delta_{n,n'} \left\{ \frac{1}{n[1 + (\frac{x}{2n})^2]} + \sum_{l=1}^{n-1} \frac{2}{l[1 + (\frac{x}{2l})^2]} \right\} + (1 - \delta_{n,n'}) \left\{ \frac{2}{|n-n'|[1 + (\frac{x}{|n-n'|})^2]} \right. \\ &\quad \left. + \frac{2}{(n+n')[1 + (\frac{x}{n+n'})^2]} + \sum_{l=1}^{\frac{n+n'-|n-n'|}{2}-1} \frac{4}{(|n-n'|+2l)[1 + (\frac{x}{|n-n'|+2l})^2]} \right\}. \end{aligned} \quad (\text{A23})$$

The f functions in the second-order terms of the energy functional, Eq. (44), can be expressed in terms of the related β pseudofermion phase shifts $2\pi \Phi_{\beta,\beta'}(q_j, q_{j'})$, Eq. (49), as follows [55],

$$\begin{aligned} f_{\beta\beta'}(q_j, q_{j'}) &= v_{\beta}(q_j) 2\pi \Phi_{\beta,\beta'}(q_j, q_{j'}) + v_{\beta'}(q_{j'}) 2\pi \Phi_{\beta',\beta}(q_{j'}, q_j) \\ &\quad + \frac{1}{2\pi} \sum_{\beta''=c,s1} \sum_{\iota=\pm 1} v_{\beta''} 2\pi \Phi_{\beta'',\beta}(\iota q_{F\beta''}, q_j) 2\pi \Phi_{\beta'',\beta'}(\iota q_{F\beta''}, q_{j'}), \end{aligned} \quad (\text{A24})$$

where the group velocities are defined in Eq. (50).

Other important quantities controlled by β pseudofermion phase shifts are the $\beta = c, s1$ lowest peak weights $A_{\beta}^{(0,0)}$ and relative weights $a_{\beta} = a_{\beta}(m_{\beta,+1}, m_{\beta,-1})$ in the β pseudofermion spectral functions, Eq. (91). These weights are derived by the use of the pseudofermion anti-commutators, Eq. (100), in Eq. (93). After some suitable algebra one finds,

$$\begin{aligned} A_{\beta}^{(0,0)} &= \left(\frac{1}{L}\right)^{2N_{\beta}^{\odot}} \prod_{j=1}^{L_{\beta}} \sin^2\left(\frac{\pi}{2} \left(1 - (1 - 2\Phi_{\beta}^T(q_j))N_{\beta}^{\odot}(q_j)\right)\right) \prod_{j=1}^{L_{\beta}-1} \left(\sin\left(\frac{\pi j}{L}\right)\right)^{2(L_{\beta}-j)} \\ &\quad \times \prod_{i=1}^{L_{\beta}} \prod_{j=1}^{L_{\beta}} \theta(j-i) \sin^2\left(\frac{\pi}{2} \left(1 - \left(1 - \frac{(2(j-i) + 2\Phi_{\beta}^T(q_j) - 2\Phi_{\beta}^T(q_i))}{L}\right) N_{\beta}^{\odot}(q_j)N_{\beta}^{\odot}(q_i)\right)\right) \\ &\quad \times \prod_{i=1}^{L_{\beta}} \prod_{j=1}^{L_{\beta}} \frac{1}{\sin^2\left(\frac{\pi}{2} \left(1 - \left(1 - \frac{2(j-i) + 2\Phi_{\beta}^T(q_j)}{L}\right) N_{\beta}^{\odot}(q_i)N_{\beta}^{\odot}(q_j)\right)\right)}, \quad \beta = c, s1, \end{aligned} \quad (\text{A25})$$

and

$$a_{\beta}(m_{\beta,+1}, m_{\beta,-1}) = \left(\prod_{\iota=\pm 1} a_{\beta,\iota}(m_{\beta,\iota})\right) \left(1 + \mathcal{O}(\ln L/L)\right), \quad \beta = c, s1, \quad (\text{A26})$$

respectively, where,

$$a_{\beta,\iota}(m_{\beta,\iota}) = \prod_{j=1}^{m_{\beta,\iota}} \frac{(2\Delta_{\beta}^{\iota} + j - 1)}{j} = \frac{\Gamma(m_{\beta,\iota} + 2\Delta_{\beta}^{\iota})}{\Gamma(m_{\beta,\iota} + 1)\Gamma(2\Delta_{\beta}^{\iota})}, \quad \beta = c, s1, \quad \iota = \pm 1. \quad (\text{A27})$$

In these expressions, $N_{\beta}^{\odot} = \sum_{j=1}^{L_{\beta}} N_{\beta}^{\odot}(q_j)$ and $N_{\beta}^{\odot}(q_j)$ are the number of $\beta = c, s1$ pseudofermions and the β band momentum distribution function, respectively, of the excited energy eigenstate generated by the PDT processes (A) and (B) defined in Section III B, L_{β} is the number of $\beta = c, s1$ band discrete momentum values given by $L_c = L$ and L_{s1} by Eq. (19) for $\alpha n = s1$, $\Phi_{\beta}^T(q_j)$ is the $\beta = c, s1$ pseudofermion phase-shift functional, Eq. (100), $\Gamma(x)$ is the usual gamma function, and the functionals $2\Delta_{\beta}^{\iota}$ are defined in Eqs. (101) and (102).

When such functionals are such that $2\Delta_{\beta}^{\iota} > 0$ and $2\Delta_{\beta}^{-\iota} = 0$, the $\beta = c, s1$ pseudofermion spectral function $B_{Q_{\beta}}(k', \omega')$, Eq. (91), has in the TL the following form,

$$\begin{aligned} B_{Q_{\beta}}(k', \omega') &= \frac{A_{\beta}^{(0,0)}}{v_{\beta}} a_{\beta,\iota} \left(\frac{L}{2\pi v_{\beta}} \omega' - \Delta_{\beta}^{\iota}\right) \delta\left(k' - \frac{\iota \omega'}{v_{\beta}}\right) \\ &\approx \frac{F_{\beta}^{(0,0)}}{v_{\beta} \Gamma(2\Delta_{\beta}^{\iota})} \Theta(\iota \omega') \left(\frac{\omega'}{2\pi S_{\beta} v_{\beta}}\right)^{-1+2\Delta_{\beta}^{\iota}} \delta\left(k' - \frac{\iota \omega'}{v_{\beta}}\right), \quad \beta = c, s1. \end{aligned} \quad (\text{A28})$$

The second expression provided here is obtained from the use of Eqs. (104) and (105).

On the other hand, when $2\Delta_\beta^t = 2\Delta_\beta^{-t} = 0$ one finds that in the TL such a function reads,

$$B_{Q_\beta}(k', \omega') = \frac{2\pi}{L} A_\beta^{(0,0)} \delta(k') \delta(\omega') \approx 2\pi F_\beta^{(0,0)} S_\beta \delta(k') \delta(\omega'), \quad \beta = c, s1. \quad (\text{A29})$$

Appendix B: Limiting behaviors of the $\beta = c, s1$ band energy dispersions, group velocities, and pseudofermion phase shifts

The one-parametric spectra of the σ one-electron spectral functions branch lines and border lines given in Eqs. (109) and (117), respectively, are expressed in terms of the c and $s1$ band energy dispersions, Eq. (47) for $\beta = c, s1$. The corresponding σ one-electron spectral weight distribution in the vicinity of the branch lines is controlled by the exponent $\xi_\beta^\sigma(k)$, Eq. (111), whose expression is linear in the functionals, Eq. (112), that involve the β pseudofermion phase shifts $2\pi \Phi_{\beta, \beta'}(q_j, q_{j'})$.

Here we provide limiting behaviors of such c and $s1$ band energy dispersions, corresponding c and $s1$ band group velocities, Eq. (50) for $\beta = c, s1$, and β pseudofermion phase shifts $2\pi \Phi_{\beta, \beta'}(q_j, q_{j'})$, Eq. (49). Except if otherwise stated, the expressions given in the following refer to electronic densities and spin densities in the ranges $n_e \in [0, 1[$ and $m \in]0, n_e]$, respectively.

In the $u \rightarrow 0$ limit the c and $s1$ energy dispersions, Eq. (47) for $\beta = c, s1$, have the following behaviors,

$$\begin{aligned} \varepsilon_c(q) &= -2t \left(2 \cos\left(\frac{q}{2}\right) - \cos k_{F\uparrow} - \cos k_{F\downarrow} \right), \quad |q| \leq 2k_{F\downarrow}, \\ &= -2t (\cos(|q| - k_{F\downarrow}) - \cos k_{F\uparrow}), \quad 2k_{F\downarrow} \leq |q| < \pi, \end{aligned} \quad (\text{B1})$$

and

$$\varepsilon_{s1}(q) = -2t (\cos q - \cos k_{F\downarrow}), \quad q \in [-k_{F\uparrow}, k_{F\uparrow}], \quad (\text{B2})$$

respectively.

On the other hand, for $u \gg 1$ and $m \rightarrow 0$ the behavior of these energy dispersions is,

$$\begin{aligned} \varepsilon_c(q) &= -2t \left(\cos q - \cos 2k_F + \frac{n \ln 2}{u} (\sin^2 q - \sin^2 2k_F) \right), \quad q \in [-\pi, \pi], \\ \varepsilon_{s1}(q) &= -\frac{\pi n_e t}{2u} \left(1 - \frac{\sin 2\pi n_e}{2\pi n_e} \right) \cos\left(\frac{q}{n_e}\right), \quad q \in [-k_F, k_F], \end{aligned} \quad (\text{B3})$$

whereas for $u \gg 1$ and $m \rightarrow n_e$ they read,

$$\begin{aligned} \varepsilon_c(q) &= -2t (\cos q - \cos 2k_F), \quad q \in [-\pi, \pi], \\ \varepsilon_{s1}(q) &= -\frac{n_e t}{u} \left(1 - \frac{\sin 2\pi n_e}{2\pi n_e} \right) \left(\cos\left(\frac{q}{n_e}\right) - 1 \right), \quad q \in [-2k_F, 2k_F]. \end{aligned} \quad (\text{B4})$$

In the $u \rightarrow 0$ limit the corresponding c and $s1$ group velocities, Eq. (50) for $\beta = c, s1$, have the following behaviors,

$$\begin{aligned} v_c(q) &= 2t \sin\left(\frac{q}{2}\right), \quad |q| \leq 2k_{F\downarrow}, \\ &= \text{sgn}\{q\} 2t \sin(|q| - k_{F\downarrow}), \quad 2k_{F\downarrow} \leq |q| < \pi, \end{aligned} \quad (\text{B5})$$

and

$$v_{s1}(q) = 2t \sin q, \quad q \in [-k_{F\uparrow}, k_{F\uparrow}], \quad (\text{B6})$$

respectively. Moreover, for $u \gg 1$ and $m \rightarrow 0$ the group velocities behavior is,

$$\begin{aligned} v_c(q) &= 2t \left(\sin q - \frac{n_e \ln 2}{u} \sin 2q \right), \quad q \in [-\pi, \pi], \\ v_{s1}(q) &= \frac{\pi t}{2u} \left(1 - \frac{\sin 2\pi n_e}{2\pi n_e} \right) \sin\left(\frac{q}{n_e}\right), \quad q \in [-k_F, k_F], \end{aligned} \quad (\text{B7})$$

whereas for $u \gg 1$ and $m \rightarrow n_e$ they are given by,

$$\begin{aligned} v_c(q) &= 2t \sin q, \quad q \in [-\pi, \pi], \\ v_{s1}(q) &= \frac{t}{u} \left(1 - \frac{\sin 2\pi n_e}{2\pi n_e} \right) \sin \left(\frac{q}{n_e} \right), \quad q \in [-2k_F, 2k_F]. \end{aligned} \quad (\text{B8})$$

In the $u \rightarrow 0$ limit the phase shifts $2\pi \Phi_{\beta, \beta'}(q_j, q_{j'})$, Eq. (49), acquired by $\beta = c, s1$ pseudofermions due to the creation or annihilation under transitions to excited energy eigenstates of other $\beta' = c, s1$ pseudofermions have the following limiting behaviors,

$$\begin{aligned} \Phi_{s1, s1}(q, q') &= 0, \\ \Phi_{s1, c}(q, q') &= -\frac{1}{2} \text{sgn} \left\{ \sin q - \sin \left(\frac{q'}{2} \right) \right\}, \quad |q'| \leq 2k_{F\downarrow} \\ &= -\frac{1}{2} \text{sgn} \{ \sin q - \text{sgn}\{q'\} \sin(|q'| - k_{F\downarrow}) \}, \quad 2k_{F\downarrow} \leq |q'| < \pi, \\ \Phi_{c, c}(q, q') &= -\frac{1}{2} \text{sgn}\{q - q'\}, \quad |q|, |q'| \leq 2k_{F\downarrow} \\ &= \frac{1}{2} \text{sgn}\{q'\}, \quad |q| \leq 2k_{F\downarrow}, \quad 2k_{F\downarrow} \leq |q'| < \pi, \\ &= 0, \quad 2k_{F\downarrow} < |q| < \pi, \\ \Phi_{c, s1}(q, q') &= -\frac{1}{2} \text{sgn} \left\{ \sin \left(\frac{q}{2} \right) - \sin q' \right\}, \quad |q| \leq 2k_{F\downarrow} \\ &= -\frac{1}{2} \text{sgn} \{ \text{sgn}\{q\} \sin(|q'| - k_{F\downarrow}) - \sin q' \}, \quad 2k_{F\downarrow} \leq |q| < \pi. \end{aligned} \quad (\text{B9})$$

Particular cases of these $\beta = c, s1$ pseudofermion phase shifts are those involved in the functionals, Eq. (112), which in the $u \rightarrow 0$ limit are then given by,

$$\begin{aligned} \Phi_{s1, s1}(\iota k_{F\downarrow}, q) &= \Phi_{c, c}(\iota 2k_F, q) = 0, \\ \Phi_{s1, c}(\iota k_{F\downarrow}, q) &= -\frac{\iota}{2}, \quad |q| < 2k_{F\downarrow}, \quad q = -\iota 2k_{F\downarrow}, \quad \iota = \pm 1 \\ &= 0, \quad q = \iota 2k_{F\downarrow}, \quad \iota = \pm 1 \\ &= -\frac{1}{2} \text{sgn} \{ \iota \sin k_{F\downarrow} - \text{sgn}\{q\} \sin(|q| - k_{F\downarrow}) \}, \quad 2k_{F\downarrow} \leq |q| < \pi, \quad \iota = \pm 1, \\ \Phi_{c, s1}(\iota 2k_F, q) &= -\frac{\iota}{2}, \quad |q| < k_{F\uparrow}, \quad \iota = \pm 1 \\ &= \frac{1}{2} \text{sgn}\{q\}, \quad |q| = k_{F\uparrow}. \end{aligned} \quad (\text{B10})$$

On the other hand, for $u \gg 1$ and spin density $m \rightarrow 0$ the above $\beta = c, s1$ pseudofermion phase shifts behave as,

$$\begin{aligned} \Phi_{s1, s1}(q, q') &= \frac{1}{\pi} \int_0^\infty d\omega \frac{\sin \left(\omega \frac{2}{\pi} \left[\text{arcsinh} \left(\tan \left(\frac{q}{n_e} \right) \right) - \text{arcsinh} \left(\tan \left(\frac{q'}{n_e} \right) \right) \right] \right)}{\omega (1 + e^{2\omega})} \\ &+ \frac{q'}{4u} \frac{\sin(\pi n_e)}{\pi n_e} \cos \left(\frac{q}{n_e} \right), \quad |q| \neq k_F \\ &= \frac{\iota}{2\sqrt{2}}, \quad q = \iota k_F, \quad q' \neq \iota k_F, \quad \iota = \pm 1 \\ &= \frac{\iota}{2\sqrt{2}} (3 - 2\sqrt{2}), \quad q = q' = \iota k_F, \quad \iota = \pm 1, \\ \Phi_{s1, c}(q, q') &= -\frac{q}{2\pi n_e} + \frac{1}{4u} \cos \left(\frac{q}{n_e} \right) \sin q', \quad |q| \neq k_F \\ &= -\frac{\iota}{2\sqrt{2}}, \quad q = \iota k_F, \quad \iota = \pm 1, \\ \Phi_{c, c}(q, q') &= -\frac{\ln 2}{2\pi u} (\sin q - \sin q'), \\ \Phi_{c, s1}(q, q') &= \frac{q'}{2\pi n_e} - \frac{1}{4u} \sin q \cos \left(\frac{q'}{n_e} \right) + q' \frac{\ln 2}{2\pi u} \frac{\sin(\pi n_e)}{\pi n_e}. \end{aligned} \quad (\text{B11})$$

Those involved in the functionals, Eq. (112), are in that limit and for the same densities then given by,

$$\begin{aligned}
\Phi_{s1,s1}(ik_F, q) &= \frac{\iota}{2\sqrt{2}}, \quad q \neq \iota k_F, \quad \iota = \pm 1 \\
&= \frac{\iota}{2\sqrt{2}}(3 - 2\sqrt{2}), \quad q = \iota k_F, \quad \iota = \pm 1, \\
\Phi_{s1,c}(ik_F, q) &= -\frac{\iota}{2\sqrt{2}}, \quad \iota = \pm 1, \\
\Phi_{c,c}(\iota 2k_F, q) &= -\frac{\ln 2}{2\pi u}(\iota \sin(\pi n_e) - \sin q), \\
\Phi_{c,s1}(\iota 2k_F, q) &= \frac{q}{2\pi n_e} - \frac{\iota}{4u} \sin 2k_F \cos\left(\frac{q}{n_e}\right) + q \frac{\ln 2}{2\pi u} \frac{\sin(\pi n_e)}{\pi n_e}.
\end{aligned} \tag{B12}$$

For $u \gg 1$ and $m \rightarrow n_e$ the $\beta = c, s1$ pseudofermion phase shifts under consideration behave as,

$$\begin{aligned}
\Phi_{s1,s1}(q, q') &= \frac{1}{\pi} \arctan\left(\frac{\tan\left(\frac{q}{2n_e}\right) - \tan\left(\frac{q'}{2n_e}\right)}{2}\right) + \frac{q'}{\pi u} \frac{\sin(\pi n_e)}{\pi n_e} \cos^2\left(\frac{q}{2n_e}\right), \\
\Phi_{s1,c}(q, q') &= -\frac{q}{2\pi n_e} + \frac{1}{\pi u} \cos^2\left(\frac{q}{2n_e}\right) \sin q', \\
\Phi_{c,c}(q, q') &= 0, \\
\Phi_{c,s1}(q, q') &= \frac{q'}{2\pi n_e} - \frac{1}{\pi u} \sin q \cos^2\left(\frac{q'}{2n_e}\right).
\end{aligned} \tag{B13}$$

As a result, in that limit in which $k_{F\downarrow} = 0$ the $\beta = c, s1$ pseudofermion phase shifts involved in the functionals, Eq. (112), read,

$$\begin{aligned}
\Phi_{s1,s1}(0, q) &= -\frac{1}{\pi} \arctan\left(\frac{1}{2} \tan\left(\frac{q}{2n_e}\right)\right) + \frac{q}{\pi u} \frac{\sin(\pi n_e)}{\pi n_e}, \\
\Phi_{s1,c}(0, q) &= \frac{\sin q}{\pi u}; \quad \Phi_{c,c}(\iota 2k_F, q) = 0, \\
\Phi_{c,s1}(\iota 2k_F, q) &= \frac{q}{2\pi n_e} - \frac{\iota}{\pi u} \sin(\pi n_e) \cos^2\left(\frac{q}{2n_e}\right), \quad \iota = \pm 1.
\end{aligned} \tag{B14}$$

The limiting behaviors of the related $\beta = c, s1$ pseudofermion phase-shift parameters, Eq. (63), which are the entries of the matrices, Eq. (64), are given in the following. In the $u \rightarrow 0$ limit such matrices read,

$$\lim_{u \rightarrow 0} Z^1 = \lim_{u \rightarrow 0} \begin{bmatrix} \xi_{cc}^1 & \xi_{cs1}^1 \\ \xi_{s1c}^1 & \xi_{s1s1}^1 \end{bmatrix} = \begin{bmatrix} 1 & 0 \\ 1 & 1 \end{bmatrix}; \quad \lim_{u \rightarrow 0} Z^0 = \lim_{u \rightarrow 0} \begin{bmatrix} \xi_{cc}^0 & \xi_{cs1}^0 \\ \xi_{s1c}^0 & \xi_{s1s1}^0 \end{bmatrix} = \begin{bmatrix} 1 & -1 \\ 0 & 1 \end{bmatrix}. \tag{B15}$$

These values apply to the limit $\lim_{u \rightarrow 0} \lim_{m \rightarrow 0}$. However, if one takes the limit $\lim_{m \rightarrow 0}$ before $\lim_{u \rightarrow 0}$ one finds instead,

$$\lim_{u \rightarrow 0} \lim_{m \rightarrow 0} Z^1 = \begin{bmatrix} \sqrt{2} & 1/\sqrt{2} \\ 0 & 1/\sqrt{2} \end{bmatrix}; \quad \lim_{u \rightarrow 0} \lim_{m \rightarrow 0} Z^0 = \begin{bmatrix} 1/\sqrt{2} & 0 \\ -1/\sqrt{2} & \sqrt{2} \end{bmatrix}. \tag{B16}$$

This singular behavior means that at $m = 0$ and for $m \rightarrow 0$ the matrices, Eq. (64), have different values at $u = 0$ and in the $u \rightarrow 0$ limit. Interestingly, this singular behavior does not show up in the physical quantities whose expressions involve the $\beta = c, s1$ pseudofermion phase-shift parameters, Eq. (63), which are the entries of the matrices under consideration.

For $m \rightarrow 0$ and all u values the matrices in Eq. (64) are given by,

$$\lim_{m \rightarrow 0} Z^1 = \begin{bmatrix} \xi_0 & \xi_0/2 \\ 0 & 1/\sqrt{2} \end{bmatrix}; \quad \lim_{m \rightarrow 0} Z^0 = \begin{bmatrix} 1/\xi_0 & 0 \\ -1/\sqrt{2} & \sqrt{2} \end{bmatrix}, \tag{B17}$$

where the $m \rightarrow 0$ parameter ξ_0 has the following limiting behaviors,

$$\begin{aligned}
\xi_0 &= \sqrt{2}, \quad u \rightarrow 0, \\
&= 1 + \frac{\ln 2}{\pi u} \sin(\pi n_e), \quad u \gg 1.
\end{aligned} \tag{B18}$$

In the $m \rightarrow n_e$ limit the matrices in Eq. (64) simplify to,

$$\lim_{m \rightarrow n_e} Z^1 = \begin{bmatrix} 1 & 0 \\ \eta_0 & 1 \end{bmatrix}; \quad \lim_{m \rightarrow n_e} Z^0 = \begin{bmatrix} 1 & -\eta_0 \\ 0 & 1 \end{bmatrix}, \quad (\text{B19})$$

where the parameter η_0 reads $\eta_0 = \frac{2}{\pi} \arctan\left(\frac{\sin(\pi n_e)}{u}\right)$ and thus has limiting behaviors,

$$\begin{aligned} \eta_0 &= 1, & u \rightarrow 0, \\ &= \frac{2}{\pi u} \sin(\pi n_e), & u \gg 1. \end{aligned} \quad (\text{B20})$$

-
- [1] E. H. Lieb, F. Y. Wu, Phys. Rev. Lett. 20 (1968) 1445.
[2] E. H. Lieb, F. Y. Wu, Physica A 321 (2003) 1.
[3] C. N. Yang, Phys. Rev. Lett. 19 (1967) 1312.
[4] M. J. Martins, P. B. Ramos, Nucl. Phys. B 522 (1998) 413.
[5] M. Takahashi, Progr. Theor. Phys 47 (1972) 69.
[6] M. C. Gutzwiller, Phys. Rev. Lett. 10 (1963) 159.
[7] J. Hubbard, Proc. Roy. Soc. (London) A 276 (1963) 238.
[8] B. S. Shastry, Bill Sutherland, Phys. Rev. Lett. 65 (1990) 243.
[9] J. M. P. Carmelo, N. M. R. Peres, D. K. Campbell, A. W. Sandvik, Z. Phys. B 103 (1997) 217; N. M. R. Peres, R. G. Dias, P. D. Sacramento, J. M. P. Carmelo, Phys. Rev. B 61 (2000) 5169.
[10] S. Tomonaga, Prog. Theor. Phys. 5 (1950) 544.
[11] J. M. Luttinger, J. Math. Phys. 4 (1963) 1154
[12] J. Sólyom, Adv. Phys. 28 (1979) 201.
[13] J. Voit, Rep. Prog. Phys. 57 (1994) 977.
[14] F. Woynarovich, H. P. Eckle, T. T. Truong, J. Phys. A 22 (1989) 4027.
[15] K.-V. Pham, M. Gabay, P. Lederer, Phys. Rev. B 61 (2000) 16 397.
[16] M. Karowski, P. Weisz, Nucl. Phys. B 139 (1978) 455;
B. Berg, M. Karowski, and P. Weisz, Phys. Rev. D 19 (1979) 2477.
[17] F. A. Smirnov, Form Factors in Completely Integrable Models of Quantum Field Theory, Advanced Series in Mathematical Physics, vol. 14, World Scientific, Singapore, 1992.
[18] J. L. Cardy, G. Mussardo, Nucl. Phys. B 340 (1990) 387;
A. Fring, G. Mussardo, P. Simonetti, Nucl. Phys. B 393 (1993) 413.
[19] V. P. Yurov, Al. B. Zamolodchikov, Int. J. Mod. Phys. A 6 (1991) 3419;
S. Lukyanov, Commun. Math. Phys. 167 (1995) 183;
S. Lukyanov, A. B. Zamolodchikov, Nucl. Phys. B 493 (1997) 2541;
S. Lukyanov, Mod. Phys. Lett. A 12 (1990) 2543.
[20] F. H. L. Essler, A. M. Tsvelik, G. Delfino, Phys. Rev. B 56 (1997) 11001;
F. H. L. Essler, A. M. Tsvelik, Phys. Rev. B 57 (1998) 10592 .
[21] B. L. Altshuler, R. M. Konik, A. M. Tsvelik, Nucl. Phys. B 739 (2006) 311.
[22] F. H. L. Essler, R. M. Konik, J. Stat. Mech. (2009) P.09018.
[23] M. Jimbo, T. Miwa, Algebraic Analysis of Solvable Lattice Models, American Mathematical Society, Providence, 1994.
[24] A. H. Bougourzi, M. Couture, M. Kacir, Phys. Rev. B 54 (2006) 12669;
A. Abada A. H. Bougourzi, B. Si-Lakhal, Nucl. Phys. B 497 (1997) 733;
M. Karbach, G. Müller, A. H. Bougourzi, A. Fledderjohann, K. H. Mütter, Phys. Rev. B 55 (1997) 12510.
[25] D. Biegel, M. Karbach, G. Müller, Europhys. Lett. 59 (2002) 882.
[26] N. Kitanine, J. M. Maillet, V. Tétraz, Nucl. Phys. B 554 (1999) 647.
[27] J.-S. Caux, J. M. Maillet, Phys. Rev. Lett. 95 (2005) 077201.
[28] J.-S. Caux, H. Konno, M. Sorrell, R. Weston, Phys. Rev. Lett. 106 (2011) 217203.
[29] H. Frahm, V. E. Korepin, Phys. Rev. B 42 (1990) 10553.
[30] H. Frahm, V. E. Korepin, Phys. Rev. B 43 (1991) 5653.
[31] M. Ogata, T. Sugiyama, H. Shiba, Phys. Rev. B 43 (1991) 8401.
[32] K. Penc, K. Hallberg, F. Mila, H. Shiba, Phys. Rev. Lett. 77 (1996) 1390.
[33] K. Penc, K. Hallberg, F. Mila, H. Shiba, Phys. Rev. B 55 (1997) 15 475.
[34] F. Woynarovich, J. Phys. C: Solid State Phys. 15 (1982) 85.
[35] F. Woynarovich, J. Phys. C: Solid State Phys. 15 (1982) 97.
[36] M. Ogata, H. Shiba, Phys. Rev. B 41 (1990) 2326.
[37] J. M. P. Carmelo, J. M. Román, K. Penc, Nucl. Phys. B 683 (2004) 387.
[38] J. M. P. Carmelo, K. Penc, D. Bozi, Nucl. Phys. B 725 (2005) 421; 737 (2006) 351, Erratum.

- [39] J. M. P. Carmelo, L. M. Martelo, K. Penc, Nucl. Phys. B 737 (2006) 237.
- [40] J. M. P. Carmelo and T. Čadež, Nucl. Phys. B 904 (2016) 39.
- [41] A. Imambekov, T. L. Schmidt, L. I. Glazman, Rev. Mod. Phys. 84 (2012) 1253.
- [42] F. H. L. Essler, Phys. Rev. B 81 (2010) 205120.
- [43] L. Seabra, F. H. L. Essler, F. Pollmann, I. Schneider, T. Veness, Phys. Rev. B 90 (2014) 245127.
- [44] J. M. P. Carmelo, D. Bozi, K. Penc, J. Phys.: Cond. Mat. 20 (2008) 415103.
- [45] M. Sing, U. Schwingenschlögl, R. Claessen, P. Blaha, J. M. P. Carmelo, L. M. Martelo, P. D. Sacramento, M. Dressel, C. S. Jacobsen, Phys. Rev. B 68 (2003) 125111.
- [46] J. M. P. Carmelo, K. Penc, L. M. Martelo, P. D. Sacramento, J. M. B. Lopes dos Santos, R. Claessen, M. Sing, U. Schwingenschlögl, Europhys. Lett. 67 (2004) 233.
- [47] J. M. P. Carmelo, K. Penc, P. D. Sacramento, M. Sing, R. Claessen, J. Phys.: Cond. Mat. 18 (2006) 5191.
- [48] M. Kohno, Phys. Rev. Lett. 105 (2010) 106402.
- [49] H. Benthien, F. Gebhard, E. Jeckelmann, Phys. Rev. Lett. 92 (2004) 256401.
- [50] A. E. Feiguin, D. A. Huse, Phys. Rev. B 79 (2009) 100507(R).
- [51] F. H. L. Essler, V. E. Korepin, K. Schoutens, Phys. Rev. Lett. 67 (1991) 3848.
- [52] D. Braak, N. Andrei, Nucl. Phys. B 542 (1999) 551.
- [53] R. G. Pereira, K. Penc, S. R. White, P. D. Sacramento, J. M. P. Carmelo, Phys. Rev. B 85 (2012) 165132.
- [54] A. A. Ovchinnikov, Sov. Phys. - JETP 30 (1970) 1160.
- [55] J. M. P. Carmelo, P. Horsch, P. A. Bares, A. A. Ovchinnikov, Phys. Rev. B 44 (1991) 9967; J. M. P. Carmelo, P. Horsch, A. A. Ovchinnikov, Phys. Rev. B 45 (1992) 7899;
- [56] J. M. P. Carmelo, P. D. Sacramento, Phys. Rev. B 68 (2003) 085104.
- [57] C. N. Yang, Phys. Rev. Lett. 63 (1989) 2144.
- [58] C. N. Yang, S. C. Zhang, Mod. Phys. Lett. B 4 (1990) 759.
- [59] E. H. Lieb, Phys. Rev. Lett. 62 (1989) 1201.
- [60] J. M. P. Carmelo, S. Östlund, M. J. Sampaio, Ann. Phys. 325 (2010) 1550.
- [61] L. D. Faddeev, L. A. Takhtajan, Phys. Lett. 85A (1981) 375.
- [62] F. H. L. Essler, V. E. Korepin, Phys. Rev. Lett. 72 (1994) 908; F. H. L. Essler, V. E. Korepin, Nucl. Phys. B 426 (1994) 505, Section 5.
- [63] H. V. Kruis, I. P. McCulloch, Z. Nussinov, J. Zaanen, Phys. Rev. B 70 (2004) 075109.
- [64] F. D. M. Haldane, Phys. Rev. Lett. 67 (1991) 937.
- [65] Y. R. Wang, Phys. Rev. B 46 (1992) 151.
- [66] P. W. Anderson, Phys. Rev. Lett. 18 (1967) 1049.
- [67] V. L. Campo, Jr., K. Capelle, J. Quintanilla, C. Hooley, Phys. Rev. Lett. 99 (2007) 240403
- [68] D. Greif, G. Jotzu, M. Messer, R. Desbuquois, T. Esslinger, Phys. Rev. Lett. 115 (2015) 260401.
- [69] V. L. Campo, Jr., K. Capelle, J. Quintanilla, C. Hooley, Phys. Rev. Lett. 115 (2015) 215301.